www.oftalmoloji.org

E-ISSN: 2149-8709

TURKISH JOURNAL OF OPHTHALMOLOGY

TURKISH JOURNAL OF OPHTHALMOLOGY TJO

May June 2024
Volume 54
Issue 3

galenos

TURKISH JOURNAL OF OPHTHALMOLOGY

TJO

www.oftalmoloji.org

Publishing House
Molla Gürani Mah. Kaçamak Sokak No: 21,
34093 Fındıkzade-İstanbul-Türkiye
Publisher Certificate Number: 14521
Phone: +90 (530) 177 30 97
E-mail: info@galenos.com.tr
Online Publishing Date: June 2024
International scientific journal published bimonthly.
E-ISSN: 2149-8709

The Turkish Journal of Ophthalmology is an official journal of the Turkish Ophthalmological Association.

On Behalf of the Turkish Ophthalmological Association Owner

Hüban ATİLLA
Ankara University Faculty of Medicine, Department of Ophthalmology, Ankara, Türkiye

TURKISH JOURNAL OF OPHTHALMOLOGY

TJO

www.oftalmoloji.org

Please refer to the journal's webpage **(https://www.oftalmoloji.org/)** for "About Us", "Instructions to Authors" and "Ethical Policy".

The editorial and publication process of the Turkish Journal of Ophthalmology are shaped in accordance with the guidelines of ICMJE, WAME, CSE, COPE, EASE, and NISO. The journal adheres to the Principles of Transparency and Best Practice in Scholarly Publishing.

The Turkish Journal of Ophthalmology is indexed in **PubMed/MEDLINE, PubMed Central (PMC), Web of Science-Emerging Sources Citation Index (ESCI), Scopus, TÜBİTAK/ULAKBİM, Directory of Open Access Journals (DOAJ), EBSCO Database, Gale, CINAHL, Proquest, Embase, British Library, Index Copernicus, J-Gate, IdealOnline, Türk Medline, Hinari, GOALI, ARDI, OARE, AGORA,** and **Turkish Citation Index**.

Issues are published electronically six times a year.

Owner: Hüban ATİLLA on Behalf of the Turkish Ophthalmological Association Owner

Responsible Manager: Banu BOZKURT

TURKISH JOURNAL OF OPHTHALMOLOGY

TJO

www.oftalmoloji.org

CONTENTS

Research Articles

Review

Case Reports

TURKISH JOURNAL OF OPHTHALMOLOGY

TJO

www.oftalmoloji.org

AT A GLANCE

2024 Issue 3 at a Glance:

Esteemed colleagues,

This issue of our journal includes 6 original research articles, 1 review, and 3 case reports from various fields of ophthalmology that we hope will be an interesting and useful read for you.

Laser-assisted in situ keratomileusis (LASIK) is safe and effective and the most commonly performed refractive surgical method. Because corneal tissue is removed, all excimer laser procedures affect corneal biomechanics. Post-LASIK ectasia (PLE) is characterized by progressive thinning and steepening of the cornea that causes refractive aberration and severe vision loss. Tanrıverdi et al. treated 26 eyes of 16 patients with PLE with the modified Cretan protocol (combined transepithelial phototherapeutic keratectomy and accelerated corneal collagen cross-linking) and evaluated visual, refractive, tomographic, and aberrometric results and point spread function (PSF) preoperatively and 6, 12, and 24 months after treatment. They stated that the modified Cretan protocol in PLE patients is an effective and safe treatment option that can provide significant improvement in visual stabilization and topographic parameters over 24-month follow-up (See pages 120-126).

Fabry disease (FD) is a rare X-linked lysosomal storage disease characterized by impaired glycosphingolipid metabolism due to absence or deficiency of the alpha-galactosidase A enzyme (α-Gal). Cardiopathy, neuropathy, and cerebrovascular diseases are the most serious clinical findings associated with increased morbidity and mortality in FD. Although ophthalmological involvement is quite common in FD and is among the early signs of the disease, it is often overlooked. Korkmaz et al. included 30 eyes of 15 patients diagnosed based on clinical findings, genetic analysis, and biochemical evaluation in their prospective cross-sectional study evaluating the ocular findings of patients with FD admitted to a tertiary eye clinic in Türkiye. Corneal verticillata, which is considered to be the most characteristic ocular finding in FD, was not detected in approximately one-third of the patients, and only 26.6% of the patients had cataract, another well-known ocular finding in FD. The authors emphasized that awareness among ophthalmologists about the findings and incidence of FD may facilitate early and accurate diagnosis (See pages 127-132).

A prospective study by Sert et al. aimed to examine changes in tear oxidative stress levels and tear film functions after conjunctiva-Müller muscle resection (CMMR) and blepharoplasty in patients with blepharoptosis and dermatochalasis. The study included 32 healthy controls and 62 patients with blepharoptosis or dermatochalasis, in whom 20 eyes underwent CMMR surgery and 42 eyes underwent upper blepharoplasty. Tear levels of oxidative stress markers (8-2′-deoxyguanosin [8-OHdG] and 4-hydroxy-2-nonenalhydroxy [4-HNE]) were determined by enzyme-linked immunosorbent assay and tear film functions were evaluated preoperatively and at postoperative 1 and 6 months. Patients with dermatochalasis or blepharoptosis were shown to have higher levels of oxidative stress markers in the tear film compared to the healthy controls. Blepharoplasty and CMMR did not cause any difference in Schirmer or Ocular Surface Disease Index scores at postoperative 1 and 6 months, while CMMR caused a temporary decrease in tear break-up time and increase in tear oxidative stress markers levels (See pages 133-139).

Neurofibromatosis type 1 (NF-1) is an autosomal dominant disease caused by deletions or mutations in the neurofibromin gene on chromosome 17p11.2. NF-1 is characterized by a range of findings such as nerve tumors that can develop in various parts of the body, skin pigmentation changes (cafe au lait spots, axillary and inguinal freckling), vascular abnormalities, and bone lesions (pseudoarthrosis, sphenoidal wing hypoplasia), and ocular involvement is also common. The NF-1 diagnostic criteria determined by the National Institute of Health include the presence of two or more Lisch nodules on the iris and optic nerve glioma as ophthalmological findings. It has been suggested that the presence of at least two choroidal anomalies defined as "bright, patchy nodules" in optical coherence tomography (OCT) or infrared reflectance (IR) imaging should also be used as a diagnostic criterion for NF-1. These choroid-level lesions are hamartomatous nodules and are also referred to as "Yasunari nodules". In their retrospective study titled "Multimodal Imaging Characteristics and Diagnostic Value of Choroidal Nodules in Patients with Neurofibromatosis Type 1", Ahmadova et al. examined 54 eyes of 27 patients and found that Yasunari nodules were frequently observed in NF-1 cases and can be easily detected with multimodal imaging techniques, especially with IR imaging. As choroidal nodules can be seen before the appearance of Lisch nodules, this study highlights the importance of Yasunari nodules in the diagnosis of NF-1 (See pages 140-148).

Retinal vein occlusions (RVO) occur as a result thrombus blocking the retinal venous system, and the most common etiological factor is atherosclerotic retinal arteries compressing the veins at the arterial-venous junction. Risk factors for RVO include advanced age, diabetes mellitus, hypertension, atherosclerotic vascular disease, and glaucoma. The triglyceride-glucose (TyG) index, calculated with the formula ln(fasting TG [mg/dL] × fasting plasma glucose [mg/dL]/2) is a marker of atherosclerosis in cardiovascular diseases. A case-controlled observational study by Katipoğlu and Turan aiming

TURKISH JOURNAL OF OPHTHALMOLOGY

TJO

www.oftalmoloji.org

AT A GLANCE

to reveal the relationship between TyG index and RVO included 387 patients (181 females and 206 males) diagnosed with RVO and 115 patients (61 females and 54 males) as the control group. The TyG index was found to be higher in the RVO group (8.9±0.7) compared to the control group (8.8±0.6) (p=0.04), and the authors suggested that the TyG index, which is obtained by a simple calculation, could be a reliable indicator to identify individuals at high risk of RVO and to initiate treatment early (See pages 149-152).

Malik and Moin retrospectively evaluated the records of 18 patients with carotico-cavernous fistula who underwent digital subtraction angiography and subsequent endo-arterial balloon embolization and stated that this method was safe and simple with demonstrated effectiveness, especially when performed in a timely manner (See pages 153-158).

Tissue engineering (TE) aims to treat, repair, or replace damaged tissues and organs using cells and appropriate physiological factors together with bioengineering, biomedical engineering, and materials sciences. Areas of TE research also include developing disease models, creating tissue scaffolds for cells, and delivering active drug components to tissues. The fact that the eye is an easily accessible organ amenable to engineering applications has paved the way for the use of TE in ophthalmology. In this issue's review, Utine and Güven describe in detail the application areas of TE in ophthalmology in light of the current literature (See pages 159-169).

Iridocorneal endothelial (ICE) syndrome is a disease group in which corneal endothelial cells proliferate and migrate to the iridocorneal angle and over the iris. There are three clinical variants: Chandler syndrome, progressive iris atrophy, and Cogan-Reese syndrome. In ICE syndrome, abnormally proliferating endothelial cells form a membrane over the iridocorneal angle and peripheral iris. This membrane can cause pupillary disorder, high intraocular pressure (IOP), corneal decompensation, and corneal edema due to peripheral anterior synechiae and peripheral iris traction. Güler Canözer et al. presented the in vivo confocal microscopy (IVCM) and anterior segment optical coherence tomography (AS-OCT) findings of three female patients who presented due to low vision and high IOP. The authors pointed out that ICE syndrome should be suspected especially in female patients with pupil irregularity and corneal edema accompanying unilateral IOP elevation, and noted that IVCM and AS-OCT are diagnostically useful non-invasive imaging methods that can reveal the abnormal structures and anterior segment migration of endothelial cells with epithelial characteristics in ICE syndrome (See pages 170-174).

Kayabaşı et al. detected multiple yellowish-white retinitis foci, vascular engorgement, and scattered intraretinal hemorrhages extending from the posterior pole to the peripheral retina in the right eye of a 78-year-old male patient who presented with complaints of a gradual decrease in vision in the right eye for 2 weeks and a history of chemotherapy and radiotherapy for lung cancer and Coronavirus Disease 2019 infection. The patient was diagnosed with endogenous endophthalmitis and received intravitreal vancomycin, ceftazidime, clindamycin, and dexamethasone. Vitreous culture demonstrated the presence of *Aspergillus lentulus*, and the patient was treated with intravitreal amphotericin-B and voriconazole injections and systemic amphotericin-B, voriconazole, posaconazole, and micafungin therapy. Vitreoretinal surgery was performed due to rhegmatogenous retinal detachment during follow-up. However, despite retinal reattachment, the patient required enucleation due to the development of a painful red eye. On histopathological examination, atypical squamous cells compatible with metastasis were detected beneath the neurosensory retina. By presenting this case, the authors emphasized that timely eye examination is vital in all immunosuppressed patients with ocular symptoms, and fungal pathogens should be considered as possible causes of endogenous endophthalmitis (See pages 175-179).

In traumatic injuries, cerebrospinal fluid (CSF) fistula can develop for various reasons. It most commonly presents as rhinorrhea and otorrhea, but oculorrhea can also occur in some cases, especially in patients with direct eye trauma. Akbulut and Bolat present the case of a 4-year-old child who was referred to a tertiary care center due to a dog bite to the left eyelid and was observed to have lid edema and increased lacrimation secondary to inflammation on initial examination. However, observation of an increase in clear discharge in the reverse Trendelenburg position and upon Valsalva maneuver during follow-up and subsequent positive halo sign and beta-transferrin test led to the diagnosis of a CSF fistula. A supraorbital craniotomy was performed via an eyebrow incision and the dural tear was repaired by primary suturing supported with a galeal graft and fibrin glue. The authors concluded that oculorrhea may be mistaken for lacrimation in patients with penetrating orbital trauma and CSF fistula must be considered (See pages 180-182).

We hope that the articles featured in the third issue of this year will be of interest to you and will guide your medical practice.

Respectfully on behalf of the Editorial Board,

Özlem Yıldırım, MD

Original Article

Efficacy and Safety of the Modified Cretan Protocol in Patients with Post-LASIK Ectasia

Burak Tanrıverdi*, Özge Saraç**, Berke Temel***, Esra Dağ Şeker****, Nurullah Çağıl*

*Lokman Hekim University, Akay Hospital, Clinic of Ophthalmology, Ankara, Türkiye
**Ankara Yıldırım Beyazıt University Faculty of Medicine, Department of Ophthalmology, Ankara, Türkiye
***Antalya City Hospital, Clinic of Ophthalmology, Antalya, Türkiye
****Ankara City Hospital, Clinic of Ophthalmology, Ankara, Türkiye

Abstract

Objectives: To investigate the clinical efficacy and safety of the modified Cretan protocol in patients with post-laser in situ keratomileusis ectasia (PLE).

Materials and Methods: In this retrospective study, 26 eyes of 16 patients with PLE were treated with the modified Cretan protocol (combined transepithelial phototherapeutic keratectomy and accelerated corneal collagen cross-linking). Visual, refractive, tomographic, and aberrometric outcomes and point spread function (PSF) were recorded preoperatively and at 6, 12, and 24 months after treatment.

Results: Both uncorrected and best corrected visual acuity were stable at 24 months postoperatively compared to baseline (from 0.89±0.36 to 0.79±0.33 logarithm of the minimum angle of resolution [LogMAR] and 0.31±0.25 to 0.24±0.19 LogMAR, respectively, p>0.05 for all values). The mean K1, K2, Kmean, thinnest corneal thickness, and spherical aberration at baseline were 45.76±5.75 diopters (D), 48.62±6.17 D, 47.13±5.89 D, 433.16±56.86 µm, and -0.21±0.63 µm respectively. These values were reduced to 42.86±6.34 D, 45.92±6.74 D, 44.21±6.4 D, 391.07±54.76 µm, and -0.51±0.58 µm at 24 months postoperatively (p<0.001, p=0.002, p<0.001, p=0.001, and p=0.02, respectively). The mean spherical equivalent, manifest cylinder, Kmax, central corneal thickness, other corneal aberrations (root mean square, trefoil, coma, quatrefoil, astigmatism), and PSF remained stable (p>0.05 for all variables), while anterior and posterior elevation were significantly improved at 24 months postoperatively (p<0.001 and p=0.02, respectively). No surgical complications occurred during the 24-month follow-up.

Conclusion: The modified Cretan protocol is a safe and effective treatment option for PLE patients that provides visual stabilization and significant improvement in topographic parameters during the 24-month follow-up. Further studies are needed to support our results.

Keywords: Post-LASIK ectasia, corneal collagen cross-linking, transepithelial phototherapeutic keratectomy, corneal topography

Introduction

Post-laser in situ keratomileusis (LASIK) ectasia (PLE) is characterized as progressive thinning and steepening of the cornea resulting in refractive aberrations and severe visual loss.[1] Iatrogenic keratectasia, a potentially vision-threatening complication following LASIK, manifests in 0.1% of instances.[2] Due to the removal of corneal tissue, corneal biomechanics can potentially be compromised by all excimer laser procedures.

Corneal collagen crosslinking (CXL) is a minimally invasive surgical procedure that utilizes riboflavin and ultraviolet A (UVA) to strengthen the biomechanical properties of an ectatic cornea by creating covalent bonds within and between the collagen and proteoglycan molecules. It is effective in stabilizing the progression of corneal ectasias including progressive keratoconus (KC), pellucid marginal degeneration (PMD), and post-refractive corneal ectasia. In the conventional CXL procedure, a dosage of 5.4 J/cm^2 energy is applied at an intensity of 3 mW/cm^2 over a duration of 30 minutes.[3] Accelerated CXL (aCXL) is an alternative approach that utilizes a higher UVA irradiance intensity and shorter overall exposure time, following the principles of the Bunsen-Roscoe law.[4] The aCXL protocol is as effective and safe as the conventional CXL protocol in both adult and pediatric KC patients.[5,6] Mechanical debridement or excimer

Cite this article as: Tanrıverdi B, Saraç Ö, Temel B, Dağ Şeker E, Çağıl N. Efficacy and Safety of the Modified Cretan Protocol in Patients with Post-LASIK Ectasia. Turk J Ophthalmol 2024;54:120-126

This article was presented as an oral presentation at the 52nd TOA National Congress (13-18 November 2018, Antalya).

Address for Correspondence: Burak Tanrıverdi, Lokman Hekim University, Akay Hospital, Clinic of Ophthalmology, Ankara, Türkiye
E-mail: drburak23@gmail.com **ORCID-ID:** orcid.org/0000-0002-3709-3955
Received: 24.08.2023 **Accepted:** 25.03.2024

DOI: 10.4274/tjo.galenos.2024.82342

laser ablation (transepithelial phototherapeutic keratectomy, tPTK) may be used to remove the epithelium during CXL. The Cretan protocol, introduced by Kymionis et al.[7], employs tPTK for the removal of corneal epithelium in the conventional CXL procedure. The utilization of this protocol leads to superior visual and refractive outcomes in KC patients when compared to mechanical epithelial debridement.[8,9] Our group demonstrated that the combined tPTK+aCXL (modified Cretan protocol) is an effective treatment option for PMD and pediatric KC patients.[10,11] However, no study in the literature has reported the efficacy of this protocol in patients with PLE.

In this retrospective study, we evaluated the visual, refractive, topographic, and optical quality outcomes of combined tPTK+aCXL treatment in PLE patients over 24 months.

Materials and Methods

Study Population

The single-center study adhered to the principles of the Declaration of Helsinki and received approval from the Ankara City Hospital-No.1 Clinical Research Ethics Committee (date: 23.06.2021, no: E1/1910/2021). Written informed consent was obtained from all patients. The records of PLE patients who received the combined tPTK+aCXL and had 24 months of follow-up were retrospectively reviewed. Clinical and topographic evaluations of all patients were performed preoperatively and at 6, 12, and 24 months after treatment. Exclusion criteria included corneal thickness <400 µm, presence of a central or paracentral corneal scar, previous ocular surgeries other than LASIK, a history of herpetic keratitis, active ophthalmic inflammation or infection, contact lens usage, and pregnancy or lactation.

Patients were diagnosed with corneal ectasia when they exhibited progressive corneal steepening, along with a worsening myopic and/or astigmatic refractive error, occurring at least two months after LASIK surgery. All patients demonstrated progression of the myopic refractive error with or without an increase in manifest astigmatism, a decrease in uncorrected visual acuity (UCVA) and best corrected visual acuity (BCVA), progressive inferior corneal steepening on topography, and/or decreasing inferior corneal thickness.[12]

Ophthalmologic and Topographic Examination

Patients underwent a comprehensive ophthalmologic examination that included measurements of spherical refractive error, spherical equivalent (SE), manifest cylinder (CYL) value, UCVA, and BCVA. VA was assessed using the Snellen chart, and the results were subsequently transformed into the logarithm of the minimum angle of resolution scale for statistical analysis. The examination also involved a slit-lamp examination, intraocular pressure measurement, fundoscopic examination, and topographic analysis of the cornea using the Sirius 3D rotating Scheimpflug camera and topography system (CSO, Italy).

The topographic corneal analysis included measurements of simulated keratometry values (flat: K1, steep: K2, mean: Kmean, maximum: Kmax), central corneal thickness (CCT), corneal thickness at the thinnest point (TCT), anterior and posterior elevation, and point spread function (PSF). Corneal higher-order aberrations (HOAs) in the central 6.0 mm, including total root mean square (RMS), coma, trefoil, astigmatism, and spherical aberration, were quantified using Zernike coefficients, considering aberrations ranging from 3rd to 8th order. PSF evaluation is used to assess image quality, which is related to the theoretical performance of the optical system.[13] We computed the Strehl ratio of the PSF in addition to HOAs to assess the impact of treatment on corneal optical performance using the Sirius imaging system. For all eyes in the study, two-dimensional corneal PSFs were computed, and the Strehl ratio was employed to represent them.[14]

Surgical Technique

All procedures were performed in an operating room by the same surgeon (Ö.S.) under sterile conditions and topical anesthesia with 0.5% proxymetacaine hydrochloride eyedrops (Alcaine, Alcon Laboratories Inc.). The tPTK method was used to remove the corneal epithelium with a scanning spot excimer laser (Esiris, Schwind eye-tech-solutions GmbH&Co., Kleinostheim, Germany). The laser ablation was performed in a single-step in an 8.5-mm zone at a fixed depth of 50 µm. The laser profiles were independent of refractive parameters, topography, or wavefront guidance.[10]

We used an ultrasonic pachymeter (Palmscan AP-2000-Ultima, Micromedical Devices, Inc.) to measure corneal thickness before and after epithelial removal. Following epithelial removal (by tPTK), we applied hypotonic 0.1% riboflavin in 0.9% sodium chloride drops (Meran Medical, BNM Inc., Istanbul, Türkiye) to the cornea every 2 minutes for 30 minutes until the cornea swelled to more than 400 µm and the aqueous became stained yellow. UVA radiation was then applied for 10 minutes at 9 mW/cm^2 power using a commercially available UVA system (Meran Medical, BNM, Inc., Istanbul, Türkiye), with the riboflavin solution being applied every 2 minutes to maintain saturation during the procedure.[10] After surgery, we placed a therapeutic silicone hydrogel contact lens (Acuvue Oasys, Johnson & Johnson Vision Care, Inc.) and left it in place until reepithelialization was complete. Postoperatively, the patient received topical ofloxacin drops (Exocin, Allergan, Inc.) 4 times a day for 1 week, topical fluorometholone drops (FML, Allergan, Inc.) 4 times a day for 1 month (with a tapering schedule), and artificial tears 4 times a day for 6 months.

Statistical Analysis

The statistical analysis was performed using SPSS Statistics 21.0 (IBM Corp, Armonk, NY). Before conducting the analysis, we verified the normal distribution of the data using the Shapiro-Wilk W test. All variables are expressed as mean and standard deviation. Changes from the preoperative value at each follow-up were assessed using the paired-sample t-test. Statistical significance was attributed to differences with a p value <0.05.

Results

This study included 26 eyes of 16 PLE patients (11 men, 5 women) who were treated with combined tPTK+aCXL. The mean age was 37.06±6.28 years (range 29 to 49 years). Therapeutic contact lenses were taken out within 5 days

postoperatively, and the epithelium was found to be intact in all eyes. None of the patients experienced any complications during the procedure or the 24-month follow-up period.

Table 1 displays the preoperative and postoperative visual, refractometric, and topographic outcomes of the patients. During the 24 months of follow-up, the mean UCVA and BCVA values remained stable compared to baseline (p>0.05). There was a stabilization in both UCVA and BCVA at 24 months postoperatively (p>0.05 for both values). While 10 eyes (38.4%) had at least one Snellen line of improvement in UCVA (mean 1.9 Snellen lines, range 1-7), 14 eyes (53.8%) had stable UCVA at postoperative 24 months. While 8 eyes (30.7%) had at least one Snellen line of improvement in CDVA (mean 2.1 Snellen lines, range 1-4), 16 eyes (61.5%) had stable CDVA at postoperative 24 months. Among the eyes that underwent the treatment, 2 eyes (7.69%) had one Snellen line of decrease in their UCVA, and 2 eyes (7.69%) had two Snellen lines of decrease in their CDVA. The mean SE and CYL started to decrease in 6 months. However, this decrease could not reach a statistically significant level and remained stable throughout the follow-up period (p>0.05 for all visits).

As seen in Table 1, regarding the topographic values, a significant reduction in the mean K1, K2, and Kmean values was noted at 6, 12, and 24 months when compared to preoperative values (p=0.009, p=0.001, and p=0.02 for K1; p=0.002, p<0.001, and p<0.001 for K2; and p=0.002, p<0.001, and p<0.001 for Kmean, respectively). The reduction in K1, K2, and Kmean values was also observed at 6 and 12 months compared to the previous visit, with stabilization noted after 12 months (Table 2). Although the mean Kmax increased at 6 months, it decreased at 12 and 24 months of follow-up, but this difference was not statistically significant (p>0.05 for all visits). The mean CCT value was significantly decreased at postoperative 6 months, although it started to recover at postoperative 12 months (p<0.001 and p=0.002, respectively). It was stable compared to baseline throughout the 24 months of follow-up (p=0.08). A significant decrease in mean TCT was observed at postoperative 6 months, and this decrease was stable during the 24-month follow-up period (p<0.001, p<0.001, and p=0.005, respectively) (Table 1). Both CCT and TCT values remained stable after postoperative month 6 when compared to the previous visit (Table 2). There was also a significant decrease in the mean anterior elevation value that started at postoperative 6 months and continued throughout the follow-up period (p=0.03, p<0.001, and p<0.001, respectively). The

Table 1. Visual acuity, refractometric, and topographic values before and after transepithelial phototherapeutic keratectomy and accelerated corneal collagen cross-linking treatment

	Preoperative	6 months	12 months	24 months
LogMAR UCVA p value*	0.89±0.36	0.76±0.31 p=0.093	0.77±0.44 p=0.734	0.79±0.33 p=0.327
LogMAR BCVA p value*	0.31±0.25	0.31±0.18 p=0.974	0.26±0.22 p=0.520	0.24±0.19 p=0.439
Spherical equivalent (D) p value*	-5.19±4.56	-4.8±3.6 p=0.315	-3.25±2.6 p=0.237	-2.77±2.27 p=0.234
Manifest cylinder (D) p value*	-2.44±1.63	-2.59±1.68 p=0.820	-2.17±1.15 p=0.105	-2.26±1.26 p=0.166
CCT (µm) p value*	441.08±56.35	404.83±53.0 **p<0.001**	408.25±52.07 **p=0.002**	429.5±55.91 p=0.08
TCT (µm) p value*	433.16±56.86	387.7±51.62 **p<0.001**	388.93±48.98 **p<0.001**	391.07±54.76 **p=0.005**
K1 (D) p value*	45.76±5.75	45.57±5.92 **p=0.009**	44.61±6.41 **p=0.001**	42.86±6.34 **p=0.02**
K2 (D) p value*	48.62±6.17	48.28±6.3 **p=0.002**	47.26±6.67 **p<0.001**	45.92±6.74 **p<0.001**
Kmean (D) p value*	47.13±5.89	46.87±6.06 p=0.002	45.89±6.51 **p<0.001**	44.21±6.4 p<0.001
Kmax (D) p value*	59.56±8.87	61.67±9.39 p=0.117	57.82±8.89 p=0.109	58.8±7.9 p=0.836
Posterior elevation (µm) p value*	73.40±47.76	68.83±39.0 p=0.131	57.0±41.24 p=0.716	69.7±41.1 **p=0.02**
Anterior elevation (µm) p value*	20.32±18.76	15.62±20.35 **p=0.03**	13.68±19.94 **p<0.001**	9.07±20.73 **p<0.001**

Data expressed as mean ± standard deviation. *Compared to preoperative value with paired-samples t-test, significant values shown in bold (p<0.05). LogMAR: Logarithm of the minimum angle of resolution, UCVA: Uncorrected visual acuity, BCVA: Best corrected visual acuity, D: Diopters, CCT: Central corneal thickness, TCT: Thinnest corneal thickness, K1: Flat keratometry, K2: Steep keratometry, Kmean: Mean keratometry, Kmax: Maximum keratometry

mean posterior elevation value significantly decreased from 73.40±47.76 µm to 69.70±41.1 µm at postoperative 24 months (p=0.02) (Table 1). Anterior elevation values were significantly decreased at 6 and 12 months, while posterior elevation values were significantly decreased at 12 months compared to the previous visit. Both values exhibited stabilization from the 12th month onwards (Table 2).

At 24 months of follow-up, all measured aberrometric values except for spherical aberration (RMS, trefoil, coma, quadrafoil, and astigmatism) and PSF value remained stable compared to the preoperative values (p>0.05 for each variable). There was a statistically significant change in spherical aberration value from -0.21±0.63 µm to -0.51±0.58 µm at postoperative 24 months (p=0.02). During both preoperative and postoperative evaluations, the measured HOAs of all included eyes with PLE deviated from the normal corneal HOA values (Table 3).

Discussion

LASIK is the most commonly performed refractive surgical procedure and is known for its effectiveness and safety.[15] Although postoperative complications are rare, they can be devastating.[16] PLE with progressive corneal steepening, either centrally or inferiorly, leads to severe progressive irregular astigmatism and decreased UCVA and BCVA.[1,16,17] Ectatic changes can occur shortly after LASIK or may be delayed for several years.[18,19] The underlying cause of postoperative ectasia is related to a biomechanical instability of the cornea.[1,17]

The treatment of corneal ectasia involves addressing two key aspects: enhancing corneal biomechanical stability and improving the optical characteristics of the irregular cornea. CXL is a minimally invasive treatment that induces corneal crosslinking to increase corneal stiffness and stability and has shown clinical success in effectively preventing the progression of ectasia.[3] Kohlhaas et al.[20] were the first to describe the successful use of CXL to treat PLE in 2005. Yildirim et al.[21] showed in a retrospective study including 20 eyes with PLE that UCVA and BCVA improved significantly and CYL and Kmax decreased significantly over a 42-month follow-up period after conventional CXL. In recent years, several additional procedures have been suggested in combination with CXL to enhance the visual outcome, such as tPTK, topography-guided photorefractive keratectomy (PRK), intrastromal corneal ring segment implantation, and phakic intraocular lens implantation.[22] These procedures have varying degrees of impact on the cornea or anterior chamber structure.[23] To prevent changes in the anterior chamber, our focus in treating eyes with PLE was on corneal surgery. During the CXL procedure, it is necessary to remove the corneal epithelium to ensure uniform and sufficient absorption of riboflavin into the corneal stroma.[24] Traditionally, mechanical removal of the epithelium has been used,[3] but more recently, excimer lasers have been employed for this purpose.[8] The tPTK procedure removes the irregular epithelial layer of an ectatic cornea with localized thinning over the cone apex and ring-shaped thickening around the cone. The procedure utilizes excimer lasers to smooth out the Bowman layer and irregular stroma, which can effectively reduce optical irregularities and astigmatism. It typically involves an ablation depth of around 50 µm.[7,25] Additionally, it has been found that removal of the Bowman layer during tPTK may enhance the effectiveness of CXL treatment.[25] The Cretan protocol incorporates tPTK

Table 2. Topographic values before and after transepithelial phototherapeutic keratectomy and accelerated corneal collagen cross-linking treatment

	Preoperative	6 months	12 months	24 months
CCT (µm) p value*	441.08±56.35	404.83±53.0 **p<0.001**	408.25±52.07 p=0.104	429.5±55.91 p=0.079
TCT (µm) p value*	433.16±56.86	387.7±51.62 **p<0.001**	388.93±48.98 p=0.568	391.07±54.76 p=0.054
K1 (D) p value*	45.76±5.75	45.57±5.92 **p=0.009**	44.61±6.41 **p=0.014**	42.86±6.34 p=0.105
K2 (D) p value*	48.62±6.17	48.28±6.3 **p=0.002**	47.26±6.67 **p=0.003**	45.92±6.74 p=0.132
Kmean (D) p value*	47.13±5.89	46.87±6.06 **p=0.002**	45.89±6.51 **p=0.004**	44.21±6.4 p=0.102
Kmax (D) p value*	59.56±8.87	61.67±9.39 p=0.117	57.82±8.89 p=0.071	58.8±7.9 p=0.214
Posterior elevation (µm) p value*	73.40±47.76	68.83±39.01 p=0.131	57.0±41.24 **p=0.026**	69.7±41.1 p=0.091
Anterior elevation (µm) p value*	20.32±18.76	15.62±20.35 **p=0.03**	13.68±19.94 **p=0.009**	9.07±20.73 p=0.068

Data expressed as mean ± standard deviation. *Compared to the previous time point with paired-samples t-test, significant values shown in bold (p<0.05). CCT: Central corneal thickness, TCT: Thinnest corneal thickness, K1: Flat keratometry, D: Diopters, K2: Steep keratometry, Kmean: Mean keratometry

Table 3. Corneal aberration and point spread function values before and after transepithelial phototherapeutic keratectomy and accelerated corneal collagen cross-linking treatment

	Preoperative	6 months	12 months	24 months
RMS (µm) p value*	2.32±1.02	3.06±1.53 **p=0.001**	2.65±1.07 p=0.212	2.51±1.42 p=0.077
Trefoil (µm) p value*	0.75±0.48	0.87±0.52 p=0.144	0.69±0.40 **p=0.004**	0.80±0.43 p=0.959
Coma (µm) p value*	1.77±0.96	1.51±1.11 p=0.065	1.31±0.88 **p=0.001**	1.59±0.94 p=0.142
Quadrifoil (µm) p value*	0.24±0.13	0.34±0.23 p=0.08	0.24±0.07 p=0.725	0.20±0.19 p=0.868
Astigmatism (µm) p value*	0.50±0.34	0.51±0.35 p=0.778	0.49±0.28 p=0.759	0.52±0.26 p=0.751
Spherical aberration (µm) p value*	-0.21±0.63	-0.27±0.66 p=0.085	-0.26±0.67 p=0.398	-0.51±0.58 **p=0.02**
Strehl ratio of PSF p value*	0.05±0.02	0.04±0.02 p=0.88	0.04±0.01 p=0.511	0.04±0.02 p=0.897

Data expressed as mean ± standard deviation, *Compared to preoperative value with paired-samples t-test, significant values shown in bold (p<0.05). RMS: Root mean square, PSF: Point spread function

for corneal epithelium removal during conventional CXL[7] and has demonstrated better visual and refractive outcomes in comparison to mechanical debridement at 1-year follow-up in studies of progressive KC.[26,27] In our previous study, we compared the outcomes of using tPTK (modified Cretan protocol) versus mechanical epithelial removal during aCXL for pediatric KC and observed enhanced visual outcomes in the first year after the procedure compared to mechanical epithelial removal.[11] However, at 36-month follow-up, both techniques showed similar results. We also used tPTK+aCXL for progressive PMD patients and observed stabilization in VA and Kmax, as well as a decrease in cylindrical refraction and SE after 36 months of follow-up.[10] In our current study, we performed a new technique, tPTK+aCXL, for the treatment of PLE.

In this retrospective study, we treated 26 eyes of 16 PLE patients with combined tPTK+aCXL and reported both short and long-term outcomes. The aCXL technique shortens the duration of UV irradiation, potentially enhancing patient comfort during treatment compared to conventional CXL. Performing mechanical epithelial debridement before conventional CXL poses a risk of damaging the LASIK flap. The lack of this risk can be seen as advantageous for tPTK. Research has demonstrated that the excimer laser for corneal epithelial removal may increase the risk of corneal complications, including epithelial hypertrophy, delayed epithelial healing, hyperopic shift, and corneal haze, compared to mechanical debridement methods.[28,29] In our current study, no complication was observed during 24-month follow-up. According to our visual outcomes, although the improvement in UCVA and BCVA during the 24-month follow-up period was not statistically significant, 38.4% of eyes showed at least one Snellen line UCVA improvement, and 30.7% had at least one Snellen line CDVA improvement. In a study by Richoz et al.[1] involving 23 PLE eyes and 3 PRK-induced ectasia eyes that underwent mechanical epithelial debridement followed by conventional CXL treatment, significant improvements in mean BCVA and Kmax were observed at 25 months of follow-up. However, it is worth noting that their patients had thinner corneas than the patients in our study. Toprak et al.[30] demonstrated that preoperative TCT serves as one of the predictive factors for the outcome of CXL treatment in KC patients, influencing changes in VA and maximum keratometry. The flattening effect of CXL treatment may be greater in thinner corneas, potentially resulting in increased VA and reduced Kmax in patients with advanced PLE.

Furthermore, our study revealed promising topographic outcomes. Keratometry values showed a flattening during the 24 months of follow-up compared to preoperative values. Specifically, K1, K2, and Kmean decreased significantly by approximately 0.3 diopters (D) at 6 months and 3.0 D by 24 months postoperatively. These values also demonstrated stabilization after the 12th month. However, Kmax, SE, and CYL remained stable throughout the entire 24 months of follow-up. Changes in the profile of corneal epithelial thickness can be observed in various corneal pathologies, including corneal ectasias.[31] It was advocated that a corneal epithelial thickness of 51-60 µm was the therapeutic window for highly aberrated corneas when performing tPTK.[31,32] It can be considered that although applying the tPTK (50 µm depth) without preoperative corneal epithelial mapping may reduce the flattening effect of CXL in the cone region, the progressive steepening in the cone region of a PLE cornea can be halted with tPTK+aCXL treatment. It could be a reason for the stabilization in VA, refraction values, and Kmax after the modified Cretan protocol in PLE. Kymionis et al.[9] reported beneficial outcomes with the Cretan protocol in the treatment of 23 eyes with KC, with UCVA and BCVA improving and the K1 and K2 decreasing at a mean follow-up of 33.83 months. They concluded that the combined approach was effective and safe for the long-term treatment of KC patients. In a comparative study showing 36-month results in progressive KC, the modified Cretan protocol was more effective in improving

UCVA, BCVA, K1, K2, Kmax, and PSF than mechanical debridement-assisted aCXL.[33] On the other hand, another study by our group comparing mechanical debridement-assisted aCXL with tPTK+aCXL in pediatric KC patients demonstrated no superiority of tPTK over mechanical debridement in the long term.[11] Gaster et al.[27] proposed that despite tPTK being as effective as manual debridement before CXL, it does not yield significant and enduring visual, topographic, or refractive benefits for progressive KC. Due to the variable results reported with tPTK+CXL treatment in corneal ectasias, we believe that prospective comparative studies with larger patient series are needed in patients with corneal ectasia, including PLE.

A reduction in corneal thickness is expected after CXL treatments, especially when combined with excimer laser procedures. This reduction in thickness is usually significant and can last for months.[8] Similarly, we observed a significant decrease in both CCT and TCT values at postoperative 6 months in the current study. The decrease in CCT and TCT at 6 months after CXL might also be affected by the Scheimpflug imaging artifact that arises from the stromal scatter that is commonly observed during the early postoperative period.[10] Although TCT remained decreased throughout the 24-month follow-up, CCT started to increase after 6 months, and there was no statistically significant difference compared to baseline at the 24-month follow-up. The mean anterior elevation value improved during the 24-month follow-up, with a total reduction of 11 µm compared to baseline. The mean posterior elevation value also showed a significant reduction at 24-month follow-up compared to the preoperative value.

Evaluation of PSF and corneal aberrations is crucial for assessing the optical quality of the eye. However, Zernike polynomials exhibit a varying effect on visual function. In this study, we observed stability in PSF and all aberration values except for spherical aberrations, which is consistent with our VA results. The spherical aberration value decreased at postoperative 24 months, which might be linked to the flattening of the central cornea following CXL treatment.

Excimer laser ablation alone is not considered the established treatment option to enhance refractive results for patients with PLE. Combined therapies, such as tPTK+CXL or topography-guided PRK+CXL, have demonstrated advantages in terms of both halting progression and enhancing visual function.[34] Zhou et al.[23] used a combined therapy (tPTK+PRK+CXL) for the treatment of 16 eyes with PLE. PTK ablation was performed in an 8.5-mm zone at a depth of 50 µm (like our ablation depth), while PRK ablation was limited to a maximum depth of 80 µm for all cases before conventional CXL. They demonstrated that UCVA improved significantly, while K1, K2, and CYL decreased significantly. The mean CCT and endothelial cell count did not change significantly at 24 months of follow-up. The tPTK+PRK+CXL therapy seems to be effective and safe in the treatment of PLE. Nonetheless, it was suggested that tPTK+CXL should be considered as an alternative in cases of low corneal thickness or when PRK+CXL cannot be performed for better outcomes.[7] Therefore, the combined tPTK+aCXL therapy may be a better treatment option for ectatic corneal diseases such as PLE with low corneal thickness.

Study Limitations

Our study has several limitations. It is retrospective, has a small sample size, and lacks preoperative corneal epithelium data, a group of PLE patients treated with mechanical debridement-assisted aCXL, and a group of untreated PLE patients as controls. Nevertheless, our study included a substantial number of eyes with PLE compared to other studies in the literature, likely due to the rarity of PLE as a complication of LASIK. Another potential study limitation is not measuring the stromal demarcation line. This boundary marks the transition between cross-linked stroma and untreated tissue after CXL, which some researchers consider crucial for the procedure's success. However, there has been debate recently about whether the depth of the stromal demarcation line accurately reflects CXL effectiveness.[35] Furthermore, safety concerns, particularly the risk of endothelial damage, are significant considerations for both combined and conventional CXL procedures.[34] Unfortunately, we could not assess the count and morphology of endothelial cells in the central cornea using specular microscopy. Despite these limitations, our study provides valuable insights into the effectiveness of tPTK+aCXL combined therapy for PLE.

Conclusion

Our long-term results demonstrate that tPTK+aCXL treatment (modified Cretan protocol) effectively and safely halts progressive PLE over 24 months. Additional prospective studies with larger cohorts and extended follow-up are essential to validate these results in this challenging ectatic condition.

Ethics

Ethics Committee Approval: Ankara City Hospital-No. 1 Clinical Research Ethics Committee (date: 23.06.2021, no: E1/1910/2021).

Informed Consent: Obtained.

Authorship Contributions

Surgical and Medical Practices: Ö.S., Concept: B.T., Ö.S., N.Ç., Design: B.T., Ö.S., N.Ç., Data Collection or Processing: B.Te., E.D.Ş., Analysis or Interpretation: Ö.S., B.Te., E.D.Ş., B.T., Literature Search: B.T., Ö.S., B.Te., Writing: B.T., Ö.S., B.Te., N.Ç.

Conflict of Interest: No conflict of interest was declared by the authors.

Financial Disclosure: The authors declared that this study received no financial support.

References

1. Richoz O, Mavrakanas N, Pajic B, Hafezi F. Corneal collagen cross-linking for ectasia after LASIK and photorefractive keratectomy: long-term results. Ophthalmology. 2013;120:1354-1359.
2. Binder PS. Ectasia after laser in situ keratomileusis. J Cataract Refract Surg. 2003;29:2419-2429.

3. Wollensak G, Spoerl E, Seiler T. Riboflavin/ultraviolet-a-induced collagen crosslinking for the treatment of keratoconus. Am J Ophthalmol. 2003;135:620-627.
4. Gatzioufas Z, Richoz O, Brugnoli E, Hafezi F. Safety profile of high-fluence corneal collagen cross-linking for progressive keratoconus: preliminary results from a prospective cohort study. J Refract Surg. 2013;29:846-848.
5. Tomita M, Mita M, Huseynova T. Accelerated versus conventional corneal collagen crosslinking. J Cataract Refract Surg. 2014;40:1013-1020.
6. Sarac O, Caglayan M, Uysal BS, Uzel AGT, Tanriverdi B, Cagil N. Accelerated versus standard corneal collagen cross-linking in pediatric keratoconus patients: 24 months follow-up results. Cont Lens Anterior Eye. 2018;41:442-447.
7. Kymionis GD, Grentzelos MA, Kankariya VP, Pallikaris IG. Combined transepithelial phototherapeutic keratectomy and corneal collagen crosslinking for ectatic disorders: cretan protocol. J Cataract Refract Surg. 2013;39:1939.
8. Kymionis GD, Grentzelos MA, Kounis GA, Diakonis VF, Limnopoulou AN, Panagopoulou SI. Combined transepithelial phototherapeutic keratectomy and corneal collagen cross-linking for progressive keratoconus. Ophthalmology. 2012;119:1777-1784.
9. Kymionis GD, Grentzelos MA, Kankariya VP, Liakopoulos DA, Karavitaki AE, Portaliou DM, Tsoulnaras KI, Pallikaris IG. Long-term results of combined transepithelial phototherapeutic keratectomy and corneal collagen crosslinking for keratoconus: Cretan protocol. J Cataract Refract Surg. 2014;40:1439-1445.
10. Cagil N, Sarac O, Yesilirmak N, Caglayan M, Uysal BS, Tanriverdi B. Transepithelial Phototherapeutic Keratectomy Followed by Corneal Collagen Crosslinking for the Treatment of Pellucid Marginal Degeneration: Long-term Results. Cornea. 2019;38:980-985.
11. Sarac O, Kosekahya P, Caglayan M, Tanriverdi B, Taslipinar Uzel AG, Cagil N. Mechanical versus transepithelial phototherapeutic keratectomy epithelial removal followed by accelerated corneal crosslinking for pediatric keratoconus: Long-term results. J Cataract Refract Surg. 2018;44:827-835.
12. Kanellopoulos AJ, Binder PS. Management of corneal ectasia after LASIK with combined, same-day, topography-guided partial transepithelial PRK and collagen cross-linking: the athens protocol. J Refract Surg. 2011;27:323-331.
13. Mafusire C, Krüger TP. Strehl ratio and amplitude-weighted generalized orthonormal Zernike-based polynomials. Appl Opt. 2017;56:2336-2345.
14. Uysal BS, Sarac O, Yaman D, Akcay E, Cagil N. Optical Performance of the Cornea One Year Following Keratoconus Treatment with Corneal Collagen Cross-Linking. Curr Eye Res. 2018;43:1415-1421.
15. Sandoval HP, Donnenfeld ED, Kohnen T, Lindstrom RL, Potvin R, Tremblay DM, Solomon KD. Modern laser in situ keratomileusis outcomes. J Cataract Refract Surg. 2016;42:1224-1234.
16. Seiler T, Koufala K, Richter G. Iatrogenic keratectasia after laser in situ keratomileusis. J Refract Surg. 1998;14:312-317.
17. Giri P, Azar DT. Risk profiles of ectasia after keratorefractive surgery. Curr Opin Ophthalmol. 2017;28:337-342.
18. Lifshitz T, Levy J, Klemperer I, Levinger S. Late bilateral keratectasia after LASIK in a low myopic patient. J Refract Surg. 2005;21:494-496.
19. Rao SN, Epstein RJ. Early onset ectasia following laser in situ keratomileusus: case report and literature review. J Refract Surg. 2002;18:177-184.
20. Kohlhaas M, Spoerl E, Speck A, Schilde T, Sandner D, Pillunat LE. Eine neue Behandlung der Keratektasie nach LASIK durch Kollagenvernetzung mit Riboflavin/UVA-Licht [A new treatment of keratectasia after LASIK by using collagen with riboflavin/UVA light cross-linking]. Klin Monbl Augenheilkd. 2005;222:430-436.
21. Yildirim A, Cakir H, Kara N, Uslu H, Gurler B, Ozgurhan EB, Colak HN. Corneal collagen crosslinking for ectasia after laser in situ keratomileusis: long-term results. J Cataract Refract Surg. 2014;40:1591-1596.
22. Kymionis GD, Grentzelos MA, Portaliou DM, Kankariya VP, Randleman JB. Corneal collagen cross-linking (CXL) combined with refractive procedures for the treatment of corneal ectatic disorders: CXL plus. J Refract Surg. 2014;30:566-576.
23. Zhou W, Wang H, Zhang X, Tian M, Cui C, Li X, Mu G. Management of Corneal Ectasia after LASIK with Phototherapeutic Keratectomy Combined with Photorefractive Keratectomy and Collagen Cross-Linking. J Ophthalmol. 2019;2019:2707826.
24. Shalchi Z, Wang X, Nanavaty MA. Safety and efficacy of epithelium removal and transepithelial corneal collagen crosslinking for keratoconus. Eye (Lond). 2015;29:15-29.
25. Kanellopoulos AJ. Comparison of sequential vs same-day simultaneous collagen cross-linking and topography-guided PRK for treatment of keratoconus. J Refract Surg. 2009;25:812-818.
26. Kapasi M, Dhaliwal A, Mintsioulis G, Jackson WB, Baig K. Long-Term Results of Phototherapeutic Keratectomy Versus Mechanical Epithelial Removal Followed by Corneal Collagen Cross-Linking for Keratoconus. Cornea. 2016;35:157-161.
27. Gaster RN, Ben Margines J, Gaster DN, Li X, Rabinowitz YS. Comparison of the Effect of Epithelial Removal by Transepithelial Phototherapeutic Keratectomy or Manual Debridement on Cross-linking Procedures for Progressive Keratoconus. J Refract Surg. 2016;32:699-704.
28. Cagil N, Sarac O, Cakmak HB, Can G, Can E. Mechanical epithelial removal followed by corneal collagen crosslinking in progressive keratoconus: short-term complications. J Cataract Refract Surg. 2015;41:1730-1737.
29. Deshmukh R, Reddy JC, Rapuano CJ, Vaddavalli PK. Phototherapeutic keratectomy: Indications, methods and decision making. Indian J Ophthalmol. 2020;68:2856-2866.
30. Toprak I, Yaylalı V, Yildirim C. Factors affecting outcomes of corneal collagen crosslinking treatment. Eye (Lond). 2014;28:41-46.
31. Abtahi MA, Beheshtnejad AH, Latifi G, Akbari-Kamrani M, Ghafarian S, Masoomi A, Sonbolastan SA, Jahanbani-Ardakani H, Atighechian M, Banan L, Nouri H, Abtahi SH. Corneal Epithelial Thickness Mapping: A Major Review. J Ophthalmol. 2024;2024:6674747.
32. Reinstein DZ, Archer TJ, Gobbe M, Rothman RC. Epithelial thickness changes following realignment of a malpositioned free cap. J Cataract Refract Surg. 2014;40:1237-1239.
33. Ozdas D, Yesilirmak N, Sarac O, Cagil N. 36-Month Outcomes of Mechanical and Transepithelial PTK Epithelium Removal Techniques Prior to Accelerated CXL for Progressive Keratoconus. J Refract Surg. 2022;38:191-200.
34. Zhu W, Han Y, Cui C, Xu W, Wang X, Dou X, Xu L, Xu Y, Mu G. Corneal Collagen Crosslinking Combined with Phototherapeutic Keratectomy and Photorefractive Keratectomy for Corneal Ectasia after Laser in situ Keratomileusis. Ophthalmic Res. 2018;59:135-141.
35. Gatzioufas Z, Balidis M, Kozeis N. Is the corneal stromal demarcation line depth a true indicator of corneal collagen crosslinking efficacy? J Cataract Refract Surg. 2016;42:804.

Original Article

Ocular Manifestations of Fabry Disease: Report from a Tertiary Eye Care Center in Türkiye

İlayda Korkmaz*, Sema Kalkan Uçar**, Hüseyin Onay***, Eser Yıldırım Sözmen****, Mahmut Çoker**, Melis Palamar*

*Ege University Faculty of Medicine, Department of Ophthalmology, İzmir, Türkiye
**Ege University Faculty of Medicine, Department of Pediatric Metabolism, İzmir, Türkiye
***Multigen Genetic Diseases Diagnosis Center, İzmir, Türkiye
****Ege University Faculty of Medicine, Department of Medical Biochemistry, İzmir, Türkiye

Abstract

Objectives: To report ocular manifestations in patients with Fabry disease (FD) from a tertiary eye care center in Türkiye.

Materials and Methods: This prospective, cross-sectional study included 30 eyes of 15 patients with FD. The diagnosis of FD was made based on a combination of clinical findings, genetic analysis, and biochemical evaluation. All participants underwent a detailed ophthalmic examination with special focus on the typical ocular features of FD (cornea verticillata, conjunctival aneurysms, cataract, retinal vessel tortuosity).

Results: The mean age was 45±17 years (range: 22-75 years), with a female/male ratio of 2:3. All patients had tortuous conjunctival vessels and 12 patients (80%) had conjunctival aneurysms. Cornea verticillata was present in 10 patients (66.6%), lens opacification in 4 patients (26.6%), and retinal vascular tortuosity in 8 patients (53.3%). All patients had at least two different ocular findings; most (3 heterozygotes/7 hemizygotes) had a combination of corneal verticillata and conjunctival vessel abnormality. The conjunctiva, cornea, and retina were affected together in 5 hemizygous patients (33.3%). One hemizygous patient had all FD-related ocular manifestations in both eyes.

Conclusion: To our knowledge, this study is the first to describe the ocular manifestations of FD in the Turkish population. Although cornea verticillata is considered a hallmark of FD, it was absent in approximately one-third of patients. Moreover, cataract, another well-known feature of FD, was present in only 26.6% of the patients. Conjunctival vascular abnormality alone seems to be quite rare in FD, although it often accompanies other ocular manifestations. Therefore, recognition of other mild findings and special consideration of their associations may increase the diagnostic value of ocular findings in FD.

Keywords: Cornea verticillata, conjunctival aneurysm, Fabry cataract, Fabry disease, metabolic diseases

Cite this article as: Korkmaz İ, Kalkan Uçar S, Onay H, Yıldırım Sözmen E, Çoker M, Palamar M. Ocular Manifestations of Fabry Disease: Report from a Tertiary Eye Care Center in Türkiye. Turk J Ophthalmol 2024;54:127-132

Address for Correspondence: Melis Palamar, Ege University Faculty of Medicine, Department of Ophthalmology, İzmir, Türkiye
E-mail: melispalamar@hotmail.com **ORCID-ID:** orcid.org/0000-0002-2494-0131
Received: 20.02.2024 **Accepted:** 29.05.2024

DOI: 10.4274/tjo.galenos.2024.09482

Introduction

Fabry disease (FD) is a rare X-linked lysosomal storage disorder with an estimated prevalence of 1/40,000-1/60,000 in males and 1/339,000 in females.[1] It is characterized by abnormal glycosphingolipid metabolism due to the absence or deficiency of the alpha-galactosidase A enzyme (α-Gal). Several mutations in the *α-Gal* gene (*GLA*) have been described in FD.[2,3] Affected males are defined as hemizygotes since they only have one disease-specific allele. As they usually have no detectable α-Gal enzyme activity, they exhibit the typical clinical picture of the disease more prominently. However, affected women are defined as heterozygotes. Unlike men, they show a wide spectrum of clinical manifestations, ranging from asymptomatic to advanced disease due to skewed X inactivation.[4,5]

Cardiopathy, neuropathy, and cerebrovascular diseases are the most serious clinical findings that increase morbidity and mortality in FD.[4,5] Although ophthalmologic involvement is also quite common in FD and is among the early manifestations of the disease, it is often overlooked. However, knowing the nature and frequency of ophthalmologic findings can be beneficial in the early and accurate diagnosis of FD.[6] Data on FD-associated ocular manifestations are limited in the literature, and available studies mostly involved patients from the USA, Canada, and European

countries.[7,8,9,10] Although there are some articles on FD in the Turkish population, to the best of our knowledge, there is no study specific to ophthalmologic involvement of the disease.[11,12] The aim of this study was to report the ophthalmological manifestations of patients with FD in a tertiary eye care center from Türkiye.

Materials and Methods

This prospective, cross-sectional study was carried out in accordance with the Declaration of Helsinki after approval by the Local Ethics Committee of Ege University (decision number: 24-1.1T/33, date: 25.01.2024). Informed consent was obtained from all participants.

Participants were recruited after referral from the Pediatric Metabolism and Nutrition Department and Medical Genetics Department of Ege University. All patients were diagnosed with FD and were referred to the Ege University Ophthalmology Department as a part of a comprehensive systemic examination. The diagnosis was made based on a combination of clinical findings, molecular genetic analysis, and biochemical evaluation.

A comprehensive case history of systemic findings and demographic data such as age and sex were recorded. All patients underwent a detailed ophthalmological evaluation, including anterior segment examination under slit lamp biomicroscopy, intraocular pressure measurement with Goldmann applanation tonometry, and fundus examination under pupil dilatation (after instillation of one drop of tropicamide 1% [Tropamid 1%, Bilim Pharmaceuticals, Türkiye]). Typical clinical features of FD such as cornea verticillata, conjunctival aneurysms, conjunctival vessel tortuosity, presence and type of lens opacification, and retinal vessel tortuosity were specifically analyzed. Best corrected visual acuities (BCVAs) were recorded as logarithm of the minimum angle of resolution (LogMAR). Tear film break-up time (TBUT) and Schirmer 1 tests were performed for the diagnosis of dry eye.

Patients with chronic systemic disease unrelated to FD (including connective tissue disorders, diabetes, etc.), who were receiving any topical or systemic treatments related to other diseases, and had a history of ocular trauma or concomitant ocular diseases were not included.

Statistical analysis

Statistical analysis was performed using IBM SPSS Statistics for Windows, Version 25.0 (IBM Corp., Armonk, NY, USA). Descriptive statistics were given as mean, standard deviation, median, minimum, maximum, number, and percentage.

Results

Thirty eyes of 15 patients with ocular manifestations associated with FD were included. The mean age was 45±17 years (range, 22-75 years), with a female to male ratio of 2:3 (Table 1).

Case histories revealed that 4 patients (26.6%) had a family history of FD. Four out of 6 heterozygote women were asymptomatic. The number and severity of systemic involvements of FD (cardiac, renal and neurological) were higher in the hemizygote men than in the women. In 9 patients (60%), α-Gal activity was found to be low in biochemical analysis, and genetic analysis strengthened the diagnosis. In the remaining 6 patients (40%), α-Gal activity was within normal limits and the diagnosis of FD was confirmed by the presence of *GLA* mutation in genetic analysis. One patient was already under enzyme replacement therapy (ERT) when he was examined for ophthalmological manifestations.

The mean BCVA was 0.03±0.06 LogMAR (range, 0-0.2 LogMAR).

Conjunctival vessel changes constituted the most frequent ophthalmological findings of FD. Increased tortuosity of the bulbar conjunctival vessels was bilaterally present in all patients. In addition, conjunctival saccular aneurysms were also evident in 24 eyes of 12 patients (80%) (Figure 1A).

Cornea verticillata was present in 20 eyes of 10 patients (66.6%) (Figure 2).

Lens opacification was observed in 4 (26.6%) of the 15 patients. The median age of patients with lens opacification was 38.5 years (mean, 40.2; standard deviation, 16.4; range, 22-62 years). One of them had bilateral "spoke-like" cataract located at the level of the posterior lens capsule, consistent with the typical "Fabry cataract" (Figure 1B). The patient's visual acuity was affected bilaterally (right: 0.20; left: 0.10 LogMAR). One patient had bilateral sectoral, wedge-shaped, white cataract at the level of the anterior subcapsular area, with non-affected visual acuity (0.00 LogMAR in both eyes). Two patients had blue-dot (cerulean) cataract. One had bilateral symmetrical opacifications at the lens periphery, and visual acuities were not affected (0.00 LogMAR in both eyes). The other patient had a BCVA of 0.20 LogMAR in the eye with cataract, and the fellow eye was pseudophakic (operated elsewhere) at 39 years of age. There was no significant difference in terms of age between patients with and without cataracts ($p>0.05$).

Vascular tortuosity was the most common retinal finding, present in 8 (53.3%) out of 15 patients. These changes were bilateral and symmetrical in all patients (Figure 3).

All patients had at least two different ocular findings of FD; 66.6% (3 heterozygous females and 7 hemizygous males) had a combination of corneal verticillata and conjunctival vessel abnormality. Conjunctiva, cornea and retina were affected together in 5 patients (33.3%), and all were hemizygous males. All Fabry-related ocular findings, including cornea verticillata, conjunctival vessel abnormalities, cataract, and retinal vascular tortuosity were bilaterally present in only 1 hemizygous male patient.

The mean TBUT was 8±3 s (range, 4-10 s). The mean Schirmer 1 result was 26.3±5.4 mm (range, 19-30 mm). Bilateral dry eye was present in one patient. Preservative-free artificial tear drops (Eyestil SD, Sifi, Italy) were initiated.

Discussion

FD is an extremely rare, inherited lysosomal storage disorder that affects numerous organs. The main life-threatening manifestations are cardiopathy, neuropathy, and cerebrovascular diseases.[13,14] Although ophthalmologic involvement in FD is not negligible, it is often underestimated because it is characterized by mild visual symptoms and signs. Therefore, data on FD-related ophthalmologic manifestations are quite limited,

Table 1. Characteristics of the patients

Patient number	Age at diagnosis (years)	Male (M)/ female (F)	Cornea verticillata	Conjunctival tortuosity	Saccular conjunctival dilatations	Cataract	Retinal tortuosity	Mutation	ACMG classification
P1	25	M	+	+	+	-	+	p.P112L (c.335G>T)	Likely pathogenic
P2	75	M	+	+	+	-	+	p.P112L (c.335G>T)	Likely pathogenic
P3	52	M	+	+	+	-	-	p.G328V (c.983 G>T)	Pathogenic
P4	28	M	+	+	+	-	+	p.R342X (c.1024C>T)	Pathogenic
P5	22	F	+	+	+	+	-	c.963_964delinsCA (p.Q321_D322_delins HN)	Variant of unknown significance
P6	38	M	+	+	+	+	+	c.719_720insA (p.S241EfsX9)	Likely pathogenic
P7	62	F	-	+	+	+	-	p.A143T (c.427G>A)*	Likely pathogenic
P8	44	M	-	+	+	-	-	p.A143T (c.427G>A)*	Likely pathogenic
P9	54	M	+	+	+	-	-	p.Y216C (c.647A>G)	Pathogenic
P10	34	M	+	+	+	-	+	p.R227X (c.679C>T)	Pathogenic
P11	39	F	-	+	+	+	+	p.R118C (c.352C>T)	Likely pathogenic
P12	74	F	+	+	-	-	-	p.Y216C (c.647A>G)	Pathogenic
P13	38	F	-	+	-	-	-	p.A143T (c.427G>A)*	Likely pathogenic
P14	62	F	+	+	+	-	+	p.R227X (c.679C>T)	Pathogenic
P15	31	M	-	+	-	-	+	p.A143T (c.427G>A)*	Likely pathogenic

*At the time of diagnosis of the patients this variant was accepted to be a disease causing variant but in the recent classifications this variant is accepted as a "benign" variant (PMID: 37937776).
ACMG: American College of Medical Genetics and Genomics

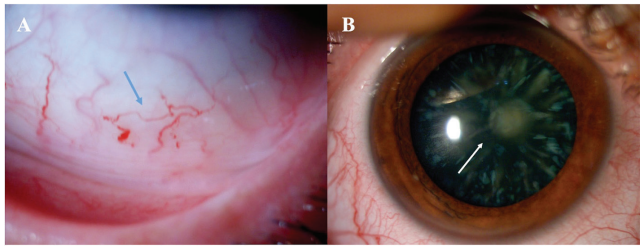

Figure 1. Representative photographs of ocular manifestations in Fabry patients. (A) Blue arrow indicates conjunctival vascular tortuosity and aneurysmal dilatations, (B) white arrow indicates Fabry cataract

and the available studies in the literature are mostly from the USA, Canada, and Europe.[7,8,9,10]

Ethnicity is a significant modifier in hereditary diseases and can strongly influence the characteristics of the disease. Therefore, studies with FD patients originating from different countries do not always reflect the entire population.[9,15] Comprehensive studies on FD from Türkiye are mostly in the fields of cardiology, nephrology, and neurology, and data on ophthalmologic involvement is very limited.[11,12,16,17] İnan et al.[17] evaluated peripheral nervous system involvement in 14 patients with FD and reported that half of the patients had additional ophthalmological findings, including cornea verticillata (2 patients) and retinal vascular tortuosity (2 patients). In a recent consensus statement, Ezgu et al.[18] conveyed Türkiye's multidisciplinary perspective on FD. Although they mentioned

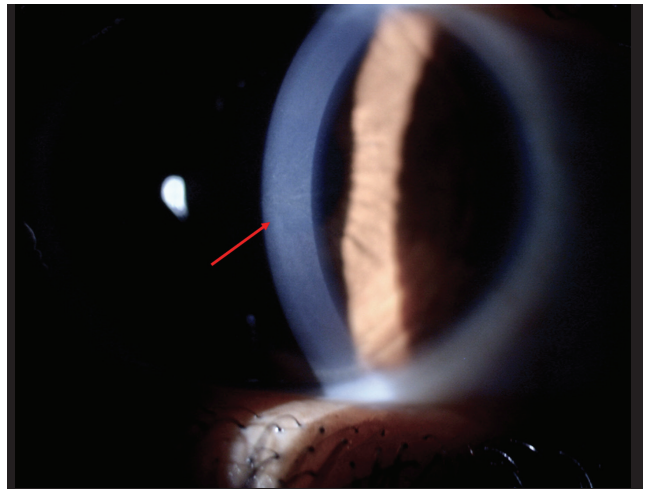

Figure 2. Cornea verticillata in a patient with Fabry disease. Red arrow indicates whorl-like gray opacities irradiating from the central cornea

the characteristic features of ophthalmologic involvement in their review, they did not make a population-based assessment of its prevalence.[18] Moreover, ophthalmological studies of FD in the Turkish population have mostly focused on microvascular signs of ocular involvement before visible symptoms appear.[19,20,21,22] In summary, although there are various studies on FD among the Turkish population, there is a lack of detailed and specific data on the nature and frequency of ophthalmologic findings of FD.

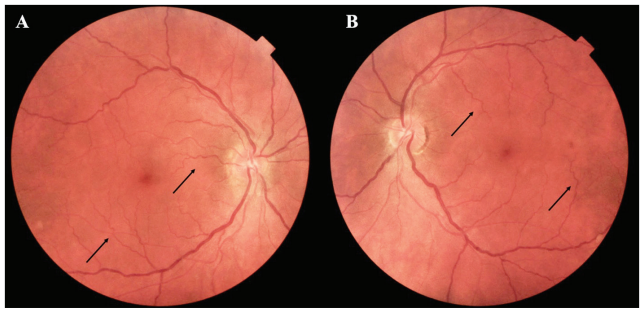

Figure 3. (A) Right and (B) left eye of a patient with Fabry disease. Black arrows show increased retinal vascular tortuosity, which is more evident at the posterior pole

To the best of our knowledge, this study is the first to specifically describe the nature and frequency of ocular manifestations of FD in the Turkish population.

The diagnosis of FD is challenging and often delayed, especially in cases without a clear family history. Fuller et al.[23] reported that the diagnosis of FD was made years after symptom onset (approximately 16 years in women and 14 years in men). In the natural course of FD, accumulation of undegraded glycosphingolipids causes progressive cell damage and eventual failure of organs such as the kidneys, heart, and the central and peripheral nervous systems. Therefore, delay in diagnosis is associated with further damage to the affected organs and causes an increased risk of morbidity and mortality.[24] Moreover, FD is one of the rare genetic lysosomal storage diseases with a medical treatment option. The widespread use of ERT, a major breakthrough in its treatment, has reinforced the importance of early detection of FD.[25,26,27] A high index of suspicion for FD is essential for timely recognition, but whole-population screening is not very cost-effective as it is an incredibly rare clinical condition.[28,29]

The presence of ophthalmological findings gains importance here by providing important clues to the clinician. Ocular manifestations are one of the first observable findings of FD, and slit-lamp examination alone is often sufficient to identify the findings. Therefore, it is critical for an ophthalmologist to know the nature, frequency, and possible consequences of ocular manifestations of FD.[6,30] Typical ophthalmologic features are conjunctival vascular abnormalities (vascular aneurysms and tortuosity), cornea verticillata, cataract, retinal vessel tortuosity, and rarely retinal vascular occlusion.[31,32,33,34] The incidence of each is reported at varying rates in studies conducted in different regions.[8,9,10,35] Nguyen et al.[7] reported from Australia that bulbar conjunctival vascular abnormality (97.1% in hemizygotes and 78.1% in heterozygotes) is the most common ophthalmologic manifestation in patients with FD, followed by cornea verticillata (94.1% in hemizygotes, 71.9% in heterozygotes) and retinal vascular tortuosity (76.5% in hemizygotes, 18.8% in heterozygotes).[7] Similarly, in a longitudinal study conducted in Canada, the most common ocular findings were reported as conjunctival vascular tortuosity (85.7%) and cornea verticillata (89.2%).[8] Consistent with the literature, in the present study, conjunctival vascular tortuosity (100%) and aneurysmal dilatations (80%) were the most frequent ocular signs of FD, followed by cornea verticillata (66.6%).

Cornea verticillata is considered to be the hallmark of FD and is a well-known manifestation of the disease. It is characterized by whorl-like opacities concentrated in the epithelial and subepithelial layers of the cornea and is typically bilateral.[32,36] Although cornea verticillata is highly suggestive of FD, it may also occur secondary to pharmacological (e.g., amiodarone, chloroquine, hydroxychloroquine) and non-pharmacological (e.g., multiple myeloma) etiologies.[37] In the literature, cornea verticillata has been reported at a frequency ranging from 43.7% to 94.5% in patients with FD.[8,9] This diversity may be related to the age, genotypes, and ethnicities of the patients, as well as to the subjectivity of the clinician's assessment. In the present study, approximately one-third of the patients did not have cornea verticillata. However, conjunctival vascular abnormalities were detected in a significant proportion of the patients. Although cornea verticillata is considered to be the most distinctive ophthalmologic finding of FD, it may not be present in every patient. Therefore, it is important to recognize other mild and easily overlooked findings of FD in addition to already well-known classical findings.

Cataract is another classical manifestation of FD which, unlike other findings, causes symptoms such as decreased vision and dysphotopsia. Theoretically, subcapsular lens opacification with a spoke-like appearance at the posterior capsule is defined as typical "Fabry cataract". In addition, cataract may present as a wedge-shaped white deposit at the anterior subcapsular level in FD.[7,8] However, the incidence of cataract is lower compared to other ophthalmological features.[9] In a multicenter study conducted across Europe, Fabry cataracts were reported in 9.8% of heterozygotes and 23.1% of hemizygotes.[9] Higher rates of cataract were reported from Canada (67.7%) and Australia (62.4%), although still relatively low compared to other ophthalmologic manifestations.[7,8] In the current study, the least common ophthalmologic manifestation was cataract, with a rate of 26.6%. The lower rate of cataract in this study can be explained by the sex distribution, as 40% of patients were female heterozygotes. Because FD is an X-linked inherited disease, sex disparity strongly affects the disease characteristics. As a general rule, FD symptoms are more pronounced in men due to the greater disease severity.[14,31] This sex difference may be more decisive and striking in cataract, which has a lower incidence compared to other ocular findings of FD.

Different ocular structures can be affected in FD. Therefore, the coexistence of multiple ophthalmologic findings is not uncommon. In fact, conjunctival vascular tortuosity rarely occurs in isolation in FD and is usually associated with other ocular findings.[9] Sodi et al.[9] reported local associations of tortuous vessels with cornea verticillata or cataract in FD. This coexistence seems to be more prominent in males. Consistent with this, all participants in the current study had at least two detectable ocular findings, most of which were a combination of corneal verticillata and conjunctival vessel abnormalities. In addition,

the coexistence of three or more clinical features was observed in 33.3% of the patients and all of them were male. This supports that sex differences also affect the number of ophthalmological areas affected. In parallel with other systemic involvements, typical ophthalmological manifestations of FD can be seen more frequently and more prominently in men.

Dry eye syndrome (DES) is a multifactorial disease that accompanies a significant proportion of systemic diseases. It has been suggested that the accumulation of abnormal deposits in the autonomic ganglia and lacrimal glands may lead to diminished lacrimal gland function.[31,38] Consequently, it has been hypothesized that the frequency of DES increases in FD due to decreased tear secretion.[30,31] Davey[30] reported in a visual symptom survey analysis that FD patients had significantly more "dryness" symptoms compared to healthy individuals. Moreover, Bitirgen et al.[20] showed corneal nerve fiber damage, reduced corneal sensitivity, and increased dendritic cells in patients with FD using in vivo confocal microscopy. Although all these data support an association between dry eye and FD, the nature of their relationship remains controversial. In the present study, DES was present in only one patient, who was misdiagnosed as having a rheumatologic disease. Further studies are still needed to reach a clear conclusion about DES in FD.

Study Limitations

The main limitations of this study are the small number of subjects included and the subjective evaluation of the findings. Measurable, precise parameters are not available yet, so potential interobserver differences in the evaluation of FD-related ocular findings are inevitable. Further studies with a population-based, multicenter design and more participants are still needed to clearly define the ophthalmological features of FD. In addition, this study presents the ophthalmological clinical picture in a single time frame, immediately after the diagnosis of FD. However, a longitudinal study to see whether the ocular findings change over time will be more valuable.

Conclusion

In conclusion, slit-lamp examination alone is usually sufficient to identify the ocular findings and guide the diagnosis of FD, especially when there is clinical suspicion. Awareness among ophthalmologists about the nature and frequency of FD-related findings may be helpful in early and accurate diagnosis. Ethnicity is the major modifier in hereditary diseases, and FD-related ophthalmologic manifestations may vary in populations originating from different regions. To the best of our knowledge, there is no previous report of ophthalmologic involvement of FD in the Turkish population. Although cornea verticillata is considered to be the most distinctive and prevalent ophthalmologic manifestation of FD, approximately one-third of the patients did not have corneal verticillata in the present study. Furthermore, cataract, another well-known feature of FD, was present in only 26.6% of the patients. Therefore, in addition to well-known specific findings, recognition of other mild findings and special consideration of their local associations may increase the diagnostic value of ocular manifestations in FD.

Ethics

Ethics Committee Approval: Approval by the Local Ethics Committee of Ege University (decision number: 24-1.1T/33, date: 25.01.2024).

Informed Consent: Obtained.

Authorship Contributions

Surgical and Medical Practices: S.K.U., H.O., E.Y.S., M.Ç., M.P., Concept: M.P., H.O., Design: İ.K., M.P., H.O., Data Collection or Processing: İ.K., S.K.U., E.Y.S., Analysis or Interpretation: H.O., M.Ç., M.P., Literature Search: İ.K., M.P., Writing: İ.K., M.P., H.O.

Conflict of Interest: No conflict of interest was declared by the authors.

Financial Disclosure: The authors declared that this study received no financial support.

References

1. MacDermot KD, Holmes A, Miners AH. Anderson-Fabry disease: clinical manifestations and impact of disease in a cohort of 60 obligate carrier females. J Med Genet. 2001;38:769-775.
2. Germain DP. Fabry disease: recent advances in enzyme replacement therapy. Expert Opin Investig Drugs. 2002;11:1467-1476.
3. Zarate YA, Hopkin RJ. Fabry's disease. Lancet. 2008;372:1427-1435.
4. Bernardes TP, Foresto RD, Kirsztajn GM. Fabry disease: genetics, pathology, and treatment. Rev Assoc Med Bras (1992). 2020;66 (Suppl 1):s10-s16.
5. Schiffmann R, Fuller M, Clarke LA, Aerts JM. Is it Fabry disease? Genet Med. 2016;18:1181-1185.
6. Samiy N. Ocular features of Fabry disease: diagnosis of a treatable life-threatening disorder. Surv Ophthalmol. 2008;53:416-423.
7. Nguyen TT, Gin T, Nicholls K, Low M, Galanos J, Crawford A. Ophthalmological manifestations of Fabry disease: a survey of patients at the Royal Melbourne Fabry Disease Treatment Centre. Clin Exp Ophthalmol. 2005;33:164-168.
8. Michaud L. Longitudinal study on ocular manifestations in a cohort of patients with Fabry disease. PLoS One. 2019;14:e0213329.
9. Sodi A, Ioannidis AS, Mehta A, Davey C, Beck M, Pitz S. Ocular manifestations of Fabry's disease: data from the Fabry Outcome Survey. Br J Ophthalmol. 2007;91:210-214.
10. Orssaud C, Dufier J, Germain D. Ocular manifestations in Fabry disease: a survey of 32 hemizygous male patients. Ophthalmic Genet. 2003;24:129-139.
11. Barman HA, İkitimur B, Kılıçkıran Avcı B, Durmaz E, Atıcı A, Aslan S, Ceylaner S, Karpuz H. The Prevalence of Fabry Disease Among Turkish Patients with Non-Obstructive Hypertrophic Cardiomyopathy: Insights from a Screening Study. Balkan Med J. 2019;36:354-358.
12. Tomar ÖK, Bal AZ, Şirali SK, Duranay M, Korucu B, Güz G, Akdağ Sİ. The prevalence of Fabry disease in a Turkish population with chronic kidney patients. Int Urol Nephrol. 2023;55:1629-1634.
13. Gibas AL, Klatt R, Johnson J, Clarke JT, Katz J. Disease rarity, carrier status, and gender: a triple disadvantage for women with Fabry disease. J Genet Couns. 2008;17:528-537.
14. Mehta A, Ricci R, Widmer U, Dehout F, Garcia de Lorenzo A, Kampmann C, Linhart A, Sunder-Plassmann G, Ries M, Beck M. Fabry disease defined: baseline clinical manifestations of 366 patients in the Fabry Outcome Survey. Eur J Clin Invest. 2004;34:236-242.
15. Pitz S, Kalkum G, Arash L, Karabul N, Sodi A, Larroque S, Beck M, Gal A. Ocular signs correlate well with disease severity and genotype in Fabry disease. PLoS One. 2015;10:e0120814.
16. Erol Ç. Artificial Intelligence, Fabry Disease…. Anatol J Cardiol. 2023;27:178.
17. İnan R, Meşe M, Bicik Z. Multidisciplinary approach to Fabry disease: from the eye of a neurologist. Acta Neurol Belg. 2020;120:1333-1339.

18. Ezgu F, Alpsoy E, Bicik Bahcebasi Z, Kasapcopur O, Palamar M, Onay H, Ozdemir BH, Topcuoglu MA, Tufekcioglu O. Expert opinion on the recognition, diagnosis and management of children and adults with Fabry disease: a multidisciplinary Turkey perspective. Orphanet J Rare Dis. 2022;17:90.
19. Cakmak AI, Atalay E, Cankurtaran V, Yaşar E, Turgut FH. Optical coherence tomography angiography analysis of fabry disease. Int Ophthalmol. 2020;40:3023-3032.
20. Bitirgen G, Turkmen K, Malik RA, Ozkagnici A, Zengin N. Corneal confocal microscopy detects corneal nerve damage and increased dendritic cells in Fabry disease. Sci Rep. 2018;8:12244.
21. Yanık Ö, Çıkı K, Özmert E, Sivri S. Vascular and structural analyses of retinal and choroidal alterations in Fabry disease: the effect of hyperreflective foci and retinal vascular tortuosity. Ophthalmic Genet. 2022;43:344-353.
22. Cankurtaran V, Tekin K, Cakmak AI, Inanc M, Turgut FH. Assessment of corneal topographic, tomographic, densitometric, and biomechanical properties of Fabry patients with ocular manifestations. Graefes Arch Clin Exp Ophthalmol. 2020;258:1057-1064.
23. Fuller M, Meikle PJ, Hopwood JJ. Epidemiology of lysosomal storage diseases: an overview. In: Mehta A, Beck M, Sunder-Plassmann G, editors. Fabry Disease: Perspectives from 5 Years of FOS. Oxford: Oxford PharmaGenesis; 2006.
24. Aerts JM, Groener JE, Kuiper S, Donker-Koopman WE, Strijland A, Ottenhoff R, van Roomen C, Mirzaian M, Wijburg FA, Linthorst GE, Vedder AC, Rombach SM, Cox-Brinkman J, Somerharju P, Boot RG, Hollak CE, Brady RO, Poorthuis BJ. Elevated globotriaosylsphingosine is a hallmark of Fabry disease. Proc Natl Acad Sci U S A. 2008;105:2812-2817.
25. El Dib R, Gomaa H, Carvalho RP, Camargo SE, Bazan R, Barretti P, Barreto FC. Enzyme replacement therapy for Anderson-Fabry disease. Cochrane Database Syst Rev. 2016;7:CD006663.
26. Schiffmann R, Kopp JB, Austin HA 3rd, Sabnis S, Moore DF, Weibel T, Balow JE, Brady RO. Enzyme replacement therapy in Fabry disease: a randomized controlled trial. JAMA. 2001;285:2743-2749.
27. Turkmen K, Baloglu I. Fabry disease: where are we now? Int Urol Nephrol. 2020;52:2113-2122.
28. Linthorst GE, Bouwman MG, Wijburg FA, Aerts JM, Poorthuis BJ, Hollak CE. Screening for Fabry disease in high-risk populations: a systematic review. J Med Genet. 2010;47:217-222.
29. van der Tol L, Smid BE, Poorthuis BJ, Biegstraaten M, Deprez RH, Linthorst GE, Hollak CE. A systematic review on screening for Fabry disease: prevalence of individuals with genetic variants of unknown significance. J Med Genet. 2014;51:1-9.
30. Davey PG. Fabry disease: a survey of visual and ocular symptoms. Clin Ophthalmol. 2014;8:1555-1560.
31. Sivley MD. Fabry disease: a review of ophthalmic and systemic manifestations. Optom Vis Sci. 2013;90:e63-78.
32. Degirmenci C, Yilmaz SG, Onay H, Palamar M, Ucar SK, Kayikcioglu M, Coker M. A novel mutation and in vivo confocal microscopic findings in Fabry disease. Saudi J Ophthalmol. 2017;31:45-47.
33. Oto S, Kart H, Kadayifçilar S, Ozdemir N, Aydin P. Retinal vein occlusion in a woman with heterozygous Fabry's disease. Eur J Ophthalmol. 1998;8:265-267.
34. Ersoz MG, Ture G. Cilioretinal artery occlusion and anterior ischemic optic neuropathy as the initial presentation in a child female carrier of Fabry disease. Int Ophthalmol. 2018;38:771-773.
35. Nguyen ATM, Chamberlain K, Holland AJA. Paediatric chemical burns: a clinical review. Eur J Pediatr. 2021;180:1359-1369.
36. van der Tol L, Sminia ML, Hollak CE, Biegstraaten M. Cornea verticillata supports a diagnosis of Fabry disease in non-classical phenotypes: results from the Dutch cohort and a systematic review. Br J Ophthalmol. 2016;100:3-8.
37. Sahyoun JY, Sabeti S, Robert MC. Drug-induced corneal deposits: an up-to-date review. BMJ Open Ophthalmol. 2022;7:e000943.
38. Cable WJ, Kolodny EH, Adams RD. Fabry disease: impaired autonomic function. Neurology. 1982;32:498-502.

Original Article

The Effect of Conjunctiva-Müller Muscle Resection on Tear Oxidative Stress Levels in Patients with Blepharoptosis

Seda Sert*, Ceyhun Arıcı**, Burak Mergen***, Özlem Balcı Ekmekçi****

*Gümüşhane State Hospital, Clinic of Ophthalmology, Gümüşhane, Türkiye
**İstanbul University-Cerrahpaşa, Cerrahpaşa Faculty of Medicine, Department of Ophthalmology, İstanbul, Türkiye
***University of Health Sciences Türkiye, Başakşehir Çam and Sakura City Hospital, Clinic of Ophthalmology, İstanbul, Türkiye
****İstanbul University-Cerrahpaşa, Cerrahpaşa Faculty of Medicine, Department of Biochemistry, İstanbul, Türkiye

Abstract

Objectives: To examine changes in tear oxidative stress levels and tear film functions in patients with blepharoptosis and dermatochalasis following conjunctiva-Müller muscle resection (CMMR) and blepharoplasty surgeries.

Materials and Methods: This prospective study included 32 healthy controls and 62 patients with blepharoptosis or dermatochalasis. CMMR surgery was performed in 20 eyes and upper blepharoplasty was performed in 42 eyes. Tear oxidative stress markers (8-hydroxy-2'-deoxyguanosine [8-OHdG] and 4-hydroxy-2-nonenal [4-HNE]) were quantified by enzyme-linked immunosorbent assay and tear film functions were evaluated preoperatively and at 1 and 6 months postoperatively. The same assessments were performed in the control group at the same time points.

Results: Preoperative tear 8-OHdG and 4-HNE levels were lower in healthy controls (52.8±13.5 ng/mL and 27.8±6.4 ng/mL, respectively) compared to patients with dermatochalasis (86.1±37.2 ng/mL and 29.8±11.1 ng/mL, respectively) and blepharoptosis (90.4±39.3 ng/mL and 43.1±4.2 ng/mL, respectively) ($p<0.001$). 8-OHdG levels were increased at 1 month after CMMR, while both markers were decreased 1 month postoperatively in the blepharoplasty group ($p=0.034$). Schirmer 1 and OSDI scores did not change throughout the visits in both patient groups, but a temporary decrease in tear break-up time (TBUT) was observed after CMMR ($p=0.017$).

Conclusion: Dermatochalasis and blepharoptosis were associated with higher tear oxidative stress levels. CMMR surgery caused a temporary decrease in TBUT scores and an increase in oxidative stress in the first postoperative month.

Keywords: Blepharoptosis, blepharoplasty, dermatochalasis, oxidative stress, tear film

Cite this article as: Sert S, Arıcı C, Mergen B, Balcı Ekmekçi Ö. The Effect of Conjunctiva-Müller Muscle Resection on Tear Oxidative Stress Levels in Patients with Blepharoptosis. Turk J Ophthalmol 2024;54:133-139

Address for Correspondence: Seda Sert, Gümüşhane State Hospital, Clinic of Ophthalmology, Gümüşhane, Türkiye
E-mail: drsedasert@gmail.com **ORCID-ID:** orcid.org/0000-0003-0176-227X
Received: 15.01.2024 **Accepted:** 30.03.2024

DOI: 10.4274/tjo.galenos.2024.02697

Introduction

Dermatochalasis is the loss of elasticity in the eyelid skin and the formation of excess skin folds due to aging.[1] Blepharoptosis is an abnormally low positioning of the upper eyelid due to various etiologies.[2]

Conjunctiva-Müller muscle resection (CMMR) is a surgery performed for acquired moderate ptosis that responds positively to the phenylephrine test, and it works by strengthening the Müller muscle.[3,4,5,6,7] Upper blepharoplasty is a surgery performed to treat dermatochalasis associated with age-related loss of skin elasticity in the upper eyelid and the development of excessive skin folds.[1]

8-hydroxy-2'-deoxyguanosine (8-OHdG) and 4-hydroxy-2-nonenal (4-HNE) are byproducts of DNA oxidation and lipid peroxidation, respectively, and are used as biomarkers to evaluate oxidative damage to the ocular surface.[8,9,10]

A study in the literature found that dermatochalasis causes dry eye related to meibomian gland dysfunction.[11] Oxidative stress is one of the factors involved in the dry eye mechanism.[12] The relationship between tear oxidative stress values and tear film function has been examined in previous studies.[10,12,13,14] The effects of CMMR and blepharoplasty surgeries on the tear film have also been examined previously.[7,15,16,17,18,19,20,21,22,23,24,25,26] Our study examines tear film functions and levels of oxidative stress in the tear film in patients with blepharoptosis and dermatochalasis and the effects of CMMR and blepharoplasty surgeries on these levels.

Materials and Methods

Participants

This prospective study included 20 patients with blepharoptosis who underwent CMMR surgery and 42 patients with dermatochalasis who underwent blepharoplasty in the Oculoplastic Surgery Clinic of the İstanbul University-Cerrahpaşa, Cerrahpaşa Faculty of Medicine from May 2018 to March 2020. The control group consisted of 32 healthy individuals matched for age and gender. The İstanbul University-Cerrahpaşa, Cerrahpaşa Faculty of Medicine Ethics Committee approved the study (approval number: 83045809-604.01.02, date: 07.08.2018). All patients and controls provided written informed consent.

The operated eye in unilateral surgeries and one random eye in bilateral surgeries were included.

The blepharoplasty group comprised individuals with dermatochalasis but with a margin reflex distance-1 (MRD-1) of 3 mm or greater. The CMMR group consisted of patients with MRD-1 less than 3 mm, levator function greater than 10 mm, and a positive 2.5% phenylephrine test. For this test, MRD-1 was measured preoperatively, before and 5 minutes after instilling 2.5% phenylephrine into the superior fornix. A change in MRD-1 greater than 1.5 mm was accepted as a positive result. The control group included healthy participants who did not meet any of the exclusion criteria and were similar in age and gender distribution to both of the two patient groups. The exclusion criteria for all groups were as follows: (1) having dry eye, (2) smoking and alcohol consumption, (3) a history of ocular or systemic disease and topical or systemic medication that may lead to dry eye, (4) contact lens use, and (5) any eye surgery or trauma.

Surgical Interventions

All surgeries were performed by one of the authors (C.A.).

Blepharoplasty

Marking was done with dye according to the "skin pinch" technique. The skin incisions were made and the excrescent skin tissue was removed, preserving the preseptal orbicularis muscle. The eyelid skin was sutured using 6/0 propylene.

CMMR

A 4-0 silk suture was passed along the upper eyelid edge to provide traction. A retractor was utilized to flip the upper eyelid inside out to expose the conjunctiva and upper portion of the upper tarsal plate. The distance planned to be resected was measured. The retractor was displaced. The Müller muscle and the conjunctiva were clamped simultaneously. Continuous suturing was performed from the lateral side to the medial side using 6-0 propylene. The Müller muscle and conjunctiva were excised at the same time. The suture was tied on the eyelid skin with a few throws.

Visit Schedule

The examination done before the surgery was regarded as day 0. Follow-up evaluations were performed at 1 and 6 months after surgery.

Clinical Assessments

Tear specimens were collected from the participants at each visit to quantify tear 8-OHdG and 4-HNE values. Schirmer 1 test was performed without using anesthetic drops. Schirmer tear test strips (35x5 mm; Liposic-Schirmer-Test-Streifen; Dr. Mann Pharma, Berlin, Germany) were placed in the outer third of the inferior fornix and the wetted distance was recorded after 5 minutes. For the tear break-up time (TBUT) test, 5 µL of unpreserved 2% sodium fluorescein was dropped into the inferior fornix. The biomicroscopic examination was performed under a cobalt blue filter. The seconds from the last blink to the occurrence of the first break in the dye were recorded. The influence of dry eye complaints on vision was evaluated subjectively using the Ocular Surface Disease Index (OSDI) questionnaire.

The same interventions were performed at the same time points in the control group.

Tear Collection and Quantification of 8-OHdG and 4-HNE

Tear specimens were collected according to the previously described eye wash method.[27] With the help of an Eppendorf pipette, 60 µL of unpreserved saline was dropped into the lower cul-de-sac with special care not to irritate the ocular surface. Then the subjects were told to close their eyes without squeezing and to rotate them twice. Samples were collected by microcapillary tube within 1 minute at the latest to prevent reflex tearing. Tear specimens were placed in 1-mL Eppendorf microtubes and stored at -80 °C until analysis. Levels of 8-OHdG and 4-HNE were quantified using commercially available 8-OHdG and 4-HNE enzyme-linked absorbent assays (ELISA; Bioassay Technology Laboratory) and following the manufacturer's recommendations. The concentration of the markers was quantified by comparing their absorption with known standard curves. The lowest measurable levels of 8-OHdG and 4-HNE were 0.5 ng/mL and 10 ng/L, respectively.

Statistical Analysis

The findings were analyzed using SPSS version 20.0 (IBM Corp., Armonk, NY, USA). The sample size was determined based on the following parameters using the G-Power software: type of analysis: ANOVA, significance level (α): 0.05, desired statistical power: 0.80, number of groups: 3, effect type: f, and effect size: 0.4. After conducting the power analysis, it was found that a sample size of 51 would yield a statistical test power of 0.803. More than 17 patients were included in each group to meet the desired level of power. Values were shown as mean ± standard deviation. The Shapiro-Wilk test was utilized to analyze the distribution of data. The chi-square test was utilized to compare frequencies. Mann-Whitney U test was utilized to compare the values of two independent groups. Friedman test was utilized in the analysis of repeated measures. For post-hoc comparison of groups with significant differences, the p value was determined by performing the Wilcoxon test with Bonferroni correction. Comparisons of three independent groups were made using Kruskal-Wallis test followed by post-

hoc Mann-Whitney U test with Bonferroni correction. Spearman correlation coefficients were determined to analyze correlations between variables. P values <0.05 were considered statistically significant.

Results

Characteristics of the Participants

Table 1 presents the demographic characteristics of the patients and controls included in the study. All of the groups were homogenous in terms of age (p=0.52) and gender (p=0.62).

The mean MRD-1 was significantly increased at 1 month after CMMR (1.6±0.5 mm vs. 3.5±0.7 mm, p<0.001) and remained high at 6 months (3.4±0.7 mm, p=1.0).

Tear Function Test Results and Changes Between Visits

Table 2 shows the differences in Schirmer, TBUT, and OSDI scores between visits in the three groups and Table 3 shows the results of post-hoc pairwise comparisons. In the preoperative period, there was no difference among the three groups in terms of Schirmer test and TBUT scores (p=0.874 and p=0.535, respectively), but OSDI scores were lower in the control group compared to the blepharoplasty group (p=0.033).

In the analysis of repeated measures, the three groups showed no significant difference at postoperative 1 and 6 months compared to baseline values in terms of Schirmer test (p=0.779, p=0.248, and p=0.08, respectively) or OSDI scores (p=0.502, p=0.573, and p=0.793, respectively). While TBUT scores did not change in the control and blepharoplasty groups, in the CMMR group they decreased between the baseline visit and 1 month (p=0.017) and increased again between 1 and 6 months (p=0.001).

Changes in Tear Oxidative Stress Levels Between Visits

The tear 8-OHdG and 4-HNE values measured preoperatively in the three groups are presented in Figure 1 and changes in these values between visits are presented in Figure 2 and Figure 3, respectively.

Table 1. Demographic characteristics of controls and patients

		Controls	Blepharoplasty	Conjunctiva-Müller muscle resection
Age (years)		53.0±6.9	55.0±7.2	52.4±15.4
Range		33-64	40-71	24-76
Gender	**Female**	19 (59.3%)	23 (54.7%)	14 (70.0%)
	Male	13 (40.7%)	19 (45.3%)	6 (30.0%)
Total		32	42	20

Table 2. Comparison of the three groups using Kruskal-Wallis test

		Control (n=32)			Blepharoplasty (n=42)			CMMR (n=20)			p
		Mean	**SD**	**Range**	**Mean**	**SD**	**Range**	**Mean**	**SD**	**Range**	
Age		53.0	6.9	33-64	55.0	7.2	40-71	52.4	15.4	24-76	0.628
Schirmer (mm)	**Baseline**	14.6	4.5	7-23	14.3	5.1	7-27	14.4	4.4	7-22	0.874
	1 month	15.0	4.5	8-24	14.0	4.1	8-26	12.2	4.4	7-24	0.057
	6 months	14.9	4.6	8-23	14.7	5.4	8-31	14.0	4.5	8-24	0.807
TBUT (s)	**Baseline**	11.7	2.3	8-17	11.5	2.4	8-16	12.0	2.5	6-16	0.535
	1 month	11.4	2.1	9-17	11.0	1.8	8-15	9.3	2.2	6-14	0.006*
	6 months	11.5	2.2	9-17	10.9	2.0	8-16	12.2	2.7	7-17	0.085
OSDI	**Baseline**	3.6	5.7	0-19	11.2	15.2	0-60	9.7	15.1	0-50	0.042*
	1 month	4.2	5.1	0-16	8.9	10.1	0-42	10.7	10.5	0-33	0.054
	6 months	4.2	5.1	0-16	9.7	13.4	0-56	9.9	12.1	0-33	0.201
8-OHdG (ng/mL)	**Baseline**	52.8	13.5	31-84	86.1	37.2	22-156	90.4	39.3	16-163	<0.001*
	1 month	50.7	28.9	14-123	54.6	30.5	13-217	118.2	48.5	17-200	<0.001*
	6 months	56.3	29.5	14-115	66.4	29.4	13-135	95.5	36.1	20-191	<0.001*
4-HNE (ng/mL)	**Baseline**	27.8	6.4	18-48	29.8	11.1	13-65	43.1	4.2	33-52	<0.001*
	1 month	29.2	7.7	15-48	15.2	4.5	10-29	45.2	7.9	36-73	<0.001*
	6 months	29.7	6.2	18-41	15.0	4.0	10-24	43.9	6.2	36-68	<0.001*

*Statistically significant (p<0.05), CMMR: Conjunctiva-Müller muscle resection, SD: Standard deviation, TBUT: Tear break-up time, OSDI: Ocular Surface Disease Index, 8-OHdG: 8-hydroxy-2'-deoxyguanosine, 4-HNE: 4-hydroxy-2-nonenal

In the preoperative period, the mean tear 8-OHdG level was higher in the CMMR (90.4±39.3 ng/mL) and blepharoplasty groups (86.1±37.2 ng/mL) compared to the control group (52.8±13.5 ng/mL) (p<0.001), with no statistical difference between the CMMR and blepharoplasty groups (p=1.0). At the 1-month visit, 8-OHdG levels were significantly higher in the CMMR group (118.2±48.5 ng/mL) when compared to the control (50.7±28.9 ng/mL) and blepharoplasty groups (54.6±30.5 ng/mL) (p<0.001 for both), with no difference observed between the control and blepharoplasty groups (p=1.0). Similarly, at the 6-month visit, tear 8-OHdG levels were higher in the CMMR group compared to the control and blepharoplasty groups (p<0.001 and p=0.003, respectively). While no significant changes in tear 8-OHdG levels were observed between different visits in the control group (p=0.064), there was a significant decrease in the blepharoplasty group (p<0.001) and a significant increase in the CMMR group (p=0.034) between the baseline and 1-month visits. No significant change was found in terms of 8-OHdG levels between the baseline and 6-month visits or between the 1- and 6-month visits in the CMMR group.

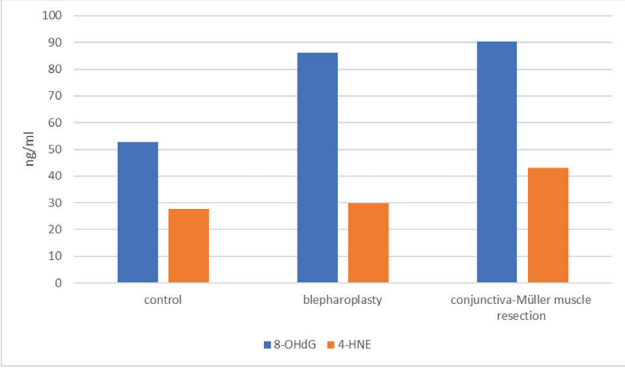

Figure 1. Baseline mean tear 8-hydroxy-2'-deoxyguanosine (8-OHdG) and 4-hydroxy-2-nonenal (4-HNE) levels in the three groups

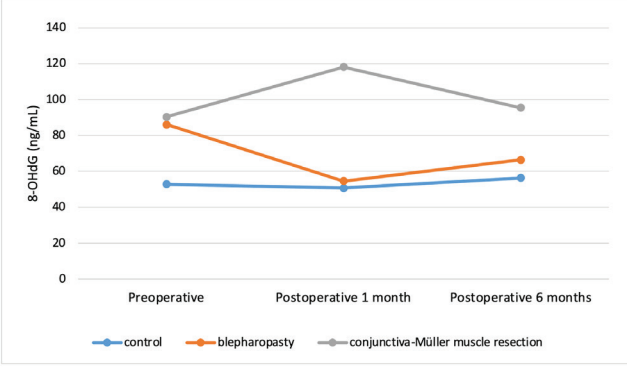

Figure 2. Changes in mean tear 8-hydroxy-2'-deoxyguanosine (8-OHdG) concentration between consecutive visits in the three groups

In the preoperative period, tear 4-HNE levels were lower in the control (27.8±6.4 ng/mL) and blepharoplasty groups (29.8±11.4 ng/mL) compared to the CMMR group (43.1±4.2 ng/mL) (p<0.001 for both). At the 1-month visit, tear 4-HNE levels were higher in the CMMR group (45.2±7.9 ng/mL) compared to the control group (29.2±7.7 ng/mL) and lower in the blepharoplasty group (15.3±4.5 ng/mL) compared to the control group (p<0.001 for both). Similarly, tear 4-HNE levels at 6 months were also higher in the CMMR group and lower in the blepharoplasty group when compared to the control group (p<0.001 for both). While no significant change in 4-HNE levels was observed in the control and CMMR groups between visits (p=0.061 and p=0.58, respectively), the blepharoplasty

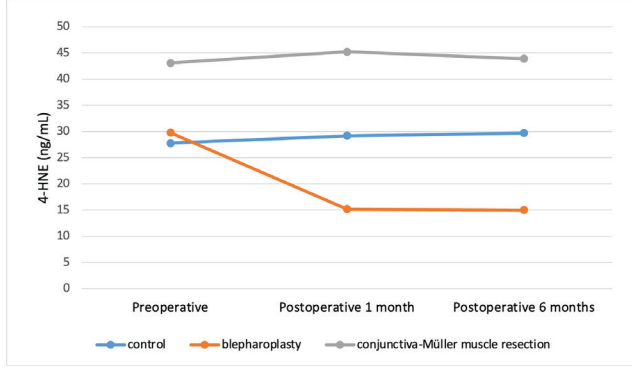

Figure 3. Changes in mean tear 4-hydroxy-2-nonenal (4-HNE) concentration between consecutive visits in the three groups

Table 3. The results (p values) of pairwise comparisons of the study groups using the Mann-Whitney U test with Bonferroni correction

	Control vs. blepharoplasty group	Control vs. CMMR group	Blepharoplasty vs. CMMR group
TBUT - 1 month	1.0	0.009*	0.015*
OSDI - baseline	0.033*	0.504	1.0
8-OHdG - baseline	<0.001*	<0.001*	1.0
8-OHdG - 1 month	1.0	<0.001*	<0.001*
8-OHdG - 6 months	0.477	<0.001*	0.003*
4-HNE - baseline	1.0	<0.001*	<0.001*
4-HNE - 1 month	<0.001*	<0.001*	<0.001*
4-HNE - 6 months	<0.001*	<0.001*	<0.001*

*Statistically significant (p<0.05), CMMR: Conjunctiva-Müller muscle resection, TBUT: Tear break-up time, OSDI: Ocular Surface Disease Index, 8-OHdG: 8-hydroxy-2'-deoxyguanosine, 4-HNE: 4-hydroxy-2-nonenal

group showed a significant decrease between the baseline and 1-month visits and between the baseline and 6-month visits ($p<0.001$ for both).

Correlation of Tear Oxidative Stress Levels to Tear Function Parameters

In the correlation analysis performed with all patients at the baseline visit, tear 8-OHdG and 4-HNE values were found to be positively correlated ($p=0.001$, $r=0.338$). Although 8-OHdG did not show a correlation with any tear parameter, 4-HNE showed a positive correlation only with Schirmer test results ($p=0.012$, $r=0.258$).

At postoperative 1 month, tear 8-OHdG and 4-HNE values were found to be positively correlated ($p<0.001$; $r=0.384$). 8-OHdG values were negatively correlated with Schirmer test ($p=0.039$; $r=-0.214$) and TBUT scores ($p=0.017$; $r=-0.246$) and positively correlated with OSDI score ($p=0.048$; $r=0.205$). 4-HNE values were found to be negatively correlated with TBUT scores ($p=0.006$; $r=-0.281$).

At postoperative 6 months, neither oxidative stress marker was correlated with any tear parameter.

Discussion

Although blepharoptosis and dermatochalasis sometimes occur together, patients with dermatochalasis without accompanying blepharoptosis were included in our study. Even though the influence of CMMR and blepharoplasty surgeries on tear function has been researched in the past,[7,15,16,17,18,19,20,21,22,23,24,25,26] the influence of these surgeries on tear oxidative stress levels has not been investigated. Our study reveals important findings about the role of these surgeries on tear oxidative stress markers and tear film function.

We observed that tear 8-OHdG values were higher in patients with dermatochalasis and both tear 8-OHdG and 4-HNE levels were higher in patients with blepharoptosis compared to controls. This may be due to impaired blinking dynamics. It has been previously found that blinking functions are impaired in patients with blepharoptosis.[28] Similarly, blinking dynamics may be impaired in patients with dermatochalasis due to increased mechanical weight on the eyelid.[29] The effective blinking which ensures the release of lipids from the meibomian glands is the principal factor in the generation of the lipid layer of the tear film.[30] In cases of impaired blinking, the lipid layer thickness of the tear film becomes thinner, causing the aqueous layer of the tear film to evaporate and leading to instability of the tear film.[31,32] Hollander et al.[29] hypothesized that excess tissue in the upper eyelid may cause mechanical eyelid dysfunction and increase dry eye complaints. The high OSDI score in dermatochalasis patients in the preoperative period may be due to this mechanical weight on the eyelid. In addition, it has also been reported that dermatochalasis causes dry eyes due to meibomian gland dysfunction.[10]

The higher tear 8-OHdG levels and lower TBUT scores 1 month after CMMR might be explained by several factors. First, inflammation is known to increase reactive oxygen products.[33] The increase of 8-OHdG and decrease of TBUT scores may have occurred due to transient inflammation on the ocular surface after CMMR, probably associated with conjunctival surgical manipulations and suturing. A previous study showed that levels of 4-HNE and malondialdehyde in the tear film were higher in patients with dry eye and were negatively correlated with Schirmer and TBUT scores.[14] Similarly, we observed a negative correlation between 8-OHdG and TBUT in our study. Therefore, we speculate that oxidative stress may cause temporary tear film dysfunction after CMMR surgery. Zloto et al.[17] also reported significant decreases in Schirmer and TBUT test results and significant increases in OSDI scores and corneal staining 90 days after CMMR. In terms of the possible causes of these findings, it has been suggested that the loss of accessory lacrimal glands might lead to aqueous tear deficiency, increased MRD-1 might result in increased tear evaporation, and the palpebral conjunctival scar might lead to increased dry eye complaints. Actually, significant loss of accessory glands and goblet cells is not expected after CMMR because the glands of Wolfring are located at the superior edge of the tarsus, the glands of Krause are located in the fornices, and goblet cells are located mostly in the bulbar conjunctiva and fornices.[15,18] In this study, observing no change in Schirmer test results after CMMR supports the hypothesis that CMMR might not cause a reduction in tear production. However, some reports have claimed the opposite.[18,19] The increased oxidative stress might also be explained by greater exposure to ultraviolet (UV) radiation due to an increase in MRD-1. It has previously been found that photooxidative reactions associated with UV light cause dry eye, and in a study conducted with rabbits, oxidation increased in corneal epithelial cells due to UV light.[34] In our previous study, we found that 8-OHdG in the tear film increased in patients whose blepharoptosis was corrected by an anterior approach.[25] The increase in tear 8-OHdG levels despite less conjunctival manipulation and thus less ocular surface inflammation can be explained by the increased UV exposure due to an increase in MRD-1. Another explanation for the increase in tear oxidative stress markers that were seen after blepharoptosis surgery performed via the anterior or posterior approach is the increase in evaporation due to the increase in MRD-1.[23]

In the blepharoplasty group, the decrease in 8-OHdG and 4-HNE levels in the tears at 1 month after surgery may be related to a possible decrease in the mechanical weight on the eyelid and the resulting reduction in the muscle strength needed to open the eyelid. However, this theory has to be verified by further studies with electrophysiological tests. We observed no change in Schirmer, TBUT, or OSDI scores between visits in this group. The lack of change in MRD-1 and the preservation of the orbicularis muscle may have ensured the stability of tear function parameters. Floegel et al.[35] previously found that there were no significant changes in Schirmer and TBUT tests 3 months after blepharoplasty but there were improvements in subjective symptoms and a decrease in the inflammatory reaction. Similar to our findings, previous studies revealed no significant

change in Schirmer, TBUT, and OSDI scores 90 days after surgery or in TBUT scores 6 weeks after blepharoplasty.[17,21,22] Another study also demonstrated no difference in tear volume 6 months after blepharoplasty.[23] Prior use of artificial tears, hypothyroidism, and diabetes are risk factors that may cause dry eyes after blepharoplasty.[36,37] Therefore, such patients were not included in our study. Some authors have suggested that excising the eyelid skin conservatively and not excising the orbicularis muscle reduces the deterioration of tear function after blepharoplasty.[24,33,34,38,39,40,41] However, other authors claim that resection of the preseptal orbicularis muscle does not impair blinking function.[42,43] In this study, the orbicularis muscle was preserved in blepharoplasty surgery and we observed no tear film dysfunction.

Study Limitations

One of the limitations of our study is that tear film functions were examined only with Schirmer, TBUT, and OSDI tests. The assessment of dry eye is complex; a single test is insufficient and the correlation between different tests is limited.[44] Objective and subjective assessments of dry eye are reported to show weak correlation,[45] and this discrepancy may be affected by various factors such as age, personal perceived health, and mental health.[46] Although we used more than one test to increase specificity and sensitivity in our study, the use of more additional tests such as non-invasive TBUT, tear osmolarity measurement, meniscal height measurement, meibography, and interferometry will be more useful in evaluating the results and understanding the mechanism. The evaluation of oxidative stress only with 8-OHdG and 4-HNE is also a limitation of this study. Further studies evaluating changes in other oxidative stress markers would offer a deeper understanding of the influence of blepharoplasty and CMMR on oxidative stress in the tear film.

Conclusion

In conclusion, we found that oxidative stress markers in the tear film of patients with dermatochalasis or blepharoptosis were higher than in healthy controls. We demonstrated that blepharoplasty and CMMR did not cause any differences in Schirmer and OSDI scores at postoperative 1 and 6 months, but CMMR caused a temporary decrease of TBUT and an increase in tear oxidative stress levels. Furthermore, at the postoperative 1-month visit, tear oxidative stress markers were negatively correlated with Schirmer and TBUT scores and positively correlated with OSDI. The findings suggest that dry eye after CMMR surgery may be caused by oxidative stress. Additional studies are needed to better reveal the relationship between tear oxidative stress status and dry eye syndrome.

Ethics

Ethics Committee Approval: İstanbul University-Cerrahpaşa, Cerrahpaşa Faculty of Medicine Ethics Committee approved the study (approval number: 83045809-604.01.02, date: 07.08.2018).

Informed Consent: Obtained.

Authorship Contributions

Surgical and Medical Practices: C.A., Concept: S.S., C.A., B.M., Ö.B.E., Design: S.S., C.A., B.M., Ö.B.E., Data Collection or Processing: S.S., C.A., B.M., Ö.B.E., Analysis or Interpretation: S.S., C.A., B.M., Ö.B.E., Literature Search: S.S., C.A., Ö.B.E., Writing: S.S., C.A., B.M., Ö.B.E.

Conflict of Interest: No conflict of interest was declared by the authors.

Financial Disclosure: This study was funded by the Scientific Research Projects Coordination Unit of İstanbul University-Cerrahpaşa, Cerrahpaşa Faculty of Medicine (project number: 31993).

References

1. Nalcı H, Hoşal MB, Gündüz ÖU. Effects of Upper Eyelid Blepharoplasty on Contrast Sensitivity in Dermatochalasis Patients. Turk J Ophthalmol. 2020;50:151-155.
2. Bacharach J, Lee WW, Harrison AR, Freddo TF. A review of acquired blepharoptosis: prevalence, diagnosis, and current treatment options. Eye (Lond). 2021;35:2468-2481.
3. Putterman AM. A clamp for strengthening Müller's muscle in the treatment of ptosis. Modification, theory, and clamp for the Fasanella-Servat ptosis operation. Arch Ophthalmol. 1972;87:665-667.
4. Zauberman NA, Koval T, Kinori M, Matani A, Rosner M, Ben-Simon GJ. Müller's muscle-conjunctival resection for upper eyelid ptosis: correlation between amount of resected tissue and outcome. Br J Ophthalmol. 2013;97:408-411.
5. Peter NM, Khooshabeh R. Open-sky isolated subtotal Muller's muscle resection for ptosis surgery: a review of over 300 cases and assessment of long-term outcome. Eye (Lond). 2013;27:519-524.
6. Elbakary M. Posterior approach levator aponeurosis advancement in aponeurotic ptosis repair. Delta J Ophthalmol. 2015;16:32.
7. Rymer BL, Marinho DR, Cagliari C, Marafon SB, Procianoy F. Effects of Muller's muscle-conjunctival resection for ptosis on ocular surface scores and dry eye symptoms. Orbit. 2017;36:1-5.
8. Wakamatsu TH, Dogru M, Matsumoto Y, Kojima T, Kaido M, Ibrahim OM, Sato EA, Igarashi A, Ichihashi Y, Satake Y, Shimazaki J, Tsubota K. Evaluation of lipid oxidative stress status in Sjögren syndrome patients. Invest Ophthalmol Vis Sci. 2013;54:201-210.
9. Choi W, Li Y, Ji YS, Yoon KC. Oxidative stress markers in tears of patients with Graves' orbitopathy and their correlation with clinical activity score. BMC Ophthalmol. 2018;18:303.
10. Seen S, Tong L. Dry eye disease and oxidative stress. Acta Ophthalmol. 2018;96:e412-e420.
11. Wu WL, Chang SW. Dermatochalasis Aggravates Meibomian Gland Dysfunction Related Dry Eyes. J Clin Med. 2022;11:2379.
12. Wakamatsu TH, Dogru M, Ayako I, Takano Y, Matsumoto Y, Ibrahim OM, Okada N, Satake Y, Fukagawa K, Shimazaki J, Tsubota K, Fujishima H. Evaluation of lipid oxidative stress status and inflammation in atopic ocular surface disease. Mol Vis. 2010;16:2465-2475.
13. Choi JH, Li Y, Kim SH, Jin R, Kim YH, Choi W, You IC, Yoon KC. The influences of smartphone use on the status of the tear film and ocular surface. PLoS One. 2018;13:e0206541.
14. Choi W, Lian C, Ying L, Kim GE, You IC, Park SH, Yoon KC. Expression of Lipid Peroxidation Markers in the Tear Film and Ocular Surface of Patients with Non-Sjogren Syndrome: Potential Biomarkers for Dry Eye Disease. Curr Eye Res. 2016;41:1143-1149.
15. Dailey RA, Saulny SM, Sullivan SA. Müller muscle-conjunctival resection: effect on tear production. Ophthalmic Plast Reconstr Surg. 2002;18:421-425.
16. Wee SW, Lee JK. Clinical outcomes of conjunctiva-Müller muscle resection: association with phenylephrine test-negative blepharoptosis and dry eye syndrome. J Craniofac Surg. 2014;25:898-901.

17. Zloto O, Matani A, Prat D, Leshno A, Ben Simon G. The Effect of a Ptosis Procedure Compared to an Upper Blepharoplasty on Dry Eye Syndrome. Am J Ophthalmol. 2020;212:1-6.
18. Uğurbaş SH, Alpay A, Bahadır B, Uğurbaş SC. Tear function and ocular surface after Muller muscle-conjunctival resection. Indian J Ophthalmol. 2014;62:654-655.
19. Lake S, Mohammad-Ali FH, Khooshabeh R. Open sky Müller's muscle-conjunctiva resection for ptosis surgery. Eye (Lond). 2003;17:1008-1012.
20. Kim HH, De Paiva CS, Yen MT. Effects of upper eyelid blepharoplasty on ocular surface sensation and tear production. Can J Ophthalmol. 2007;42:739-742.
21. Lima CG, Siqueira GB, Cardoso IH, Sant'Anna AE, Osaki MH. Avaliação do olho seco no pré e pós-operatório da blefaroplastia [Evaluation of dry eye in before and after blepharoplasty]. Arq Bras Oftalmol. 2006;69:227-232.
22. Soares A, Faria-Correia F, Franqueira N, Ribeiro S. Effect of superior blepharoplasty on tear film: objective evaluation with the Keratograph 5M - a pilot study. Arq Bras Oftalmol. 2018;81:471-474.
23. Watanabe A, Selva D, Kakizaki H, Oka Y, Yokoi N, Wakimasu K, Kimura N, Kinoshita S. Long-term tear volume changes after blepharoptosis surgery and blepharoplasty. Invest Ophthalmol Vis Sci. 2014;56:54-58.
24. Prischmann J, Sufyan A, Ting JY, Ruffin C, Perkins SW. Dry eye symptoms and chemosis following blepharoplasty: a 10-year retrospective review of 892 cases in a single-surgeon series. JAMA Facial Plast Surg. 2013;15:39-46.
25. Sert S, Arici C, Mergen B, Ekmekci OB. Effect of Ptosis Surgery on Tear Oxidative Stress Levels in Patients with Blepharoptosis and Pseudoptosis. Beyoglu Eye J. 2023;8:266-272.
26. Aksu Ceylan N, Yeniad B. Effects of Upper Eyelid Surgery on the Ocular Surface and Corneal Topography. Turk J Ophthalmol. 2022;52:50-56.
27. Markoulli M, Papas E, Petznick A, Holden B. Validation of the flush method as an alternative to basal or reflex tear collection. Curr Eye Res. 2011;36:198-207.
28. Mak FH, Harker A, Kwon KA, Edirisinghe M, Rose GE, Murta F, Ezra DG. Analysis of blink dynamics in patients with blepharoptosis. J R Soc Interface. 2016;13:20150932.
29. Hollander MHJ, Pott JWR, Delli K, Vissink A, Schepers RH, Jansma J. Impact of upper blepharoplasty, with or without orbicularis oculi muscle removal, on tear film dynamics and dry eye symptoms: A randomized controlled trial. Acta Ophthalmol. 2022;100:564-571.
30. McMonnies CW. Incomplete blinking: exposure keratopathy, lid wiper epitheliopathy, dry eye, refractive surgery, and dry contact lenses. Cont Lens Anterior Eye. 2007;30:37-51.
31. Salmon JF. Kanski's Clinical Ophtalmology (9th ed). Elsevier; 2020;156-157.
32. Gomes JAP, Azar DT, Baudouin C, Efron N, Hirayama M, Horwath-Winter J, Kim T, Mehta JS, Messmer EM, Pepose JS, Sangwan VS, Weiner AL, Wilson SE, Wolffsohn JS. TFOS DEWS II iatrogenic report. Ocul Surf. 2017;15:511-538.
33. Agita A, Alsagaff MT. Inflammation, Immunity, and Hypertension. Acta Med Indones. 2017;49:158-165.
34. Shimmura S, Suematsu M, Shimoyama M, Tsubota K, Oguchi Y, Ishimura Y. Subthreshold UV radiation-induced peroxide formation in cultured corneal epithelial cells: the protective effects of lactoferrin. Exp Eye Res. 1996;63:519-526.
35. Floegel I, Horwath-Winter J, Muellner K, Haller-Schober EM. A conservative blepharoplasty may be a means of alleviating dry eye symptoms. Acta Ophthalmol Scand. 2003;81:230-232.
36. Fagien S. Reducing the incidence of dry eye symptoms after blepharoplasty. Aesthet Surg J. 2004;24:464-468.
37. Bhattacharjee K, Misra D, Singh M, Deori N. Long-term changes in contrast-sensitivity, corneal topography and higher-order aberrations after upper eyelid blepharoplasty: A prospective interventional study. Indian J Ophthalmol. 2020;68:2906-2910.
38. Kiang L, Deptula P, Mazhar M, Murariu D, Parsa FD. Muscle-sparing blepharoplasty: a prospective left-right comparative study. Arch Plast Surg. 2014;41:576-583.
39. Mohammed F. Impact of orbicularis oculi muscle strip excision during upper lid blepharoplasty on tear film break up time and postoperative dry eye symptoms. Al-Azhar Med J. 2018;539-549.
40. Saadat D, Dresner SC. Safety of blepharoplasty in patients with preoperative dry eyes. Arch Facial Plast Surg. 2004;6:101-104.
41. Zhang SY, Yan Y, Fu Y. Cosmetic blepharoplasty and dry eye disease: a review of the incidence, clinical manifestations, mechanisms and prevention. Int J Ophthalmol. 2020;13:488-492.
42. Mak FHW, Ting M, Edmunds MR, Harker A, Edirisinghe M, Duggineni S, Murta F, Ezra DG. Videographic Analysis of Blink Dynamics following Upper Eyelid Blepharoplasty and Its Association with Dry Eye. Plast Reconstr Surg Glob Open. 2020;8:e2991.
43. Abell KM, Cowen DE, Baker RS, Porter JD. Eyelid kinematics following blepharoplasty. Ophthalmic Plast Reconstr Surg. 1999;15:236-242.
44. Sullivan BD, Crews LA, Messmer EM, Foulks GN, Nichols KK, Baenninger P, Geerling G, Figueiredo F, Lemp MA. Correlations between commonly used objective signs and symptoms for the diagnosis of dry eye disease: clinical implications. Acta Ophthalmol. 2014;92:161-166.
45. Bartlett JD, Keith MS, Sudharshan L, Snedecor SJ. Associations between signs and symptoms of dry eye disease: a systematic review. Clin Ophthalmol. 2015;9:1719-1730.
46. Vehof J, Sillevis Smitt-Kamminga N, Nibourg SA, Hammond CJ. Predictors of Discordance between Symptoms and Signs in Dry Eye Disease. Ophthalmology. 2017;124:280-286.

Original Article

Multimodal Imaging Characteristics and Diagnostic Value of Choroidal Nodules in Patients with Neurofibromatosis Type 1

Nargiz Ahmadova*, Mustafa Kayabaşı**, Seher Köksaldı**, Eda Hümaz*, Ali Osman Saatci*

*Dokuz Eylül University Faculty of Medicine, Department of Ophthalmology, İzmir, Türkiye
**Muş State Hospital, Clinic of Ophthalmology, Muş, Türkiye

Abstract

Objectives: Yasunari nodules are choroidal lesions observed in patients diagnosed with neurofibromatosis type 1 (NF-1) and characterized by relatively irregular dome-shaped, plaque-like, or patchy boundaries. The present study examines the multimodal imaging characteristics of Yasunari nodules and their value in the diagnosis of NF-1.

Materials and Methods: Medical records including optical coherence tomography (OCT), enhanced depth imaging OCT, infrared reflectance (IR) imaging, OCT angiography, and color fundus images of NF-1 patients who were examined at the Department of Ophthalmology in Dokuz Eylül University Faculty of Medicine between January 2022 and December 2023 were retrospectively reviewed for the presence of Yasunari nodules.

Results: A total of 54 eyes of 27 patients were included in the study. At least one choroidal nodule was detected on IR imaging in 52 eyes (96.3%). In 31 (72.1%) of the 43 eyes (79.6%) with available high-quality OCT angiography images, choroidal nodules were observed as areas showing a flow deficit in the choriocapillaris layer. Of the total 54 eyes included, Lisch nodules without choroidal nodules were observed in 2 eyes (3.7%). In 16 eyes (29.6%), Lisch nodules were not detected despite the presence of choroidal nodules. Both Lisch nodules and choroidal nodules were detected in the other 36 eyes (66.7%).

Conclusion: Yasunari nodules are frequently observed in NF-1 cases and can be easily detected with multimodal imaging techniques, especially IR imaging. The ability to visualize choroidal nodules before the appearance of Lisch nodules demonstrates the importance of Yasunari nodules in the diagnosis of NF-1.

Keywords: Choroidal nodules, infrared imaging, multimodal imaging, neurofibromatosis type 1, Yasunari nodules

Cite this article as: Ahmadova N, Kayabaşı M, Köksaldı S, Hümaz E, Saatci AO. Multimodal Imaging Characteristics and Diagnostic Value of Choroidal Nodules in Patients with Neurofibromatosis Type 1. Turk J Ophthalmol 2024;54:140-148

Address for Correspondence: Ali Osman Saatci, Dokuz Eylül University Faculty of Medicine, Department of Ophthalmology, İzmir, Türkiye
E-mail: osman.saatci@deu.edu.tr **ORCID-ID:** orcid.org/0000-0001-6848-7239
Received: 11.03.2024 **Accepted:** 09.05.2024

DOI: 10.4274/tjo.galenos.2024.48017

Introduction

Neurofibromatosis type 1 (NF-1) is an autosomal dominant disease caused by deletions or mutations in the neurofibromin gene located on chromosome 17p11.2.[1] It has a reported incidence of approximately 1/3000 and a prevalence between 1/4000 and 1/5000.[2] NF-1 is characterized by a range of findings, including nerve tumors that can develop in various parts of the body, cutaneous pigmentation changes (cafe au lait spots, axillary and inguinal freckling), vascular abnormalities, and bone lesions (pseudoarthrosis, sphenoidal wing hypoplasia), and is also commonly associated with ocular involvement.[3,4,5]

The NF-1 diagnostic criteria determined by the National Institutes of Health include the presence of two or more Lisch nodules on the iris and optic nerve glioma as ophthalmological findings.[6] In 2021, Legius et al.[7] suggested that the presence of at least two choroidal abnormalities described as "bright, patchy nodules" on optical coherence tomography (OCT) or infrared reflectance (IR) imaging should also be used as a diagnostic criterion for NF-1. These lesions, which occur at the level of the choroid, are hamartomatous nodules also referred to as "Yasunari nodules".[8] Their reported prevalence in NF-1 cases ranges from 28% to 100%.[8,9,10,11]

The aim of this study was to evaluate the incidence of choroidal nodules in patients with NF-1, their multimodal imaging characteristics, and their place in the diagnosis of NF-1.

Materials and Methods

This retrospective study was conducted within the framework of the principles of the Declaration of Helsinki and approved by the Dokuz Eylül University Local Ethics Committee (approval number: 2023/10-01, date: 29.03.2023). We retrospectively

analyzed the medical records and recorded OCT, enhanced depth imaging OCT (EDI-OCT), IR, OCT angiography (OCTA), and color fundus images of patients who were examined in the Dokuz Eylül University Faculty of Medicine, Department of Ophthalmology between January 2022 and December 2023 and had at least two of the National Institutes of Health diagnostic criteria for NF-1.[6] Exclusion criteria were optic media opacity that could interfere with posterior segment imaging, comorbid systemic or ocular disease other than NF-1, and a history of systemic drug use.

All patients included in the study underwent a comprehensive ophthalmological assessment including anterior and posterior segment examination. Spectral-domain OCT images (7-mm fovea-centered radial B-scan sections with a 30-degree lens, ART: 9), EDI-OCT images (9-mm horizontal sections passing through the fovea) and IR images (fovea-centered 55-degree area) were obtained with a standard protocol using the Heidelberg Spectralis (Heidelberg Engineering, Heidelberg, Germany) device. OCTA images covering a 12x12-mm area centered on the fovea and/or optic disc were obtained using the DRI OCT Triton (TOPCON, Tokyo, Japan) device, and central 45-degree color fundus images including the optic disc and macula were obtained using the VISUCAM 500 (Carl Zeiss Meditec, Jena, Germany) or DRI OCT Triton device. We recorded the patients' age, gender, presence of cafe au lait spots, and cranial magnetic resonance imaging (MRI) findings for each patient; central macular thickness (CMT) and presence of Lisch nodules, eyelid plexiform neurofibroma, optic glioma, and Yasunari nodules in each eye; and subfoveal choroidal thickness (SFCT) for eyes with EDI-OCT images passing through the fovea.

Using the device software, CMT was determined by manually measuring the shortest vertical distance between the internal limiting membrane and Bruch's membrane in OCT images passing through the fovea, and SFCT was determined by manually measuring the shortest vertical distance between the hyperreflective outer border of the retinal pigment epithelium (RPE) and the choroid-sclera junction in EDI-OCT images passing through the fovea.

The presence of optic glioma was evaluated by examining contrast-enhanced orbital MRI.

Lisch nodules were defined as yellowish brown dome-shaped solid hamartomatous lesions 1-2 mm in diameter on the iris surface on slit-lamp examination.[10]

Choroidal nodules were identified on IR images as domed, placoid, or patchy choroidal lesions with relatively irregular borders and high reflectivity.[8] The presence of these nodules was also evaluated on OCT images with image quality ≥18 and OCTA images with image quality ≥40 for patients with recorded images.

Informed consent was not obtained because the study was retrospective and used no identifying data or images.

Statistical Analysis

Statistical analyses were performed using the SPSS statistical program (IBM Corp, Armonk, NY, USA). Descriptive statistics were used to summarize the data. Categorical variables are presented as numbers and percentages, and quantitative variables are presented as mean ± standard deviation.

Results

The study included a total of 54 eyes of 27 patients. Descriptive statistics of the study group are given in Table 1; detailed demographic and clinical characteristics are shown in Table 2.

Fourteen (51.9%) of the patients were male and 13 (48.1%) were female. The mean age of the patients was 22.33±14.62 years (range, 8-57 years). All patients (100%) had at least 6 cafe au lait spots.

Table 1. Descriptive statistics of the patients and eyes included in the study

Number of patients/eyes, n	27/54
Age, years	22.33±14.62[a]
Gender, M/F	14/13[a]
Cafe au lait spots, n (%)	27 (100)[a]
Lisch nodule, n (%)	40 (74.1)[b]
Eyelid neurofibroma, n (%)	1 (1.9)[b]
Optic glioma, n (%)	9 (64.3)[c]
Central macular thickness, µm	244.31±25.17[b]
Subfoveal choroidal thickness, µm	320.49±63.63[b]
Choroidal nodule on IR imaging, n (%)	52 (96.3)[b]
Choroidal nodule on OCTA, n (%)	31 (72.1)[d]

[a]: According to number of patients, [b]: According to number of eyes, [c]: According to number of patients with contrast-enhanced orbital magnetic resonance imaging, [d]: According to number of eyes with adequate quality OCTA images, M: Male, F: Female, IR: Infrared reflectance, OCTA: Optical coherence tomography angiography

Table 2. Demographic and clinical characteristics of the patients

Patient	Sex	Age (years)	Cranial MRI findings	Eye	Lisch nodule	Eyelid neurofibroma	Optic glioma	CMT (µm)	SFCT (µm)	Choroidal nodule on IR	Choroidal nodule on OCTA
1	M	52	No cranial MRI	Right Left	+ +	- -	- -	220 380	351 354	+ +	+ No OCTA
2	F	41	No pathology	Right Left	+ -	- -	- +	214 209	307 299	+ +	+ +
3	F	12	Hamartoma	Right Left	+ +	- -	+ -	268 243	347 337	+ +	- -
4	F	16	Hamartoma	Right Left	+ +	- -	- -	242 236	387 362	+ +	+ +
5	F	16	Hamartoma	Right Left	+ +	- -	+ -	237 228	373 408	+ +	+ +
6	F	13	Non-specific hyperintense foci	Right Left	+ -	- -	No orbital MRI No orbital MRI	227 228	349 363	+ +	No OCTA No OCTA
7	F	14	No cranial MRI	Right Left	+ +	- -	- -	232 262	345 346	+ +	+ +
8	M	10	Hamartoma	Right Left	- -	- -	No orbital MRI No orbital MRI	240 237	389 384	+ +	+ +
9	M	13	Hamartoma ICA thinning	Right Left	- -	- -	+ -	232 232	359 305	+ +	+ +
10	M	57	Encephalomalacia	Right Left	+ +	- -	No orbital MRI No orbital MRI	228 221	177 139	+ +	+ +
11	M	15	Venous anomaly	Right Left	+ +	- -	No orbital MRI No orbital MRI	244 250	277 356	+ +	+ +
12	M	24	Bone dysplasia Plexiform neurofibroma	Right Left	+ +	- +	No orbital MRI No orbital MRI	249 181	352 No EDI-OCT	+ +	+ No OCTA
13	F	25	No pathology	Right Left	+ +	- -	- -	237 236	No EDI-OCT No EDI-OCT	+ +	- -
14	F	23	Hamartoma	Right Left	+ +	- -	- -	282 263	323 316	+ +	+ +
15	M	48	Ventricular dilatation	Right Left	+ +	- -	No orbital MRI No orbital MRI	237 238	254 224	+ +	+ +
16	M	19	Hamartoma Glial tumor	Right Left	- +	- -	+ -	235 244	302 300	+ +	+ +
17	F	18	Hamartoma Chiari type I anomaly	Right Left	+ +	- -	No orbital MRI No orbital MRI	262 255	No EDI-OCT No EDI-OCT	+ +	- -
18	F	11	Hamartoma Ventricular dilatation	Right Left	+ +	- -	+ -	249 256	337 313	+ +	+ +
19	M	17	Venous anomaly	Right Left	+ +	- -	+ -	248 249	330 316	+ +	No OCTA No OCTA
20	F	47	No cranial MRI	Right Left	- +	- -	No orbital MRI No orbital MRI	240 250	206 167	+ +	No OCTA No OCTA
21	M	19	Hamartoma	Right Left	- -	- -	No orbital MRI No orbital MRI	253 268	307 271	+ +	+ +
22	F	40	No cranial MRI	Right Left	- -	- -	No orbital MRI No orbital MRI	251 258	284 275	+ +	+ +
23	F	12	Expansile lesion in pons	Right Left	- +	- -	- +	223 223	324 317	+ +	- -
24	M	11	Non-specific hyperintense foci	Right Left	+ +	- -	No orbital MRI No orbital MRI	244 254	359 360	- -	- -

Table 2. continued

Patient	Sex	Age (years)	Cranial MRI findings	Eye	Lisch nodule	Eyelid neurofibroma	Optic glioma	CMT (µm)	SFCT (µm)	Choroidal nodule on IR	Choroidal nodule on OCTA
25	M	10	No pathology	Right Left	+ +	- -	No orbital MRI No orbital MRI	245 264	No EDI-OCT No EDI-OCT	+ +	No OCTA No OCTA
26	M	12	Hamartoma Arachnoid cyst	Right Left	+ +	- -	+ +	253 248	426 469	+ +	- +
27	M	8	Hamartoma	Right Left	- +	- -	No orbital MRI No orbital MRI	238 250	302 313	+ +	No OCTA No OCTA

MRI: Magnetic resonance imaging, CMT: Central macular thickness, SFCT: Subfoveal choroidal thickness, IR: Infrared reflectance, OCTA: Optical coherence tomography angiography, ICA: Internal carotid artery, EDI-OCT: Enhanced depth imaging optical coherence tomography

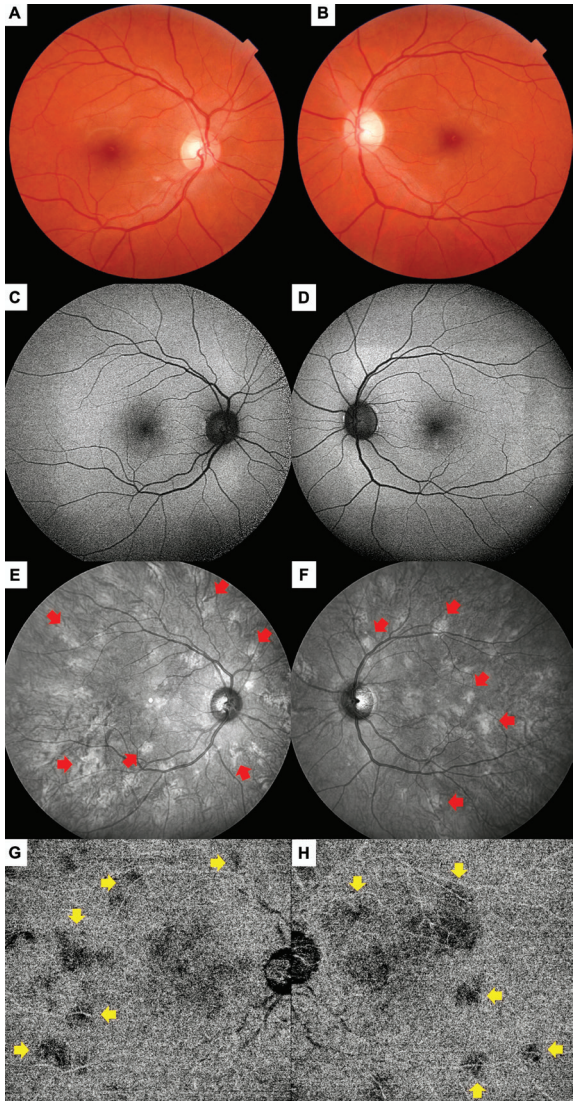

Figure 1. Patient 2 (female, 41 years old) exhibited no pathological findings in either eye on color fundus images (A and B) or fundus autofluorescence images (C and D). However, infrared reflectance imaging revealed patchy, highly reflective choroidal nodules (red arrows) widespread across the posterior pole (E and F), and corresponding areas of flow deficit (yellow arrows) in the choriocapillaris layer were observed on optical coherence tomography angiography (G and H)

Lisch nodules were observed on slit-lamp examination in 40 (74.1%) of the 54 eyes. Neurofibroma on the upper eyelid was noted in 1 eye (1.9%) (patient 12, left eye).

Contrast-enhanced cranial MRI was performed in 23 patients (85.2%). Hamartoma was detected in 12 patients (52.2%); non-specific hyperintense foci, venous anomaly, and ventricular dilatation were each detected in 2 patients (8.7%); and thinning of the internal carotid artery, encephalomalacia, sphenoid bone dysplasia, plexiform neurofibroma, glial tumor, Chiari malformation type I, expansile lesion in the pons, and arachnoid cyst were each detected in 1 patient (4.3%). Three patients (12.9%) had no pathological findings.

Of 14 patients (51.8%) who underwent contrast-enhanced orbital MRI, 9 (33.3%) had optic glioma (unilateral in 8 patients [57.1%] and bilateral in 1 patient [7.1%]).

The mean CMT for all eyes was 244.31±25.17 µm (range, 181-380 µm), while the mean SFCT for 47 eyes with EDI-OCT images passing through the fovea was 320.49±63.63 µm (range, 139-469 µm).

IR imaging revealed at least one choroidal nodule in 52 eyes (96.3%). One pediatric patient (3.7%) had bilateral Lisch nodules but no detectable choroidal nodule in either eye (patient 11, 11 years old). Adequate quality OCTA images were available for 43 eyes (79.6%). In 31 (72.1%) of these eyes, choroidal nodules were observed as areas of low reflectivity in the choriocapillaris layer.

Two (3.7%) of the 54 eyes included in the study had no choroidal nodules despite the presence of Lisch nodules. In contrast, 16 eyes (29.6%) had no Lisch nodules despite the presence of choroidal nodules. In the remaining 36 eyes (66.7%), both Lisch nodules and choroidal nodules were detected.

The multimodal imaging characteristics of patient 2 are shown in Figures 1 and 2, and those of patient 18 are presented in Figures 3 and 4 as examples.

Discussion

Histopathological studies have revealed that the choroidal nodules observed in NF-1 are hamartomatous in character, consisting of ovoid bodies that contain Schwann cells which proliferate in an annular structure around axons, and may also include neural crest-derived melanocytes and ganglion cells.[1,12,13]

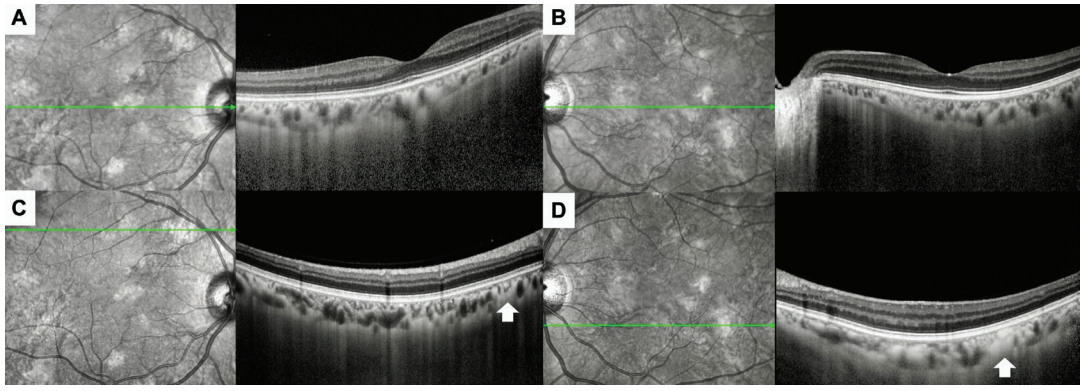

Figure 2. On enhanced depth imaging optical coherence tomography in patient 2, no pathology was detected in sections passing through the fovea (A and B), whereas sections passing through areas of high reflectivity on infrared reflectance imaging showed the surrounding large-caliber choroidal vessels with highly reflective choroidal nodules (white arrows) causing relative compression of the adjacent choroidal vascular structures (C and D)

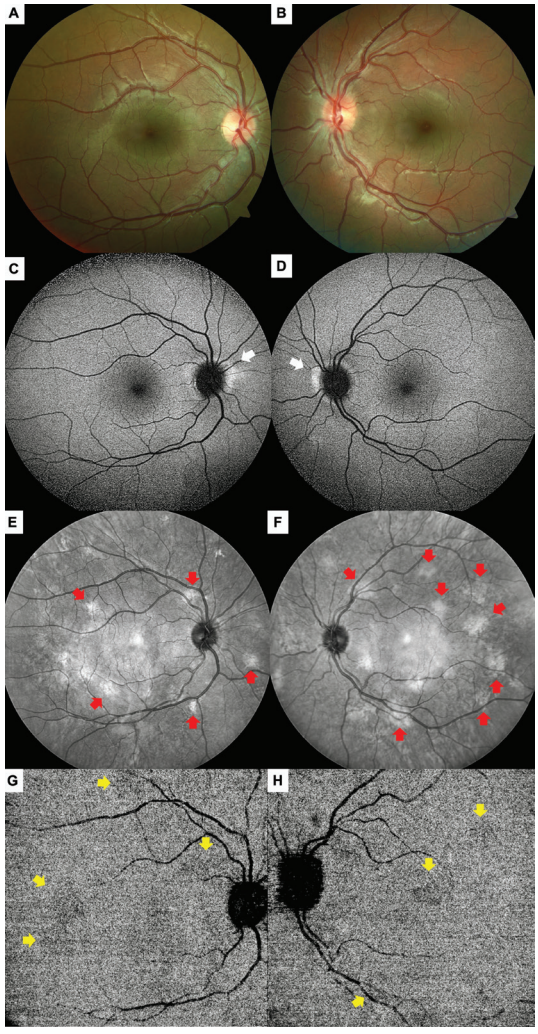

Figure 3. Patient 18 (female, 11 years old) exhibited no pathological findings in colored fundus images (A and B), while fundus autofluorescence imaging showed areas of hyperautofluorescence (white arrows) nasal to the optic disc in both eyes (C and D). Patchy, highly reflective choroidal nodules (red arrows) widespread across the posterior pole were observed on infrared reflectance imaging (E and F), and areas of flow deficit (yellow arrows) in the choriocapillaris layer were seen on optical coherence tomography angiography (G and H)

These nodules are reported to impact choroidal blood flow, causing compression and thinning of the choriocapillaris and subsequently leading to choroidal and retinal thinning.[14,15] These lesions also show structural similarities to the cutaneous neurofibromas and Lisch nodules observed in the iris.[16]

Due to the high wavelength light used, IR imaging is a suitable modality for evaluating the ocular structures that lie beyond the RPE and is useful in detecting changes at the choroidal level.[15] Although the choroidal nodules of NF-1 patients are not visible on fundoscopic examination, fundus autofluorescence imaging, or fluorescein angiography, they appear as bright, patchy areas in IR imaging and as hypocyanescent, patchy areas in the early phases of indocyanine green angiography.[8,13] In addition, the bright, patchy areas observed on IR imaging were found to be areas of high flow in the deep choroidal segment of OCTA.[17] In our study, choroidal nodules were observed in 31 (72.1%) of 43 eyes with adequate quality OCTA images, appearing as areas of flow deficit in the choriocapillaris layer. Although it is generally accepted that these nodules cannot be observed on fundoscopic examination, some authors have stated that the degree of pigmentation may vary and as a result, areas of hyperpigmentation in the fundus might be detectable in some cases.[11,13]

Studies in the literature that used IR imaging to examine choroidal nodules in NF-1 are summarized in Table 3.[8,11,13,18,19,20,21,22,23,24,25,26,27,28,29,30,31,32]

There are publications reporting that choroidal abnormalities, which can be detected up to 100% of NF-1 patients, are much more common than cafe au lait spots (98%) and Lisch nodules (41-68%) (classically considered the most common findings of the disease) and may actually be the most common sign of NF-1.[13,33] Similar to cutaneous findings and Lisch nodules, choroidal findings are observed more frequently with older age, but they occur earlier than Lisch nodules. The prevalence of choroidal findings and Lisch nodules in pediatric cases has been reported to be 64-95% and 41-52%, respectively.[19,28]

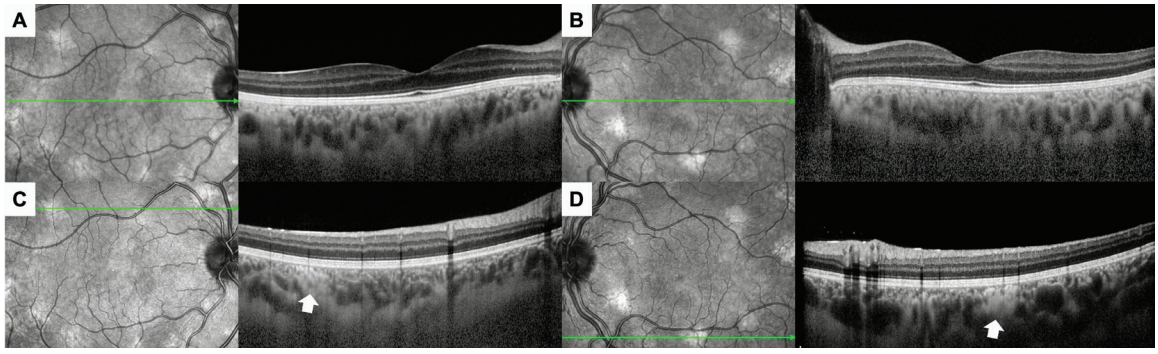

Figure 4. Enhanced depth imaging optical coherence tomography images of patient 18 showed no pathology in sections passing through the fovea (A and B), whereas in sections passing through the areas of high reflectivity on infrared reflectance imaging, choroidal nodules (white arrows) were observed as highly reflective lesions causing relative compression of the adjacent choroidal vasculature, along with the surrounding large-caliber choroidal vessels (C and D)

Table 3. Studies evaluating the presence of choroidal nodules with infrared reflectance imaging in neurofibromatosis type 1

Authors (reference)	Number of patients/eyes, n	Age (years) mean ± SD	CN presence, n (%)	Remarks
Yasunari et al.[8]	17 patients	29.2±18.0	17 (100%)	- The bright patchy areas seen on infrared fundus examination and the hypofluorescent areas corresponding to these areas on indocyanine green angiography are likely of choroidal origin. - The high frequency of these abnormalities suggests that choroidal tissue is one of the most commonly affected structures in NF-1.
Arigon et al.[11]	211 patients	32.0±14.0	61 (28.9%)	- CN have a hamartomatous character and increase in incidence with age, similar to Lisch nodules. - CN are the most common ophthalmologic finding in NF-1 patients after Lisch nodules. - Red-free imaging is the most effective method for detecting CN. - CN may appear hypopigmented or hyperpigmented on ophthalmoscopic examination and hypofluorescent or hyperfluorescent on fluorescein angiography.
Moramarco et al.[13]	249 patients	33.0±17.1	238 (95.6%)	- Hyperpigmentation can be observed on fundoscopic examination in areas corresponding to the location of CN. - These areas tend to be located at the posterior pole because the area between the vascular arcades has thick choroidal tissue and is rich in melanocytes and neural cells.
Abdolrahimzadeh et al.[18]	19 patients	42.8±14.3	17 (89.4%)	- In NF-1 patients, CN may appear as a dome or placoid shape. - These lesions lead to changes in choroidal thickness and morphology.
Vagge et al.[19]	78 patients	8.1±3.5	54 (69.2%)	- CN are very common in children with NF-1. - CN can be visualized on IR imaging as bright patchy areas and are diagnostic.
Cassiman et al.[20]	34 patients	22.0	23 (68%)	- CN are easily detected with a confocal laser scanning ophthalmoscope. - CN may vary in prevalence and number according to different genotypic subtypes of NF-1 and aid in the differential diagnosis from Legius syndrome. - Detecting CN facilitates the diagnosis, especially in young patients without the fully developed clinical picture.
Chilibeck et al.[21]	74 patients	Unspecified	56 (75.7%)*	- CN detected by IR imaging are common in NF-1 and appear at an early age. - IR imaging can aid in the diagnosis of NF-1 in young children.
Godinho et al.[22]	44 eyes	16.4±7.3	28 (63.4%)	- The presence of CN correlates with the presence of central nervous system findings in NF-1 patients.
de Rivas et al.[23]	30 patients	57.0	25 (83.3%)	- CN, which can be detected on IR imaging, are common in NF-1 patients, similar to Lisch nodules, and are even more common than Lisch nodules when high myopic eyes are excluded.
Goktas et al.[24]	19 patients	8.6±3.2	15 (78.9)	- Choroidal abnormalities are common in NF-1 patients. - Choroidal abnormalities detectable by OCT and IR imaging can be used to diagnose NF-1.

Table 3. continued

Authors (reference)	Number of patients/eyes, n	Age (years) mean ± SD	CN presence, n (%)	Remarks
Viola et al.[25]	95 patients	28.0±16.0	79 (82%)	- CN appear as bright, patchy areas on IR imaging and are common in NF-1. - IR imaging should be considered as a new diagnostic criterion in order to detect CN in NF-1 patients.
Makino et al.[26]	10 patients	20.6±13.2	9 (90%)	- Choroidal abnormalities in NF-1 patients increase with age and are correlated with the number of Lisch nodules.
Vagge et al.[27]	31 patients	22.7±13.7	24 (77.4%)	- Retinal thickness changes and CN are among the ocular symptoms described in NF-1 cases. - OCTA is an important technique in detecting the retinal and choroidal vascular flow changes that may occur early in NF-1.
Moramarco et al.[28]	160 patients	32.0±17.0	156 (97%)	- IR imaging is a non-invasive, sensitive, and reproducible in vivo imaging method that can be used to detect CN in NF-1 patients. - Choroidal changes are a diagnostic feature of NF-1.
Estrela et al.[29]	41 patients	11.8±3.3	39 (47.6%)	- Choroidal abnormalities are common in children with NF-1 and optic glioma but may not be detected in all cases. - Although choroidal abnormalities are a diagnostic criterion for NF-1, their presence and size have no impact on visual function.
Touzé et al.[30]	141 patients	8.6	97 (68.8%)	- With age, NF-1 patients show an increase in CN number and area on IR imaging.
Flores Pimentel et al.[31]	94 patients	10.3±4.2	60 (64%)	- In pediatric NF-1 patients, CN are more common than Lisch nodules, regardless of age and genetic confirmation. - Combining ophthalmological examination with IR imaging will be beneficial for early diagnosis in children.
Parrozzani et al.[32]	119 patients	8.3±4.5	72 (60.5%)	- Choroidal abnormalities can be regarded as a diagnostic criterion for the diagnosis of NF-1 in children. - The main advantage of this finding is that it aids early diagnosis, while the main drawback is that patient cooperation is required for its detection.
Ahmadova et al.	54 eyes	22.3±14.6	52 (96.3%)	- CN are more common than Lisch nodules in NF-1 patients. - The earlier appearance of CN compared to Lisch nodules may facilitate early diagnosis in these patients.

SD: Standard deviation, NF-1: Neurofibromatosis type 1, CN: Choroidal nodules, IR: Infrared reflectance

Moreover, choroidal findings without Lisch nodules have been observed in 14-37% of NF-1 cases, while Lisch nodules without choroidal findings were observed in 2.5-16%.[28,31,33] In our series, choroidal nodules were observed in 29.6% of eyes without Lisch nodules, whereas 3.7% of the eyes had only Lisch nodules.

Study Limitations

The main limitations of this study are that it was retrospective and single-centered with a relatively small number of patients. In addition, assessments that can indicate functional status, such as visual acuity and visual field, were not included in our study. However, the reason for this is that most previous publications examining choroidal nodules in NF cases have stated that these findings are asymptomatic and do not cause functional problems. Furthermore, as the OCTA images in our study were recorded for the purpose of evaluating for choroidal nodules, 12x12-mm images were obtained in order to evaluate the largest possible area. However, due to the features of the OCTA device we used, we could not obtain data on quantitative parameters such as vascular density and the foveal avascular zone with 12x12-mm images. Considering that choroidal nodules can lead to vascular alterations, especially at the choriocapillaris level, this can also be considered a limitation.

Conclusion

As NF-1 can cause ophthalmological findings, patients often present or are referred to ophthalmology clinics, both through outpatient clinic admissions and consultations by other medical disciplines. Therefore, it is important for ophthalmologists to recognize the ocular findings of NF-1. Although the presence of Lisch nodules can be evaluated by biomicroscopic examination, choroidal nodules can be observed much more frequently in these patients, as in our series, and can be easily detected using IR imaging, which is a rapid and non-invasive method. The presence of choroidal nodules before the appearance of Lisch nodules may facilitate early diagnosis in these patients.

Ethics

Ethics Committee Approval: Dokuz Eylül University Local Ethics Committee (approval number: 2023/10-01, date: 29.03.2023).

Informed Consent: Retrospective study.

Authorship Contributions

Concept: M.K., S.K., A.O.S., Design: M.K., E.H., Data Collection or Processing: N.A., M.K., E.H., Analysis or Interpretation: M.K., S.K., A.O.S., Literature Search: N.A., M.K., S.K., Writing: N.A., M.K., A.O.S.

Conflict of Interest: No conflict of interest was declared by the authors.

Financial Disclosure: The authors declared that this study received no financial support.

References

1. Abdolrahimzadeh S, Plateroti AM, Recupero SM, Lambiase A. An Update on the Ophthalmologic Features in the Phakomatoses. J Ophthalmol. 2016;2016:3043026.
2. Ratner N, Miller SJ. A RASopathy gene commonly mutated in cancer: the neurofibromatosis type 1 tumour suppressor. Nat Rev Cancer. 2015;15:290-301.
3. Bajaj A, Li QF, Zheng Q, Pumiglia K. Loss of NF1 expression in human endothelial cells promotes autonomous proliferation and altered vascular morphogenesis. PLoS One. 2012;7:e49222.
4. Saatci AO, Saylam GS, Yasti ZO, Söylev M, Saatci I, Kavukçu S, Memişoğlu B. Neurofibromatosis type I and unilateral ophthalmic artery occlusion. Ophthalmic Genet. 1998;19:87-91.
5. Özdemir Zeydanlı E, Özdek Ş. Neurofibromatosis Type 1 Vasculopathy Presenting as Branch Retinal Vein Occlusion: Case Report and Review of the Literature. Turk J Ophthalmol. 2023;53:390-394.
6. No authors listed. Neurofibromatosis. Conference statement. National Institutes of Health Consensus Development Conference. Arch Neurol. 1988;45:575-578.
7. Legius E, Messiaen L, Wolkenstein P, Pancza P, Avery RA, Berman Y, Blakeley J, Babovic-Vuksanovic D, Cunha KS, Ferner R, Fisher MJ, Friedman JM, Gutmann DH, Kehrer-Sawatzki H, Korf BR, Mautner VF, Peltonen S, Rauen KA, Riccardi V, Schorry E, Stemmer-Rachamimov A, Stevenson DA, Tadini G, Ullrich NJ, Viskochil D, Wimmer K, Yohay K; International Consensus Group on Neurofibromatosis Diagnostic Criteria (I-NF-DC); Huson SM, Evans DG, Plotkin SR. Revised diagnostic criteria for neurofibromatosis type 1 and Legius syndrome: an international consensus recommendation. Genet Med. 2021;23:1506-1513.
8. Yasunari T, Shiraki K, Hattori H, Miki T. Frequency of choroidal abnormalities in neurofibromatosis type 1. Lancet. 2000;356:988-992.
9. Safi A, Borruat FX. Yasunari Nodules: A New Sensitive and Specific Marker of Neurofibromatosis Type 1, Readily Detectable by Ophthalmologists. Klin Monbl Augenheilkd. 2019;236:480-482.
10. Lubs ML, Bauer MS, Formas ME, Djokic B. Lisch nodules in neurofibromatosis type 1. N Engl J Med. 1991;324:1264-1266.
11. Arigon V, Binaghi M, Sabouret C, Zeller J, Revuz J, Soubrane G, Wolkenstein P. Usefulness of systematic ophthalmologic investigations in neurofibromatosis 1: a cross-sectional study of 211 patients. Eur J Ophthalmol. 2002;12:413-418.
12. Kurosawa A, Kurosawa H. Ovoid bodies in choroidal neurofibromatosis. Arch Ophthalmol. 1982;100:1939-1941.
13. Moramarco A, Mallone F, Sacchetti M, Lucchino L, Miraglia E, Roberti V, Lambiase A, Giustini S. Hyperpigmented spots at fundus examination: a new ocular sign in Neurofibromatosis Type I. Orphanet J Rare Dis. 2021;16:147.
14. Cassiman C, Casteels I, Stalmans P, Legius E, Jacob J. Optical Coherence Tomography Angiography of Retinal Microvascular Changes Overlying Choroidal Nodules in Neurofibromatosis Type 1. Case Rep Ophthalmol. 2017;8:214-220.
15. Formisano M, Lodesani M, Rullo D, Fabrizio L, Guglielmelli F, Scuderi G. Unusual case of enlarged choroidal vessels in neurofibromatosis type 1 observed with near-infrared reflectance and spectral domain optical coherence tomography. Clin Ter. 2021;172:507-510.
16. Richetta A, Giustini S, Recupero SM, Pezza M, Carlomagno V, Amoruso G, Calvieri S. Lisch nodules of the iris in neurofibromatosis type 1. J Eur Acad Dermatol Venereol. 2004;18:342-344.
17. Kumar V, Singh S. Multimodal imaging of choroidal nodules in neurofibromatosis type-1. Indian J Ophthalmol. 2018;66:586-588.
18. Abdolrahimzadeh S, Felli L, Plateroti R, Plateroti AM, Giustini S, Calvieri S, Recupero SM. Morphologic and vasculature features of the choroid and associated choroid-retinal thickness alterations in neurofibromatosis type 1. Br J Ophthalmol. 2015;99:789-793.
19. Vagge A, Camicione P, Capris C, Sburlati C, Panarello S, Calevo MG, Traverso CE, Capris P. Choroidal abnormalities in neurofibromatosis type 1 detected by near-infrared reflectance imaging in paediatric population. Acta Ophthalmol. 2015;93:667-671.
20. Cassiman C, Casteels I, Jacob J, Plasschaert E, Brems H, Dubron K, Keer KV, Legius E. Choroidal abnormalities in café-au-lait syndromes: a new differential diagnostic tool? Clin Genet. 2017;91:529-535.
21. Chilibeck CM, Shah S, Russell HC, Vincent AL. The presence and progression of choroidal neurofibromas in a predominantly pediatric population with neurofibromatosis type-1. Ophthalmic Genet. 2021;42:223-239.
22. Godinho G, Esteves-Leandro J, Alves G, Madeira C, Faria O, Brandão E, Magalhães A, Falcão-Reis F, Penas S. Correlation Between Ophthalmologic and Neuroradiologic Findings in Type 1 Neurofibromatosis. J Neuroophthalmol. 2022;42:101-107.
23. de Rivas MO, Gabás JM, Cabeza MÁT, Floría OE, Latorre RH, Moscarda EN, Clavería JA, Rivasés GP, Puyuelo JA. Choroidal Hyperreflective Nodules Detected by Infrared Reflectance Images Are a Diagnostic Criterion for Neurofibromatosis Type 1 Patients Excluding Those with High Myopia. Diagnostics (Basel). 2023;13:1348.
24. Goktas S, Sakarya Y, Ozcimen M, Alpfidan I, Uzun M, Sakarya R, Yarbag A. Frequency of choroidal abnormalities in pediatric patients with neurofibromatosis type 1. J Pediatr Ophthalmol Strabismus. 2014;51:204-208.
25. Viola F, Villani E, Natacci F, Selicorni A, Melloni G, Vezzola D, Barteselli G, Mapelli C, Pirondini C, Ratiglia R. Choroidal abnormalities detected by near-infrared reflectance imaging as a new diagnostic criterion for neurofibromatosis 1. Ophthalmology. 2012;119:369-375.
26. Makino S, Tampo H, Arai Y, Obata H. Correlations between choroidal abnormalities, Lisch nodules, and age in patients with neurofibromatosis type 1. Clin Ophthalmol. 2014;8:165-168.
27. Vagge A, Corazza P, Ferro Desideri L, Camicione P, Agosto G, Vagge R, Maria Grazia C, Carnevali A, Giannaccare G, Nicolò M, Traverso CE. Ocular biometric parameters changes and choroidal vascular abnormalities in patients with neurofibromatosis type 1 evaluated by OCT-A. PLoS One. 2021;16:e0251098.
28. Moramarco A, Giustini S, Nofroni I, Mallone F, Miraglia E, Iacovino C, Calvieri S, Lambiase A. Near-infrared imaging: an in vivo, non-invasive diagnostic tool in neurofibromatosis type 1. Graefes Arch Clin Exp Ophthalmol. 2018;256:307-311.

29. Estrela T, Truong S, Garcia A, He J, Ying GS, Devakandan K, Reginald YA, Fisher MJ, Liu GT, Ullrich NJ, Avery RA, Heidary G. The Relationship Between Choroidal Abnormalities and Visual Outcomes in Pediatric Patients With NF1-Associated Optic Pathway Gliomas. J Neuroophthalmol. 2024;44:5-9.
30. Touzé R, Manassero A, Bremond-Gignac D, Robert MP. Long-term follow-up of choroidal abnormalities in children with neurofibromatosis type 1. Clin Exp Ophthalmol. 2021;49:516-519.
31. Flores Pimentel M, Heath A, Wan MJ, Hussein R, Leahy KE, MacDonald H, Tavares E, VandenHoven C, MacNeill K, Kannu P, Parkin PC, Heon E, Reginald A, Vincent A. Prevalence of Choroidal Abnormalities and Lisch Nodules in Children Meeting Clinical and Molecular Diagnosis of Neurofibromatosis Type 1. Transl Vis Sci Technol. 2022;11:10.
32. Parrozzani R, Clementi M, Frizziero L, Miglionico G, Perrini P, Cavarzeran F, Kotsafti O, Comacchio F, Trevisson E, Convento E, Fusetti S, Midena E. In Vivo Detection of Choroidal Abnormalities Related to NF1: Feasibility and Comparison With Standard NIH Diagnostic Criteria in Pediatric Patients. Invest Ophthalmol Vis Sci. 2015;56:6036-6042.
33. Mallone F, Lucchino L, Giustini S, Lambiase A, Moramarco A. An update on choroidal abnormalities and retinal microvascular changes in neurofibromatosis type 1. Orphanet J Rare Dis. 2022;17:223.

Original Article

Could Triglyceride-Glucose Index, a Predictor of Atherosclerosis, Be Associated with Retinal Vein Occlusion?

Zeynep Katipoğlu, Meydan Turan

Atatürk City Hospital, Clinic of Ophthalmology, Balıkesir, Türkiye

Abstract

Objectives: The triglyceride-glucose (TyG) index is a sign of atherosclerosis in cardiovascular diseases. The TyG index is thought to have clinical significance for the assessment of vascular damage. In this study we aimed to demonstrate the connection between the TyG index and retinal vein occlusion (RVO).

Materials and Methods: This case-control observational study involved 492 participants aged 40-90, admitted to the ophthalmology outpatient clinic of our hospital. TyG index was calculated using the formula: ln(fasting TG [mg/dL] × fasting plasma glucose [mg/dL]/2).

Results: The RVO group included 387 patients (181 women and 206 men) and the control group included 115 patients (61 women and 54 men). The average patient age was 62.9±11.1 years in the RVO group and 56.7±8.7 years in the control group. The TyG index was higher in the RVO group (8.9±0.7) than in the control group (8.8±0.6). This difference was statistically significant (p=0.04). The correlation was statistically significant when evaluated according to age and sex by multivariate logistic regression analysis (odds ratio: 1.45, confidence interval: 1.03-2.02, p=0.03).

Conclusion: The TyG index is a novel atherogenicity index that is derived from routine blood tests and can be used to determine the risk of RVO in at-risk individuals with a simple calculation. Therefore, the TyG index could help as a reliable guide to identify individuals at RVO with high risk and initiate early intervention.

Keywords: Atherogenic index, retinal vein occlusion, triglyceride-glucose index, vascular disease

Cite this article as: Katipoğlu Z, Turan M. Could Triglyceride Glucose Index, a Predictor of Atherosclerosis, Be Associated with Retinal Vein Occlusion? Turk J Ophthalmol 2024;54:149-152

Address for Correspondence: Zeynep Katipoğlu, Atatürk City Hospital, Clinic of Ophthalmology, Balıkesir, Türkiye
E-mail: zynp_nal@hotmail.com **ORCID-ID:** orcid.org/0000-0002-6935-3221
Received: 11.01.2024 **Accepted:** 28.05.2024

DOI: 10.4274/tjo.galenos.2024.69841

Introduction

Retinal vein occlusion (RVO) is the occlusion of the retinal venous system by thrombi and can occur in three different forms: central, hemicentral, or branch RVO. The most common etiologic factor for the disease is the compression of atherosclerotic retinal arteries at the arterial-venous junction.[1] Risk factors for RVO include advanced age, diabetes mellitus (DM), hypertension, atherosclerotic disease, and glaucoma. Studies show mixed results regarding the involvement of hypercoagulability and inflammatory factors in its development.[2,3] Moreover, hypertension and diabetes may accelerate the progression of atherosclerosis, contributing to the development of RVO.[4] While the cause of RVO in younger people is not well understood, some case reports suggest inflammation, physical exercise, dehydration, and congenital anomalies as possible factors.[5]

The triglyceride-glucose (TyG) index is a marker of insulin resistance in healthy populations. Various studies have demonstrated that the TyG index is linked to the development of diabetes, high blood pressure, and metabolic syndrome. Recent research has also used this index as a marker for atherosclerosis in cardiovascular disease (CVD). The TyG index is considered clinically significant for evaluating vascular damage.[6] However, the normal range of the TyG index has not been determined in the literature, as varying results from different studies hinder a consensus. Thai et al.[7] reported that a higher TyG index value was related to a greater number of narrowed coronary arteries and more severe coronary stenosis. This suggests that the TyG index might be an effective parameter in assessing risk of atherosclerosis in patients with type 2 DM.

Clinicians need different non-invasive and simple tools to predict the presence of atherosclerosis.[8] A recent study with a small sample size (57 RVO patients) and age- and gender-matched controls examined the connection between the TyG index and RVO.[9] However, this study did not assess the burden of comorbidities in multivariate analysis. We hypothesized that a high TyG index may be linked to RVO independent of age, gender, and multiple comorbidities. Thus, this study aimed

to investigate the relationship between TyG index and other measurements in patients with RVO.

Materials and Methods

Study Population, Design, and Setting

This retrospective, observational, case-control study involved 492 participants aged 40-90 years who presented to the ophthalmology clinic of a tertiary center from January 2018 to March 2023. Patients with eye diseases other than RVO that were previously diagnosed by an ophthalmologist, patients under 40 years old, patients with advanced liver and kidney failure, patients who had active infections or uncontrolled chronic diseases, smokers and alcohol users, patients with impaired cognitive function, and patients who did not have blood test results recorded in the hospital system within the last month were excluded from the study.

Informed consent was not obtained because the study was retrospective. The study was approved by the Atatürk City Hospital Ethics Committee (no: 2023/2/15, date: 04.05.2023) and adhered to the Declaration of Helsinki.

Assessment of Atherosclerosis (TyG Index)

The TyG index is calculated as ln(fasting TG [mg/dL] × fasting plasma glucose [mg/dL]/2).[10]

Covariates for All Participants

Demographic (age, gender, chronic disease) and laboratory data of all patients, including hemograms and biochemical tests (glucose, triglycerides, total cholesterol, high-density lipoprotein, low-density lipoprotein) performed in the last month during routine outpatient follow-up visits were retrieved from the hospital's electronic records system.

We used the Deyo-Charlson comorbidity index to score the total comorbidity burden of multiple comorbid conditions.[11,12,13]

Statistical Analysis

The statistical analysis was performed using IBM SPSS Statistics version 22.0 (IBM Corp., Armonk, NY, USA). Kolmogorov-Smirnov test was used to assess whether the data showed normal distribution. Normally distributed values were expressed as mean ± standard deviation, while non-normally distributed values were expressed as median (min-max). Student's t-test or the Mann-Whitney U test was used to compare continuous variables. Chi-square test was used to compare categorical data. Multivariate and univariate logistic regression analyses were used to identify independent factors associated with RVO. A p value <0.05 was noted as statistically significant.

Results

The study included 492 participants (61.0% men) with an average age of 68.2±1.2 years. The RVO group consisted of 387 patients (181 women and 206 men) with a mean age of 62.9±11.1 years, while the control group consisted of 115 patients (61 women and 54 men) with a mean age of 56.7±8.7 years. Statistically significant age and sex differences were found between the two groups (p=0.01 and p=0.04, respectively).

There was no significant difference between the groups in Deyo-Charlson comorbidity index values (p=0.46) or triglyceride levels (p=0.35). However, a statistically significant difference was found between the RVO and control groups in terms of glucose (p=0.01) and mean TyG index value (p=0.04). The RVO group had a mean TyG index value of 8.9±0.7, while the control group had a mean TyG index value of 8.8±0.6 (Figure 1).

Associations of TyG Index with RVO

In the univariate logistic regression analysis, we observed an association between RVO and TyG index (odds ratio [OR]: 1.39, 95% confidence interval [CI]: 1.01-1.93, p=0.04), age (OR: 1.05, 95% CI: 1.03-1.08, p=0.01), and female sex (OR: 1.57, 95% CI: 1.02-2.44, p=0.04).

In the multivariate logistic regression analysis (Model), RVO was significantly associated with TyG index (OR: 1.45, 95% CI: 1.03-2.02, p=0.03) and age (OR: 1.06, 95% CI: 1.03-1.08, p=0.01). A 1.45-fold increased risk of RVO was observed among subjects with higher TyG index when compared to healthy individuals (Table 1).

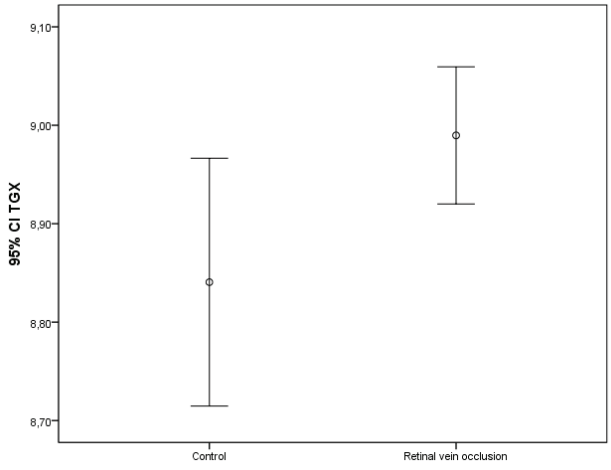

Figure 1. Comparison of triglyceride-glucose index between the retinal vein occlusion and control group
CI: Confidence interval, TGX: Triglyceride-glucose index

Table 1. Association between triglyceride-glucose index and retinal vein occlusion

	Unadjusted		Model	
	OR (95% CI)	p	OR (95% CI)	p
TyG index	1.39 (1.01-1.93)	0.04	1.45 (1.03-2.02)	0.03
Age	1.05 (1.03-1.08)	0.01	1.06 (1.03-1.08)	0.01
Gender (female)	1.57 (1.02-2.44)	0.04	1.55 (0.96-2.43)	0.06

Model: Adjusted for age and sex, OR: Odds ratio, CI: Confidence interval, TyG: Triglyceride-glucose

Discussion

The results of our research show that the TyG index was higher in the RVO group compared to the control group. This difference remained significant even when age and sex were taken into account. Our findings also suggest that a high TyG index score is a predictive factor for RVO. In fact, a high TyG index increased the risk of RVO by almost 50%. This is one of the first studies to demonstrate the association of TyG index with RVO, regardless of covariates such as age, sex, and comorbidity burden.

Insulin resistance is a crucial factor in the development of CVD.[14] Therefore, it is important to identify reliable markers for its assessment to stratify and predict risk. Recently, researchers have demonstrated that the TyG index, a cost-effective measure calculated from triglyceride levels and fasting glucose, is a dependable indicator of insulin resistance. This finding suggests that the TyG index may be a valuable tool for identifying individuals at higher risk of CVD and for tailoring interventions. Its simple measurement and strong predictive power make it a promising marker for clinical use.[10,15] In a cohort study of 49,579 participants, Li et al.[16] found that a high TyG index value was an independent predictor of an increased risk of CVD. In a recent study, we examined the TyG index values of patients with pseudoexfoliation syndrome, which is potentially caused by atherosclerotic changes. The study revealed a significant association between TyG index and pseudoexfoliation syndrome.[17] Consistent with prior research, we showed in this study that the TyG index, strongly linked to atherosclerotic vascular disease, was also associated with RVO. However, additional research and validation of the TyG index in diverse populations will be crucial for its widespread adoption in clinical practice.[18,19,20,21,22,23,24,25]

RVO is a widespread and long-lasting condition that poses a significant risk to vision and is closely associated with CVD. The disease is usually associated with typical atherosclerotic risk factors that are known to be related to various forms of RVO.[26] The retinal vein and artery share a common sheath, and the thin-walled vein traverses the thick and rigid arterial wall and extends posteriorly.[27,28,29] This mechanical constriction at the transition zones between artery and vein leads to hemodynamic changes, potentially causing chronic venous endothelial damage.[27,28,30] As a result, endothelial cell proliferation and vein wall remodeling contribute significantly to occlusion at these sites. The age-related increased stiffness of the retinal artery may increase the risk of compression and vascular occlusion at these junctions. Therefore, atherosclerosis and other cardiovascular risk factors that favor arteriolar sclerosis, such as systemic hypertension or diabetes, are prevalent in RVO patients.[31,32] The results of the present study are a valuable addition to the literature on this topic.

However, it is unclear whether the high TyG index observed in patients with potential sequelae of atherosclerosis is due to underlying neuropathologic changes that occur in diseases. To clarify this, we minimized the likelihood of changes due to uncontrolled diseases (e.g., DM, hypertension, CVD) through the exclusion criteria. The notable association between RVO and high TyG index values discovered in our study may provide further insight into the relationship between cardiovascular risk factors and the development of RVO. On the other hand, there may be other factors, including insulin level, glycosylated hemoglobin (HbA1c) and body mass index (BMI), that affect the TyG index and should be considered in future research.

Study Limitations

Strengths of this study are its community-based design, considerable sample size, and comprehensive clinical and ophthalmologic evaluations. The significance of the results persisted even after adjustment for several major confounding factors (age, sex, concomitant diseases). However, the study is limited by its retrospective, single-centered, case-control design without age and sex matching. Finally, even after adjusting for certain potential demographic and clinical variables, there may still be residual confounding factors (e.g., HbA1c, BMI). Therefore, prospective studies on this issue are needed to better characterize the relationship between TyG index and RVO.

Conclusion

The TyG index, a novel atherogenicity index derived from routine blood tests, has shown promise as a potential marker for RVO. This simple calculation may serve as a reliable indicator to identify individuals at high risk of RVO and initiate early intervention. Further prospective, randomized, controlled, large-scale research is needed to validate the TyG index in various populations and to fully understand its potential impact on RVO risk assessment and management.

Ethics

Ethics Committee Approval: Atatürk City Hospital Ethics Committee (no: 2023/2/15, date: 04.05.2023) and adhered to the Declaration of Helsinki.

Informed Consent: Retrospective study.

Authorship Contributions

Surgical and Medical Practices: Z.K., M.T., Concept: Z.K., M.T., Design: Z.K., Data Collection or Processing: Z.K., Analysis or Interpretation: Z.K., M.T., Literature Search: Z.K., Writing: Z.K., M.T.

Conflict of Interest: No conflict of interest was declared by the authors.

Financial Disclosure: The authors declared that this study received no financial support.

References

1. Nicholson L, Talks SJ, Amoaku W, Talks K, Sivaprasad S. Retinal vein occlusion (RVO) guideline: executive summary. Eye (Lond). 2022;36:909-912.
2. Chen TY, Uppuluri A, Zarbin MA, Bhagat N. Risk factors for central retinal vein occlusion in young adults. Eur J Ophthalmol. 2021;31:2546-2555.
3. Klien BA, Olwin JH. A survey of the pathogenesis of retinal venous occlusion, emphasis upon choice of therapy and an analysis of the therapeutic results in fifty-three patients. AMA Arch Ophthalmol. 1956;56:207-247.

4. Shantaram V. Pathogenesis of atherosclerosis in diabetes and hypertension. Clin Exp Hypertens. 1999;21:69-77.
5. Noma H, Yasuda K, Shimura M. Cytokines and pathogenesis of central retinal vein occlusion. J Clin Med. 2020;9:3457.
6. Sánchez-Íñigo L, Navarro-González D, Fernández-Montero A, Pastrana-Delgado J, Martínez JA. The TyG index may predict the development of cardiovascular events. Eur J Clin Invest. 2016;46:189-197.
7. Thai PV, Tien HA, Van Minh H, Valensi P. Triglyceride glucose index for the detection of asymptomatic coronary artery stenosis in patients with type 2 diabetes. Cardiovasc Diabetol. 2020;19:137.
8. Schmidt-Erfurth U, Garcia-Arumi J, Gerendas BS, Midena E, Sivaprasad S, Tadayoni R, Wolf S, Loewenstein A. Guidelines for the Management of Retinal Vein Occlusion by the European Society of Retina Specialists (EURETINA). Ophthalmologica. 2019;242:123-162.
9. Aslan Sirakaya H, Sirakaya E. Association of triglycerideglucose index in branch retinal vein occlusion. Graefes Arch Clin Exp Ophthalmol. 2024.
10. Tao LC, Xu JN, Wang TT, Hua F, Li JJ. Triglyceride-glucose index as a marker in cardiovascular diseases: landscape and limitations. Cardiovasc Diabetol. 2022;21:68.
11. Deyo RA, Cherkin DC, Ciol MA. Adapting a clinical comorbidity index for use with ICD-9-CM administrative databases. J Clin Epidemiol. 1992;45:613-619.
12. Charlson ME, Carrozzino D, Guidi J, Patierno C. Charlson Comorbidity Index: A Critical Review of Clinimetric Properties. Psychother Psychosom. 2022;91:8-35.
13. Cleves MA, Sanchez N, Draheim M. Evaluation of two competing methods for calculating Charlson's comorbidity index when analyzing short-term mortality using administrative data. J Clin Epidemiol. 1997;50:903-908.
14. Simental-Mendía LE, Rodríguez-Morán M, Guerrero-Romero F. The product of fasting glucose and triglycerides as surrogate for identifying insulin resistance in apparently healthy subjects. Metab Syndr Relat Disord. 2008;6:299-304.
15. Baydar O, Kilic A, Okcuoglu J, Apaydin Z, Can MM. The Triglyceride-Glucose Index, a Predictor of Insulin Resistance, Is Associated With Subclinical Atherosclerosis. Angiology. 2021;72:994-1000.
16. Li H, Zuo Y, Qian F, Chen S, Tian X, Wang P, Li X, Guo X, Wu S, Wang A. Triglyceride-glucose index variability and incident cardiovascular disease: a prospective cohort study. Cardiovasc Diabetol. 2022;21:105.
17. Abay RN, Katipoğlu Z. The correlation between pseudoexfoliation syndrome and the Triglyceride-Glucose index. Graefes Arch Clin Exp Ophthalmol. 2022;260:3903-3908.
18. Wang X, Xu W, Song Q, Zhao Z, Meng X, Xia C, Xie Y, Yang C, Jin P, Wang F. Association between the triglyceride-glucose index and severity of coronary artery disease. Cardiovasc Diabetol. 2022;21:168.
19. Irace C, Carallo C, Scavelli FB, De Franceschi MS, Esposito T, Tripolino C, Gnasso A. Markers of insulin resistance and carotid atherosclerosis. A comparison of the homeostasis model assessment and triglyceride glucose index. Int J Clin Pract. 2013;67:665-672.
20. Park K, Ahn CW, Lee SB, Kang S, Nam JS, Lee BK, Kim JH, Park JS. Elevated TyG Index Predicts Progression of Coronary Artery Calcification. Diabetes Care. 2019;42:1569-1573.
21. Lee EY, Yang HK, Lee J, Kang B, Yang Y, Lee SH, Ko SH, Ahn YB, Cha BY, Yoon KH, Cho JH. Triglyceride glucose index, a marker of insulin resistance, is associated with coronary artery stenosis in asymptomatic subjects with type 2 diabetes. Lipids Health Dis. 2016;15:155.
22. da Silva A, Caldas APS, Hermsdorff HHM, Bersch-Ferreira ÂC, Torreglosa CR, Weber B, Bressan J. Triglyceride-glucose index is associated with symptomatic coronary artery disease in patients in secondary care. Cardiovasc Diabetol. 2019;18:89.
23. Özkalaycı F, Karagöz A, Karabay CY, Tanboga İH, Türkyılmaz E, Saygı M, Oduncu V. Prognostic value of triglyceride/glucose index in patients with ST-segment elevation myocardial infarction. Biomark Med. 2022;16:613-622.
24. Tian X, Zuo Y, Chen S, Liu Q, Tao B, Wu S, Wang A. Triglyceride-glucose index is associated with the risk of myocardial infarction: an 11-year prospective study in the Kailuan cohort. Cardiovasc Diabetol. 2021;20:19.
25. Hong S, Han K, Park CY. The triglyceride glucose index is a simple and low-cost marker associated with atherosclerotic cardiovascular disease: a population-based study. BMC Med. 2020;18:361.
26. Ip M, Hendrick A. Retinal Vein Occlusion Review. Asia Pac J Ophthalmol (Phila). 2018;7:40-45.
27. Jefferies P, Clemett R, Day T. An anatomical study of retinal arteriovenous crossings and their role in the pathogenesis of retinal branch vein occlusions. Aust N Z J Ophthalmol. 1993;21:213-217.
28. Zhao J, Sastry SM, Sperduto RD, Chew EY, Remaley NA. Arteriovenous crossing patterns in branch retinal vein occlusion. The Eye Disease Case-Control Study Group. Ophthalmology. 1993;100:423-428.
29. Duker JS, Brown GC. Anterior location of the crossing artery in branch retinal vein obstruction. Arch Ophthalmol. 1989;107:998-1000.
30. Christoffersen NL, Larsen M. Pathophysiology and hemodynamics of branch retinal vein occlusion. Ophthalmology. 1999;106:2054-2062.
31. Mitchell P, Smith W, Chang A. Prevalence and associations of retinal vein occlusion in Australia. The Blue Mountains Eye Study. Arch Ophthalmol. 1996;114:1243-1247.
32. Klein R, Klein BE, Moss SE, Meuer SM. The epidemiology of retinal vein occlusion: the Beaver Dam Eye Study. Trans Am Ophthalmol Soc. 2000;98:133-141; discussion 141-143.

Original Article

Clinical Presentation of Carotid-Cavernous Fistula and Outcomes of Endovascular Balloon Embolization

Tayyaba Gul Malik*, Muhammad Moin**

*Postgraduate Medical Institute/Lahore General Hospital, Lahore, Pakistan
**College of Ophthalmology and Vision Sciences, Lahore, Pakistan

Abstract

Objectives: To describe the clinical presentation of carotico-cavernous fistula (CCF) and outcomes of endovascular balloon embolization in a tertiary care center in a developing country.

Materials and Methods: This retrospective interventional case series included 18 patients who underwent endovascular balloon embolization from 2019 to 2022 at Lahore General Hospital in Lahore, Pakistan. The analyzed data consisted of age, gender, cause and type of CCF, clinical presentation, diagnostic technique used, intervention, and the results of two-month follow-up. Patients with incomplete records and coil embolization were excluded. Digital subtraction angiography was done in all cases followed by endo-arterial balloon embolization. Procedures were carried out under general anesthesia via femoral artery approach. A single balloon was sufficient to close the fistula in all cases.

Results: There were 18 patients who met the inclusion criteria. Sixteen patients had direct CCF, and the mean age of the patients was 27.2±12.6 years. The commonest cause of CCF was trauma, and the mean time of presentation after trauma was 7.89±7.19 months. The male-to-female ratio was 8:1. Preoperative visual acuity was worse than 6/60 in 8 patients, between 6/60 and 6/18 in 7 patients, and better than 6/18 in 3 patients. The mean intraocular pressure was 16.06±3.37 mmHg preoperatively and 14.83±3.49 mmHg postoperatively (p=0.005). Endovascular embolization was successful in 15 patients (83.3%). One patient developed epidural hematoma as a complication of the procedure, which was drained later. There was no mortality related with the procedure.

Conclusion: Balloon embolization via the femoral artery is an efficient technique in direct as well as indirect CCF. It is safe and simple with very good results if performed in a timely manner.

Keywords: Carotid-cavernous fistula, balloon embolization, arterial embolization, digital subtraction angiography

Cite this article as: Malik TG, Moin M. Clinical Presentation of Carotid-Cavernous Fistula and Outcomes of Endovascular Balloon Embolization. Turk J Ophthalmol 2024;54:153-158

Address for Correspondence: Tayyaba Gul Malik, Postgraduate Medical Institute/Lahore General Hospital, Lahore, Pakistan
E-mail: tayyabam@yahoo.com **ORCID-ID:** orcid.org/0000-0003-1040-7114
Received: 10.09.2023 **Accepted:** 26.04.2024

DOI: 10.4274/tjo.galenos.2024.32457

Introduction

A carotid-cavernous fistula (CCF) refers to an abnormal connection between the internal carotid artery and the cavernous sinus. This connection disrupts normal blood flow dynamics, causing a decrease in arterial pressure and an increase in venous pressure. Consequently, an abnormal arteriovenous gradient develops, leading to reduced perfusion pressure. Clinically, CCF manifests as hypoxia, inflammation, and edema in the orbital and ocular tissues. The classic triad associated with direct CCF consists of the sudden onset of proptosis, the presence of a bruit, and conjunctival congestion, collectively known as the "Dandy triad".[1] While the clinical presentation of CCF, particularly direct CCF, may exhibit characteristic features, confirming the diagnosis requires neuroimaging. Digital subtraction angiography (DSA) is regarded as the gold standard for diagnosis and should be conducted before considering any potential interventions.[2]

As CCF is generally not life-threatening in most cases and the eye is at maximum risk, patients typically present to the ophthalmology department. The approach to treating CCF varies depending on the individual patient and is based on the clinical presentation at the time of diagnosis. Management options encompass conservative measures, endovascular intervention, open surgery, and radiosurgery. For cases of indirect CCF with normal vision, conservative treatment with vigilant monitoring for any signs of visual disturbance is often recommended. In other instances, treatment is pursued to alleviate symptoms, preserve vision, and close the fistula. At present, endovascular treatment is considered the primary choice for many direct CCF cases. It boasts a high rate of occlusion and a lower incidence

of complications.[3] This method involves the use of detachable balloons, coils, stents, or liquid embolic agents such as Onyx.[4]

Endovascular embolization can be performed through either the transarterial or transvenous route. Both approaches are effective, but in situations involving vascular fragility, such as Ehlers-Danlos syndrome, the transvenous route is recommended to minimize the risk of arterial injury.[5]

Endovascular embolization is not commonly performed in Pakistan, leading to limited available data regarding the outcomes of this treatment modality.[6] In the United States, coil embolization has replaced balloon embolization. However, in developing countries like Pakistan, balloon embolization remains a safe and effective first-line treatment. Despite its lower prevalence, it is considered a simple and safe approach. This case series presents the results of balloon embolization in 18 patients, including demographic data and success rates.

Materials and Methods

This study was a retrospective interventional case series that included the records of 18 patients with either direct or indirect CCF. The patients underwent endovascular balloon embolization between 2018 and 2022 at Lahore General Hospital in Lahore, Pakistan. The research received approval from the U.S. Department of Health and Human Services (HHS) (certificate no: OSP-IRB/022-2022, date: 31.01.2022), and adherence to the Declaration of Helsinki was observed for the publication of human data.

The collected data included various parameters such as age, gender, cause and type of CCF, clinical presentation, visual status, intraocular pressure (IOP), fundus findings, diagnostic techniques used, interventions, and the results of two-month follow-up. Patients with incomplete records and those who underwent coil embolization were excluded.

All patients underwent detailed ocular examinations. Diagnostic tools such as computed tomography (CT), magnetic resonance imaging (MRI), and orbital B-scan ultrasound were employed to confirm the presence of the fistula, which was further verified through DSA. An interventional radiologist performed the endoarterial embolization.

Procedures were conducted under general anesthesia using a femoral artery approach. A microcatheter with detachable balloon was directed towards the cavernous sinus, inflated to a size greater than the fistula for closure, and then detached. Notably, only one balloon was needed to close the fistula in this case series. DSA was repeated after embolization. Postoperatively, patients were advised against straining to prevent balloon displacement.

Statistical Analysis

The data were analyzed in Microsoft Excel and presented as percentage, mean, and standard deviation values. A paired t-test was applied to compare pre- and postoperative IOP values.

Results

There were 18 patients who met the inclusion criteria. Sixteen patients had direct CCF, the mean age of the patients was 27.2±12.6 years, and the male-to-female ratio was 8:1. The commonest cause of CCF was trauma (n=14, 77.8%). The mean time of presentation after trauma was 7.89±7.19 months. Fracture of the skull bones was seen in 5 patients (27.8%). Other clinical features are presented in Table 1.

Figures 1 and 2 show the preoperative findings of a patient with posttraumatic CCF, while Figure 3 shows a dilated superior ophthalmic vein on the right side in a CT scan. Figure 4 shows pre- and post-embolization DSA results.

The patients' visual acuity and IOP values are presented in Table 2. There was no significant difference in terms of the distribution of pre- and postoperative visual acuities (Figure 5).

Table 1. Clinical findings at the time of presentation

Clinical feature	n (%)
Nose bleed	8 (44.4)
Unconsciousness	8 (44.4)
Diplopia	7 (38.9)
Proptosis (mean: 5.94±2.67 mm)	18 (100)
Dystopia	14 (77.8)
Chemosis	13 (72.2)
Engorged vessels	17 (94.4)
Central retinal vein occlusion	6 (33.3)
Choroidal folds	3 (16.7)
Optic atrophy	5 (27.7)
Total ophthalmoplegia	6 (33.3)
Partial oculomotor nerve palsy	2 (11.1)
Oculomotor and trochlear nerve palsy	1 (5.6)
Abducens nerve palsy	1 (5.6)
Trochlear and abducens nerve palsy	1 (5.6)
Bruit	5 (27.7)

Figure 1. Posttraumatic right carotid-cavernous fistula with proptosis, chemosis, conjunctival prolapse, and cataract

Figure 2. Positive Valsalva test

Figure 3. Dilated superior ophthalmic vein on computed tomography scan

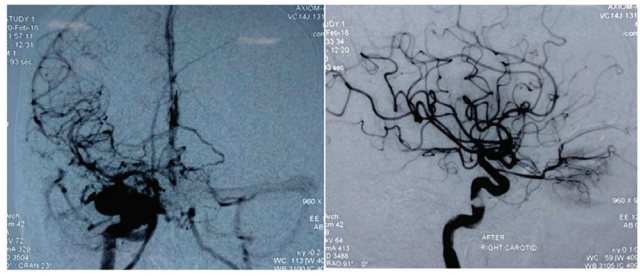

Figure 4. Digital subtraction angiography before balloon embolization (left panel) and after embolization (right panel)

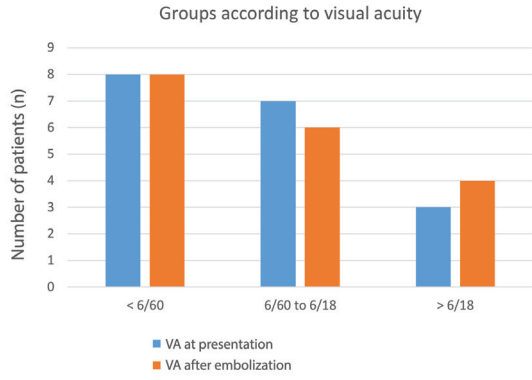

Figure 5. Comparison of visual acuity before and after balloon embolization
VA: Visual acuity (Snellen)

Table 2. Pre- and postoperative visual acuity and intraocular pressure

Patient	Preoperative IOP (mmHg)	Postoperative IOP (mmHg)	Visual acuity at presentation (Snellen)	Visual acuity after embolization (Snellen)
1	14	16	6\9	6\6
2	20	19	No light perception	No light perception
3	15	14	6\60	6\36
4	15	15	6\18	6\12
5	24	20	No light perception	No light perception
6	16	15	Counting fingers	Counting fingers
7	18	16	Light perception	No light perception
8	19	20	No light perception	No light perception
9	14	14	6\18	6\18
10	12	11	6\12	6\9
11	10	8	Hand movements	Hand movements
12	18	17	Counting fingers	Counting fingers
13	19	18	No light perception	No light perception
14	16	14	6\9	6\6
15	14	13	6\36	6\60
16	18	17	6\36	6\24
17	12	10	6\18	6\18
18	15	10	6\36	6\36

IOP: Intraocular pressure

Preoperatively, there were 8 patients with visual acuity worse than 6/60, 7 patients with visual acuity of 6/60 to 6/18, and 3 patients with visual acuity better than 6/18. There was no significant improvement in post-embolization visual acuity. The mean IOP was 16.06±3.37 mmHg preoperatively and 14.83±3.49 mmHg postoperatively (p=0.0046).

Endovascular embolization was successful in 15 patients (83.3%). Among the other three, one patient developed epidural hematoma as a complication of the procedure, which was drained later. The other two had very large fistulas which resulted in failure of the procedure. There was no mortality related to the procedure.

Discussion

CCF is a complex condition with diverse etiologies, pathogenesis, presentations, and radiographic features, necessitating various treatment strategies. The condition is relatively uncommon, especially outside of tertiary care centers with neurological facilities, making it challenging to determine its exact incidence. Notably, traumatic brain injuries are reported to contribute to 0.2% to 4% of CCF cases.[7,8]

In our case series, 77% of the patients presented with traumatic CCF following closed or penetrating head injuries and fractures at the base of the skull. The majority of these cases occurred in males, with a male-to-female ratio of 8:1 in our series. This may be attributed to a higher prevalence of outdoor trauma in males. Interestingly, these findings differ from those reported in a study by Alexander et al.[9] in which the majority of patients were females (78.3%) and the mean age was 61 years. However, in contrast to our study, Alexander et al.[9] included only patients with indirect fistulas. The mean duration from the onset of symptoms to diagnosis in our study was 234 days, providing insight into the delayed recognition of CCF in our patient cohort.

In another series reported by Iampreechakul et al.[10], a different demographic profile was observed, with a male-to-female ratio of 1:2 and a mean age of 47.3 years, contrasting with the younger patient population in our study (mean age 27.2±12.6 years). Despite these differences, the percentage of traumatic CCF in their series (71.7%) closely resembled our findings (77.8%).

Permana et al.[4] conducted a study involving 28 patients who underwent endovascular treatment. In this cohort, there was a female preponderance, with 15 females (54%) and 13 males (46%). Notably, they included patients with traumatic CCF. The presence of cephalic bruit was reported in 28% of their cases, a figure close to our percentage of 27.7%. These variations in demographic characteristics and clinical features highlight the diverse nature of CCF and underscore the importance of considering multiple factors when formulating treatment strategies.

The literature describes anterior and posterior patterns of CCF based on drainage. The anterior pattern typically presents with ocular signs, while the posterior pattern may manifest as a "white eye" associated with isolated ocular nerve palsy. Diagnosing the posterior drainage pattern can be challenging without neuroimaging, as ocular signs may be less apparent.

Some patients with CCF may present with raised IOP due to increased episcleral venous pressure, ciliary body edema, or neovascularization secondary to ischemia. Interestingly, in this study, 33.3% of patients had central retinal vein occlusion associated with CCF. Although not observed in our series, rare complications of CCF include retinal detachment, vitreous hemorrhage, and choroidal effusions.[11] These findings emphasize the diverse clinical presentations and potential complications associated with CCF, reinforcing the need for comprehensive evaluation and neuroimaging when suspecting this condition.

Diagnostic techniques for CCF have significantly advanced in recent years. On MRI, CCF is characterized by proptosis, extraocular muscle enlargement, and a dilated superior ophthalmic vein. The dilated superior ophthalmic vein is typically observed in 86%-100% of cases using contrast-enhanced CT and 75%-100% using T1-weighted post-contrast MRI. CT scans also provide the added advantage of easily visualizing fractures. Other neuroimaging techniques such as CT angiography (CTA) and magnetic resonance angiography (MRA) are employed for diagnosis. The reported sensitivities for CTA, MRA, and DSA are 87%, 80%, and 94.4%, respectively.[12,13] In this study, we used DSA, which is considered the gold standard for diagnosing and classifying CCF. These improved diagnostic modalities enhance the accuracy and efficiency of identifying and classifying CCF, allowing for more precise clinical management.

In our series, we specifically included patients who underwent balloon embolization, and our success rate reached 83.3%. This success rate aligns well with findings from another study, where the success rate for CCF treatments ranged from 75% to 88%.[14] Notably, technical challenges during the procedure, such as insufficient embolization due to early balloon detachment, balloon deflation, or rupture, did not occur in any of the 15 successful cases out of the total 18 in our study. These favorable outcomes suggest the effectiveness of balloon embolization in the management of CCF in our patient series.

Another study conducted at Aga Khan Medical University in Pakistan included 26 patients, 20 males and 6 females, with a mean age of 31.4±12.6 years.[6] This study exhibited several similarities to our case series, particularly in terms of the male predominance. However, their reported success rate was higher than that in our series. The variance in success rates could be attributed to the fact that the Aga Khan study involved repeated sessions for four patients who were unsuccessful in the initial attempt.[6] In contrast, our study only included cases treated successfully in the primary surgical intervention.

The complication rate in our study was 5.5%, whereas the Aga Khan study reported a higher complication rate of 15.3%.[6] After a 2-month follow-up period, symptom resolution was observed but there was no improvement in vision. These findings underscore the importance of considering the approach and potential complications when evaluating the outcomes of endovascular treatments for CCF.

Given the anatomical proximity of the cavernous sinus to the cranial nerves, CCF often presents with associated nerve palsies. Abducens nerve palsy is reported in 50%-80% of cases, oculomotor nerve palsy in 67%, and trochlear nerve palsy in 49%.[15] In our series, 33% of cases exhibited complete ophthalmoplegia. Among single nerve palsies, the third nerve was affected in 11%, and sixth nerve palsy occurred in 5.6%. Combined third and fourth nerve palsy or fourth and sixth nerve palsy each accounted for 5.6%. Notably, the abducens nerve, located within the cavernous sinus, is more susceptible to injury compared to other intracavernous nerves. However, in real-life scenarios, the third nerve is more commonly affected. It is crucial to acknowledge that nerve palsies can also result from the embolization process. Teng et al.[16] reported a rare complication associated with migration of the balloon during embolization, leading to iatrogenic ophthalmoplegia. These findings highlight the intricacies and potential complications associated with CCF and its management, underscoring the need for careful consideration of cranial nerve involvement during diagnosis and treatment.

In our case series, proptosis was observed in 100% of cases, and additional clinical features included engorged ocular vessels, chemosis, dystopia, nosebleeds, central retinal vein occlusion, choroidal folds, and optic atrophy. Our failure rate was 3 out of 18 cases, amounting to 16.7%. It is noted that the failure rate tends to increase with an extended interval between trauma and treatment. In our study, the mean time of presentation was 7.89±7.19 months. Another factor contributing to failure is the size of the fistula; if it exceeds the inflated balloon size, it can result in treatment failure. These considerations emphasize the importance of timely intervention and careful assessment of fistula characteristics for successful outcomes in the management of CCF.

Gao et al.[17] presented a substantial series of 188 patients who underwent balloon embolization, with a high success rate of 96.8% (n=182). The angiographic occlusion rate reached 97.3%. Notably, the study reported three cases of balloon rupture attributed to basal fracture bone pieces. The research underscored the significance of the disease course and advanced age, noting that cavernous sinus enlargement due to bone resorption secondary to flow can contribute to procedural failure.

Recurrence is also documented in the literature, with multivariate logistic regression analysis revealing that incomplete embolization is a risk factor for recurrence (odds ratio [OR]: 16.63, 95% confidence interval [CI]: 1.74-159.33, p=0.015).[18] However, in our study with limited follow-up, no recurrence was observed in the 15 cases that underwent successful embolization. These findings emphasize the need for a thorough understanding of the factors influencing the success of balloon embolization and recurrence in the management of CCF.

In a comprehensive review including 57 studies and 1575 patients, transarterial embolization of CCF resulted in complete closure in 93.93% of direct fistulas and 81.51% of indirect fistulas.[19] Transvenous embolization, on the other hand, led to closure in 91.67% of direct CCFs and 86.03% of indirect CCFs. Notably, there were no statistically significant differences between the two routes for direct CCFs (OR: 1.42, 95% CI: 0.23-8.90, I^2: 0.0%) or indirect CCFs (OR: 0.62, 95% CI: 0.31-1.23, I^2: 0.0%). These findings highlight the comparable efficacy of transarterial and transvenous embolization routes in achieving closure of both direct and indirect CCF.

In an additional series that encompassed both traumatic and spontaneous fistulas, a remarkable 100% closure of fistulas was achieved.[20] Out of the 25 cases, 20 were successfully closed in a single session, four required two sessions, and one case spontaneously closed. Unlike our case series, this study employed a combination of arterial and venous approaches for intervention. Their treatment modalities included coils, stents, detachable balloons, n-butyl cyanoacrylate, and combined embolization.

The intervention strategy varies, suggesting that different embolization techniques and materials are employed based on the size and nature of the fistula. Some authors recommend balloon embolization for medium and large fistulas, while coil embolization is suggested for smaller fistulas.[21] In cases where CCF closure is not achieved, occlusion of the affected artery is also recommended.

Although angiographic closure of CCF is typically excellent after embolization, improvement in visual acuity is contingent upon the preintervention status. However, there is often an immediate postoperative improvement in bruit, and other ocular symptoms tend to regress over the course of weeks. These diverse approaches and outcomes underscore the individualized nature of CCF management and the importance of tailoring interventions based on the specific characteristics of each case.

The strength of this series lies in its contribution to the limited available data from developing countries like Pakistan regarding CCF management. This case series adds valuable insights to the literature from a third-world perspective, where medical and health facilities may be scarce. By providing information and experiences from a region with unique healthcare challenges, this series helps broaden the understanding of CCF and its management in diverse healthcare settings. It may contribute to the development of more context-specific approaches to diagnosis and treatment, potentially benefiting patients in similar regions with limited medical resources.

Study Limitations

This study has several limitations, primarily due to its retrospective nature. The follow-up duration of only two months is relatively short, potentially limiting the ability to assess long-term outcomes and recurrence rates. The sample size is also acknowledged as small, but given the rarity of CCF, it was considered acceptable. However, it is essential to recognize that larger sample sizes would provide a more robust basis for drawing conclusions.

To address these limitations and enhance the understanding of CCF management, further research involving controlled and randomized trials is recommended. These studies could provide more comprehensive insights into the efficacy and safety of

different treatment modalities and enable a more thorough exploration of long-term outcomes and potential complications.

Conclusion

In conclusion, balloon embolization is an efficient technique for the management of CCF, especially in low-resourced countries. This approach is characterized by its safety, simplicity, and demonstrated effectiveness, particularly when performed in a timely manner. The results from this study add to the limited data from a third-world country like Pakistan. While recognizing the retrospective nature and other limitations of the study, the findings underscore the potential benefits of balloon embolization in CCF cases. Further research, including controlled trials and larger sample sizes, would be valuable to deepen our understanding and refine the approach to CCF management.

Ethics

Ethics Committee Approval: U.S. Department of Health and Human Services (HHS) (certificate no: OSP-IRB/022-2022, date: 31.01.2022).

Informed Consent: Obtained.

Authorship Contributions

Surgical and Medical Practices: T.G.M., M.M., Concept: T.G.M., M.M., Design: T.G.M., M.M., Data Collection or Processing: T.G.M., M.M., Analysis or Interpretation: T.G.M., M.M., Literature Search: T.G.M., Writing: T.G.M.

Conflict of Interest: No conflict of interest was declared by the authors.

Financial Disclosure: The authors declared that this study received no financial support.

References

1. Joshi DK, Singh DD, Garg DD, Singh DH, Tandon DM. Assessment of clinical improvement in patients undergoing endovascular coiling in traumatic carotid cavernous fistulas. Clin Neurol Neurosurg. 2016;149:46-54.
2. Williams ZR. Carotid-Cavernous Fistulae: A Review of Clinical Presentation, Therapeutic Options, and Visual Prognosis. Int Ophthalmol Clin. 2018;58:271-294.
3. Gemmete JJ, Ansari SA, Gandhi DM. Endovascular techniques for treatment of carotid-cavernous fistula. J Neuroophthalmol. 2009;29:62-71.
4. Permana GI, Suroto NS, Al Fauzi A. Clinical Improvement of Patients with Endovascular Treatment in the Traumatic Carotid-Cavernous Fistula. Asian J Neurosurg. 2021;16:376-380.
5. Ide S, Kiyosue H, Tokuyama K, Hori Y, Sagara Y, Kubo T. Direct Carotid Cavernous Fistulas. J Neuroendovasc Ther. 2020;14:583-592.
6. Hamid RS, Tanveer-ul-Haq, Shamim MS, Kazim SF, Salam B. Endovascular approach as primary treatment for traumatic carotid cavernous fistula: local experience from Pakistan. J Pak Med Assoc. 2011;61:989-993.
7. Liang W, Xiaofeng Y, Weiguo L, Wusi Q, Gang S, Xuesheng Z. Traumatic carotid cavernous fistula accompanying basilar skull fracture: a study on the incidence of traumatic carotid cavernous fistula in the patients with basilar skull fracture and the prognostic analysis about traumatic carotid cavernous fistula. J Trauma. 2007;63:1014-1020.
8. Ono K, Oishi H, Tanoue S, Hasegawa H, Yoshida K, Yamamoto M, Arai H. Direct carotid-cavernous fistulas occurring during neurointerventional procedures. Interv Neuroradiol. 2016;22:91-96.
9. Alexander MD, Halbach VV, Hallam DK, Cooke DL, Ghodke B, Dowd CF, Amans MR, Hetts SW, Higashida RT, Meyers PM. Relationship of clinical presentation and angiographic findings in patients with indirect cavernous carotid fistulae. J Neurointerv Surg. 2019;11:937-939.
10. Iampreechakul P, Tirakotai W, Tanpun A, Wattanasen Y, Lertbusayanukul P, Siriwimonmas S. Spontaneous resolution of direct carotid-cavernous fistulas: case series and literature review. Interv Neuroradiol. 2019;25:71-89.
11. Chaudhry IA, Elkhamry SM, Al-Rashed W, Bosley TM. Carotid cavernous fistula: ophthalmological implications. Middle East Afr J Ophthalmol. 2009;16:57-63.
12. Adam CR, Shields CL, Gutman J, Kim HJ, Hayek B, Shore JW, Braunstein A, Levin F, Winn BJ, Vrcek I, Mancini R, Linden C, Choe C, Gonzalez M, Altschul D, Ortega-Gutierrez S, Paramasivam S, Fifi JT, Berenstein A, Durairaj V, Shinder R. Dilated Superior Ophthalmic Vein: Clinical and Radiographic Features of 113 Cases. Ophthalmic Plast Reconstr Surg. 2018;34:68-73.
13. Henderson AD, Miller NR. Carotid-cavernous fistula: current concepts in aetiology, investigation, and management. Eye (Lond). 2018;32:164-172.
14. Lu X, Hussain M, Ni L, Huang Q, Zhou F, Gu Z, Chen J, Ding Y, Xu F. A comparison of different transarterial embolization techniques for direct carotid cavernous fistulas: a single center experience in 32 patients. J Vasc Interv Neurol. 2014;7:35-47.
15. Holland LJ, Mitchell Ranzcr K, Harrison JD, Brauchli D, Wong Y, Sullivan TJ. Endovascular treatment of carotid-cavernous sinus fistulas: ophthalmic and visual outcomes. Orbit. 2019;38:290-299.
16. Teng MM, Chang CY, Chiang JH, Lirng JF, Luo CB, Chen SS, Chang FC, Guo WY. Double-balloon technique for embolization of carotid cavernous fistulas. AJNR Am J Neuroradiol. 2000;21:1753-1756.
17. Gao BL, Wang ZL, Li TX, Xu B. Recurrence risk factors in detachable balloon embolization of traumatic direct carotid cavernous fistulas in 188 patients. J Neurointerv Surg. 2018;10:704-707.
18. Zhenxing Y, Yangyang S, Fangqin S, Dejun H, Zongzheng L. Endovascular treatment of traumatic direct carotid-cavernous fistulas: a retrospective case series study of 54 patients. Int J Cerebrovasc Dis. 2020;8:605-612.
19. Texakalidis P, Tzoumas A, Xenos D, Rivet DJ, Reavey-Cantwell J. Carotid cavernous fistula (CCF) treatment approaches: A systematic literature review and meta-analysis of transarterial and transvenous embolization for direct and indirect CCFs. Clin Neurol Neurosurg. 2021;204:106601.
20. Sanal B, Nas OF, Korkmaz M, Erdogan C, Hakyemez B. Endovascular Treatment in Traumatic and Spontaneous Carotid Cavernous Fistulas: with Different Embolization Agents and via Various Vascular Routes. J Vasc Interv Neurol. 2018;10:18-24.
21. Thohar Arifin M, Ali Akbar M, Illyasa W, Tsaniadi Prihastomo K. Neuro-Endovascular Intervention in Traumatic Carotico-Cavernous Fistulae: A Single-Center Experience. Int J Gen Med. 2020;13:917-925.

Review

Tissue Engineering and Ophthalmology

Canan Aslı Utine*,**, Sinan Güven**,***,****

*Dokuz Eylül University Faculty of Medicine, Department of Ophthalmology, İzmir, Türkiye
**İzmir Biomedicine and Genome Center, İzmir, Türkiye
***Dokuz Eylül University, İzmir International Biomedicine and Genome Institute, İzmir, Türkiye
****Dokuz Eylül University Faculty of Medicine, Department of Medical Biology and Genetics, İzmir, Türkiye

Abstract

Tissue engineering (TE) is a field of science that combines biological, engineering, and medical sciences and allows the development of disease models, drug development and gene therapy studies, and even cellular or tissue-based treatments developed by engineering methods. The eye is an organ that is easily accessible and amenable to engineering applications, paving the way for TE in ophthalmology. TE studies are being conducted on a wide range of topics, including the tear film, eyelids, cornea, optic nerve, glaucoma, and retinal diseases. With the rapid scientific advances in the field, it seems that TE is radically modifying the management of ocular disorders.

Keywords: Tissue engineering, gene therapy, disease model, drug development, regenerative medicine

Cite this article as: Utine CA, Güven S. Tissue Engineering and Ophthalmology. Turk J Ophthalmol 2024;54:159-169

Address for Correspondence: Canan Aslı Utine, Dokuz Eylül University Faculty of Medicine, Department of Ophthalmology, İzmir, Türkiye
E-mail: cananutine@gmail.com **ORCID-ID:** orcid.org/0000-0002-4131-2532
Received: 03.09.2023 **Accepted:** 12.04.2024

DOI: 10.4274/tjo.galenos.2024.49779

Introduction

Tissue engineering (TE) is a discipline based on the principles of biology, engineering, developmental biology, and the medical and morphogenesis sciences for tissue healing, treatment, and regeneration. TE aims to treat, repair, or replace damaged biological tissues and organs using cells and appropriate physiological factors combined with bioengineering, biomedical engineering, and materials sciences. TE also includes developing disease models, creating tissue scaffolds for cells, and administering active drug components to tissues.[1] Knowledge of how to control and regulate the intrinsic regeneration potential of the tissues is crucial.[2] The ultimate aim is to create artificial tissue or organ models to support medicine and the life sciences.

The eye tissues originate from epithelial, mesenchymal, connective, and neural tissue sources with precisely regulated structural and functional integration (Figure 1). TE has been used to achieve the above-mentioned objectives in the cornea, lacrimal gland, retina, optic nerve, and conditions like glaucoma, with significant progress from bench to bedside. The use of TE in ophthalmology includes, but is not limited to, the following:

a. Disease Models

Animal models may not faithfully recapitulate human pathogenic processes due to species differences.[3] With recent developmental milestones in microfluidic chips, stem cells, cellular signaling, and biomechanics, *organ-on-a-chip* technology has emerged from TE.[4] Microfluidic systems are designed to demonstrate the dynamic, functional, and pathophysiological properties of the tissues in living conditions. In a microfluidic system, specially designed channels are created in glass or polymeric materials, in which the biomaterials that constitute the tissue skeleton are seeded with specific cells that are cultivated to produce a three-dimensional (3D) structure that approximates physiologic conditions. These advanced engineered systems are

designed to recapitulate the unique microenvironment of organs *in vivo* and reproduce *in vitro* disease models.[4,5] Organ-on-a-chip systems can study the essential functions of one specific tissue/organ (i.e., "one-organ systems") or the interactions and reactions of multiple organs/tissues within a single system (i.e., "multi-organ platforms").

Recent advances have proven the feasibility of modeling human diseases with patient-specific induced pluripotent stem cells (iPSCs).[6] iPSCs are generated from a somatic cell line without using human embryos and can differentiate into any somatic cell. This represents a fundamental tool for studying disease pathogenesis and performing drug development studies (Figure 2).[7]

The organ-on-a-chip microfluidic technologies have increased our understanding of basic ocular physiology and disease pathogenesis. Overcoming the shortcomings of two-dimensional cell culture, they let us develop clinically relevant substitutes for eye treatment.[8] As an example, a microfluidic platform has been developed to dynamically cultivate the corneal epithelial barrier to study the effects of blinking shear stress on the human ocular surface and guide the development of ophthalmic drugs.[9] Similar systems can imitate and be used to evaluate the corneal epithelial wound repair process.[10] In another study, a microfluidic 3D microengineered cornea-on-a-chip was constructed based on primary mouse corneal epithelial and endothelial cells to realize basic corneal functions and facilitate research on topical drug delivery.[11]

In glaucoma research, TE approaches have been used to recreate the trabecular meshwork (TM) since the late 1980s. Cellulose porous filters with human TM cells grown on them, hydrogel molding, and photolithography techniques were used to study the effect of stiffness on gene expression and mechanotransducers, the mechanism of action of drugs on the TM, and drug repurposing.[12] Furthermore, a decellularized, tissue-engineered anterior segment eye culture was transplanted with TM cells to see if outflow structure and function would be restored. The engineered anterior segment scaffolds served as scalable ocular perfusion cultures to decrease the dependency on donor globes for outflow research and enable studies on perfusion cultures with specific genotypes and phenotypes.[13] A bioengineered synthetic 3D *in vitro* TM model can also be used to study detailed mechanisms of intraocular pressure (IOP) regulation to develop a glaucoma disease model and allow high-throughput screening of glaucoma drugs. This involves selecting and designing biomaterials for scaffold fabrication and extracellular matrix (ECM) components to mimic the trabecular architecture.[14]

Evaluation of retinal ganglion cells (RGCs) and their degeneration is also imperative in glaucoma research. TE methods to generate iPSCs from the blood or skin of glaucoma patients and induce them to differentiate into RGCs are valuable approaches in pathogenesis studies.[15]

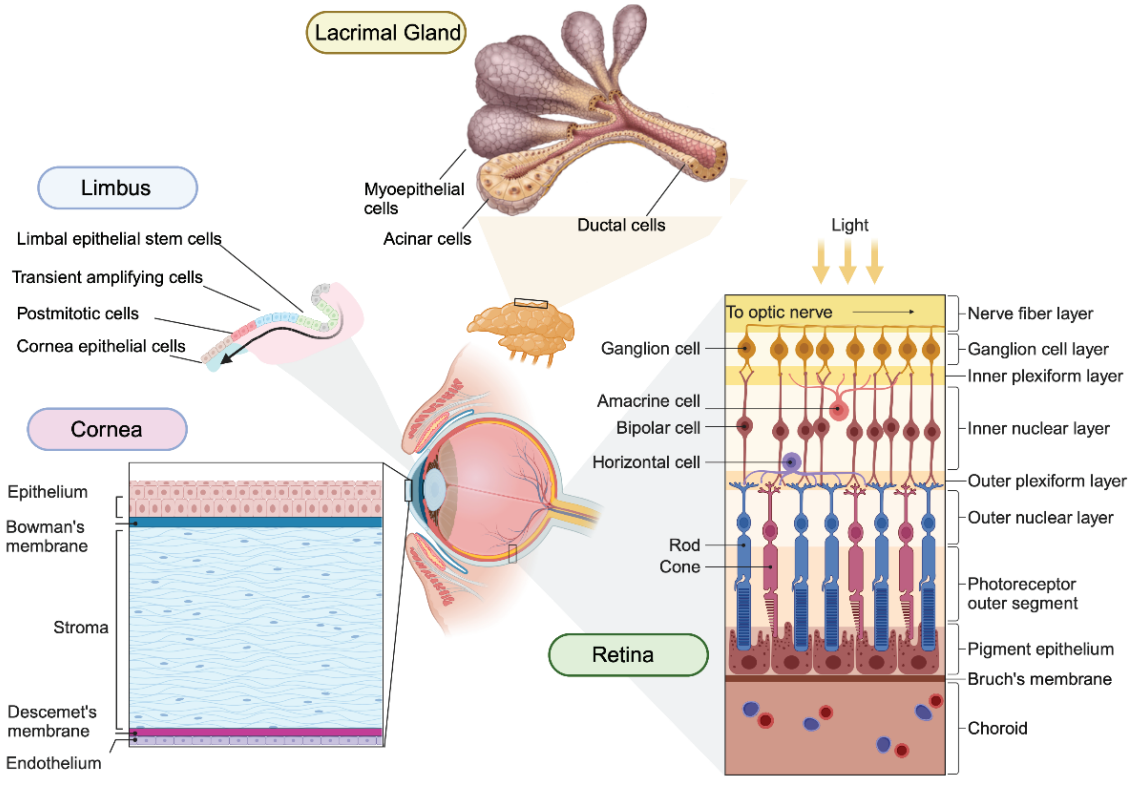

Figure 1. Schematic representation of ocular cell types and tissues. Diverse phenotypes and functions of ocular cells collectively establish and maintain vision

On the other hand, iPSCs can form self-assembled 3D structures that, upon differentiation, generate miniaturized organ mimicries named *organoids*. Organoids can recapitulate the cellular heterogeneity and architecture of organs and are excellent tools for studying the developmental phases of human tissues *in vitro*. Increasing interest in organoid research has also led to novel approaches in ophthalmology. iPSC-derived retinal organoids serve as 3D models of embryonic development, pathologies, and new therapeutic avenues for retinal diseases due to their high stability and similarity to native retinas.[16] Structures of the lens, neural retina, and retinal pigmented epithelium (RPE) cells have already been generated from undifferentiated embryonic stem cells (ESC) in a defined culture system.[17] Furthermore, 3D models of the human outer blood-retina barrier have been engineered to recapitulate critical features of healthy RPE-choriocapillaris interactions in dry and wet age-related macular degeneration (AMD) phenotypes.[18,19]

Optic nerve head (ONH) disease models have yet to be developed because of significant challenges which include the lack of a systems biology description of the ONH and large-scale gene expression and phenotype data in glaucoma, as well as insufficient knowledge about the roles of astrocytic and non-astrocytic ECM cells in tissue remodeling and the effect of actual IOP at the ONH on the tissues.[20] However, as iPSC-derived glaucomatous RGCs were shown to suffer from mitochondrial deficiency, improving mitochondrial biogenesis could be studied to reverse the disease process.[21] Merging more than one type of organoid results in more complex cellular structures named *assembloids*. Advanced *in vitro* models of diverse tissues resemble a more native-like environment, supporting and improving functional outcomes.

b. Drug Development Studies

TE provides a means for preliminary drug screening that reduces the need for highly criticized and expensive animal experiments, which are often poorly predictive of human physiology.[1] Indeed, in 2022 the FDA Modernization Act 2.0 eliminated the animal testing requirement for newly developed drugs before being given to humans. While the new law does not ban animal testing, it makes allowances for the use of new technologies such as artificial intelligence and organ-on-a-chip technology, where pharmaceuticals are tested on microchips that mimic organ function. Organ-on-a-chip models are expected to replace most drug and toxicity experiments in animal models.[22]

Bennet et al.[23] have grown immortalized human corneal epithelial cells in a microfluidic system to create a "corneal epithelial chip" to study eye drop transport. Another dynamic microengineered human corneal system has also been used for *in vitro* drug absorption studies.[24] A microfluidic plastic-based chip was used for *in vitro* 3D vascular network reconstruction in normal and pathological ocular angiogenesis studies and antiangiogenic drug testing.[25]

Drug repurposing is a feasible approach to identify new therapeutic uses for drugs approved for other diseases. The molecular mechanisms of action and the pharmacokinetic and pharmacodynamic properties of existing medicinal agents

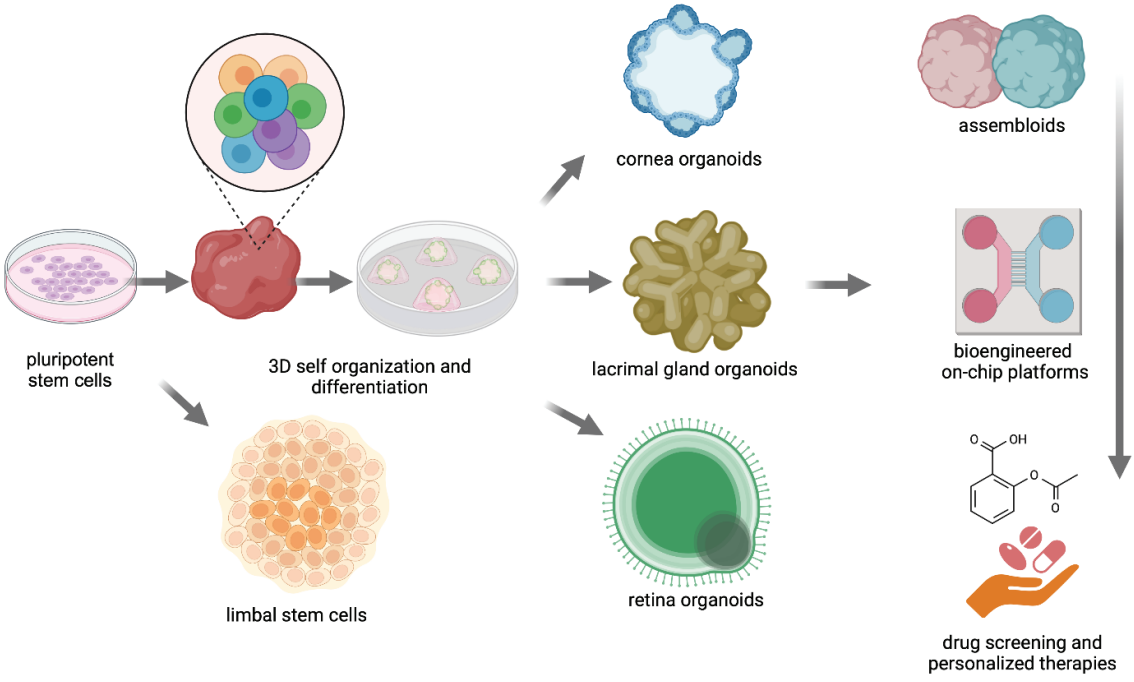

Figure 2. Pluripotent stem cells can give rise to all cell types, forming ocular cells and organoids. Ocular organoids and assembloids provide *in vitro* models to study the development of the eyes and related diseases. Bioengineered on-chip platforms can recapitulate physical and biochemical stimuli in a precisely controlled microenvironment, resulting in more realistic models in drug screening and personalized therapies in ophthalmology

are explored from the perspective of their pharmacological targets to redirect them to uncovered areas. The safety and efficacy of these drugs have already been established, saving time and cost. Structural modification, novel delivery system development, or combination with other medications are needed for some medicines requiring TE approaches. The development of controlled drug release systems is also possible.

The evolution of the use of cyclosporine A (CsA) in ophthalmology is an example of drug repurposing, per se. CsA was initially tested as an antifungal agent in the 1970s, with disappointing results. It was widely used in solid organ transplant surgery due to its potent immunosuppressive anti-T-cell potential and lack of bone marrow toxicity. Systemic CsA has also been used in noninfectious uveitis. Topically applied CsA was first used to inhibit experimental corneal allograft reactions in the 1980s. The beneficial effects of CsA in dry eye syndrome were initially noted in canine species.[26] Topical CsA has a local immunosuppressive effect in patients with Sjögren's syndrome, demonstrated by a significant reduction in CD4+ cells in both the conjunctival epithelium and substantia propria.[27] Today, it is one of the main treatment options for dry eye syndrome and various inflammatory lacrimal gland and ocular surface diseases.[28]

In glaucoma research, drug repositioning is among the most active fields.[15] The drugs being explored range from cholinergic medications to nifedipine due to vasodilatation of the ocular vascular smooth muscles.[29] In addition to IOP-lowering medications, the anti-epileptic drug valproic acid was repurposed as an adjuvant medication in glaucoma surgery. Valproic acid reduces collagen production and disrupts collagen fiber assembly in conjunctival wound healing postoperatively; thus, its anti-fibrotic activity might improve the success and prolong the survival of functional blebs.[30]

Retinitis pigmentosa (RP), AMD, and diabetic retinopathy could also be treated using repositioned medicines. In all neurodegenerative diseases, the shared signaling pathways leading to apoptotic cell death include calcium excitotoxicity, oxidative stress, mitochondrial dysfunction, and neuroinflammation. Targeting these main pathogenic mechanisms has successfully treated chronic diseases such as depression and epilepsies. The combinations include a list of possible repurposed drugs, such as brimonidine, curcumin, ceftriaxone, MitoQ, and valproic acid.[31]

Vision loss in dry AMD results mostly from RPE degeneration, partly driven by inflammation. Fluoxetine, approved by the FDA for treating clinical depression, inhibits the activation of inflammasomes and inflammatory cytokine release in RPE cells. Indeed, analyzing the data of more than 100 million Americans in two health insurance databases revealed a reduced risk of developing dry AMD among patients with clinical depression who had been treated with fluoxetine, suggesting fluoxetine as a potential drug-repurposing candidate for dry AMD.[32]

Another repurposed drug is dimethyl fumarate (DMF), which is approved for treating psoriasis and multiple sclerosis through its anti-inflammatory, immunomodulatory, and antioxidant effects. Vascular disorders of the eye, such as diabetic retinopathy and AMD, share a common pathogenesis associated with reduced nuclear factor (erythroid-derived 2)-like 2 (Nrf2) activity. DMF displayed induction of the Nrf2 pathway and related target genes, in addition to protection of photoreceptors, RGCs, and RPE. *In vivo* evidence has accumulated on its use in AMD, autoimmune uveoretinitis, cystoid macular edema, glaucoma, keratitis, optic neuritis, optic nerve crush, and retinal ischemia. Topical DMF administration needs to be studied for its repurposing in eye pathologies.[33]

Microfluidic systems have also been used to test surgical intraocular tamponades such as isopropanol silicone oil, which may emulsify and cause inflammation *in vivo*. An *in vitro* "eye-on-a-chip" microfluidic system showed that polymer silicone oil prevents decomposition and the formation of emulsion droplets.[34]

Topical treatments allow only a minority of the medicine to reach the ocular tissues. Developing *controlled-release ophthalmic drugs* aims to improve the effectiveness of drug delivery and reduce the number of times patients receive eye drops.[35] Biocompatible and biodegradable polymer particles capable of drug loading and controlled release enable non-invasive drug delivery. Poly(lactic-co-glycolic acid) (PLGA) is a frequently used biodegradable material.[36] For example, the anti-glaucomatous betaxolol or other beta-blockers combined with polymer ion exchange resin particles suspended in an adhesive medium is released more slowly and for a longer time in the eye (Japanese patent no: JPH0725698B2 - Formulation for the treatment of glaucoma with sustained release and comfortable application). Microfluidic chip studies might allow the preparation of polymer particles with uniform and controllable particle size, high drug loading, and suitable degradation. One such study involved the preparation of multidrug polymer particles by loading latanoprost and dexamethasone onto monodisperse biodegradable ~150-μm-diameter PLGA and examined the verification and optimization of drug release parameters.[37] Additionally, *drug nanosuspensions* with high bioavailability can be prepared. These are micron-sized drug particles suspended in a dispersed medium and stabilized by polymers or surfactants. For example, creating an ophthalmic hydrocortisone nanosuspension using a simple microfluidic nanoprecipitation method and nanocrystalization technology significantly prolonged its duration of effect.[38]

Combining microfluidic technology with current technologies can allow controlled *in vitro* drug delivery studies.[39] Precision *ophthalmic drug delivery devices* have mechanical, electronic, and microfluidic functions,[40] such as the contact lenses used as a platform for drug release to treat eye infections or release long-term steroids. It is crucial to adjust the composition of biomaterials to allow controlled drug release.[41]

The *in vitro* drug release studies in ophthalmology are mainly carried out under static conditions and do not consider the influence of flow dynamics of the tear volume. An *in vitro* 3D-printed eye model that included eyelids was developed to study fluconazole release from various commercial contact lenses.[42] It was designed to simulate physiological tear volume, as the volume of tears significantly speeds up drug release.[43] Another microfluidic unit was designed to simulate the tears' volumetric

flow rate.[44] The release kinetics of diclofenac were slower under dynamic conditions than static conditions. Furthermore, plasma-assisted grafting for surface modification of hydrophilic acrylic or silicon-based hydrogel materials with moxifloxacin significantly prolonged *in vitro* diclofenac release time to more than ten days.[45]

c. Gene Therapies

Gene therapies aim to alter cellular function via the delivery of genetic material, including DNA and RNA, or even proteins in some cases. Delivery can be performed *in vivo* or in cells that are removed from the body, transfected in *ex vivo* conditions, and returned to the organism later.

The cornea has the advantages of offering easy clinical access and an immune-privileged state for gene therapies, which focus on single and combination gene therapies via adeno-associated virus (AAV) and nanoparticle delivery. The potential applications of gene editing, such as Clustered Regularly Interspaced Short Palindromic Repeats/Associated Systems (CRISPR/Cas9), have been increasing.[46] Gene modulation therapies for endothelial diseases could make it possible to treat early-stage patients, reducing the need for corneal allografts.[47]

As for the posterior segment, modified gene therapy with AAV vectors was shown to be an effective neuroprotective and regenerative treatment that enhanced RGC survival and axon regeneration.[48] Voretigene neparvovec (Luxturna; Sparks Therapeutics) is based on a non-replicating AAV-2 vector that carries a modified transgene of human RPE65. It is the only approved gene therapy for treating dystrophies associated with biallelic pathological mutation of RPE65,[49] and the only approved for treating up to 1% of all RP patients.[50] The *RPE65* gene is responsible for visual cycle vitamin A metabolism, and its mutations cause approximately 6% of Leber's congenital amaurosis cases. The phase III clinical trial included patients with confirmed biallelic RPE65 mutations. Significant visual improvement with no serious adverse events and sustained improvement over 3-4 years of follow-up were reported after treatment.[51,52] Subretinal injection is the most frequent technique,[53] preferred over intravitreal injection because of its higher efficacy and lower systemic exposure.[54] However, the treated area is limited to the detached retina around the injection subretinal bleb.

d. Development of Biomaterials

One of the tasks in TE is to develop appropriate biomaterials with which the cells will interact. The biomaterials used in TE should meet certain criteria, including biocompatibility, structural stability, mechanical endurance, porosity to allow cellular integration, clinical applicability in the targeted tissue, and lack of toxicity, antigenicity, and mutagenicity.[55,56] In ophthalmology, transparency is also essential. Moreover, materials should not stimulate an inflammatory reaction and should potentially assist regeneration and healing.

Due to the cornea's complex structure featuring high refractive power and tensile strength with optical transparency, it is challenging to replicate its architecture using a single type of natural or synthetic biomaterial.[57,58] Corneal TE strategies have been primarily based on raw materials such collagen, gelatin, chitosan, amniotic membrane, and silk, as well as synthetic fabrics like polyvinylalcohol (PVA) and polyethylene glycol (PEG) derivatives. Natural biomaterials such as collagen have high biocompatibility, and gelatin has the advantage of being cheap, but their mechanical qualities are not up to standard. Decellularized cornea has similar properties to the native cornea but low bioactivity. Chitosan offers simple biofunctionalization, good biocompatibility, and manageable biodegradability. However, it must be crosslinked with other materials. As for synthetic biomaterials, the mechanical properties of PVA and PEG diacrylate (PEGDA) can be controlled, but both need additional components for corneal TE. Although collagen or amniotic membrane can be combined with PVA or PEGDA as a biocompatible biomaterial, together they might induce inflammatory responses. Combining chitosan with PVA or PEGDA yields proper mechanical properties but a lower-than-natural degradation rate.[59]

3D bioprinting is a technology that can be used to construct artificial target tissue scaffolds and imitate natural embryogenetic tissue formation with simultaneous processing of biomaterials and cells.[60,61] Using smart fiber alignment, keratocyte migration and orientation can be studied for corneal TE.[62] Conventional 3D printer heads are loaded with material into the cartridges as bioinks.[63] The extrusion-based method in a 3D printer seems the best to achieve enhanced mechanical properties. However, the droplet-based method may yield better microstructure, geometrical curvature, and enhanced elastic modulus.[63]

Nanotechnology in developing corneal scaffolds may promote cell adhesion, proliferation, and differentiation and facilitate gas, nutrient, and waste exchange in the corneal scaffold.[64,65] It is possible to enhance the functionality of the seeded stem cells, such as in chitosan nanoparticles/polycaprolactone membranes that yield a biodegradable scaffold for the maturation and growth of corneal endothelial cells (CECs).[66] Nanotechnology holds promise to personalize regenerative medicine in the damaged cornea.[67]

In addition to corneal TE, bioprinting technology was applied for the first time in 2020 to produce *tarsal plate scaffolds* using polycaprolactone, which was coated with adipose-derived mesenchymal stromal cells and seeded with sebocytes to secrete lipids, replacing meibocytes.[68] This technology might provide an alternative for treating massive eyelid defects, such as after tumor invasion or trauma.

The retina is the second most commonly studied eye tissue for bioprinting studies. The feasibility of creating 3D-printed scaffolds for retinal progenitor cells (RPCs) was demonstrated in 2017.[69] Chemically modified hyaluronic acid hydrogels and a Bruch's membrane-mimetic material have been synthesized.[70,71] The RGCs and glial cells successfully 3D printed on this scaffold remained viable with stable phenotypes.[72] When glial cells were used as a substrate for printed cells, the RGC neurite outgrowth was increased significantly.[73] Retinal disease models will be available once a complex retinal structure can be 3D-printed. As an example, an outer blood-retina-barrier 3D-printed tissue (i.e.,

RPE, Bruch's membrane, and choriocapillaris) has been created and is being studied to reveal the RPE-dependent choroidal phenotype in AMD.[74] A Müller cell-based 3D biomimetic model was also bioprinted and showed similar responses under hyperglycemic conditions as observed in an *in vivo* diabetic retinal model.[75]

e. Transplantation of Engineered Cells, Tissues, and Tissue Substitutes

Cell therapies as a subset of TE have been very promising in treating ocular diseases.[76] Stem cells are commonly used due to their plasticity and capacity to stay uncommitted and self-renewable until a signal to develop into distinct cell types is received.[77] ESCs are pluripotent stem cells that can renew through division and develop into the three primary germ cells. However, as ESCs can be potentially immunological and may be rejected, iPSCs are used as an alternative.

The success of cell therapy depends on using appropriate TE methods for cell processing and proper biophysical and biochemical stimuli to induce cells to migrate and settle in exact loci.[78] For transplanted cells to be functional, they must form new synaptic junctions and integrate with the host.[79] Certain cell types, such as human keratocytes, can be easily propagated using standard culture techniques.[80] However, the transfer and transplantation of cell lines may not be accessible in posterior segment applications. The eye is an electric-based organ; the retinal cells use endogenous electrical currents to function.[81] Electrical stimulation may improve the migration of transplanted cells, axonal regeneration, and synapse formation.[82]

Recent studies have focused more on developing artificial organs of clinically relevant sizes via TE methods using autologous or immunologically matched stem cells to address the growing need for biological tissue or substitutes.[1] With the current understanding of mechanisms in organogenesis and gene expressions, stem cell biology, and TE technologies, *regenerative medicine* has emerged. This involves isolating healthy cells from the organ in the initial stages of the disease, *in vitro* expansion of those cells, and seeding them on the tissue skeleton. Vital conditions for organogenesis are provided, and functional tissue is achieved in laboratory conditions. As the disease process resolves, the artificial organ is transplanted to replace the damaged organ. Despite the excitement about the possible use of ESCs and iPSCs in regenerative medicine, there are limited examples of actual translation into humans.

Combining a biosynthetic scaffold with cell culture-derived cells might allow a completely bioengineered cornea. Two main approaches have been used in corneal TE: to expand or create the desired cell population by tissue culture, or to support the corneal structure by providing a biomimetic/biosynthetic device that allows native cornea cells to stimulate endogenous corneal regeneration. In the first approach, the tissue culture of cornea cells can be transplanted as a sheet, or cells can be dissociated and injected into the desired part of the anterior segment.

These bioengineered corneas differ from the entirely artificial corneas (i.e., keratoprostheses) used in pathological eyes that cannot support a corneal graft. None of the keratoprostheses today integrates seamlessly into the host tissue[83] and none have addressed the reinnervation issue.[84] The quest for soft artificial corneas with improved biointegration, biofunctionality, and minimum complication rates continues.[85] Beyond the need for vision restoration, biointegration, epithelial overgrowth, and sensory innervation are crucial.[86] The strength and optical clarity of noncytotoxic, biosynthetic composites can be controlled. With further development, TE corneal replacements could address future donor cornea shortages.[87]

One artificial cornea product is worth mentioning. The CorNeat keratoprostheses has a synthetic polymeric scaffold for biointegration. It has a central poly(methyl methacrylate) optic and an integrating skirt, which imitates the microstructure of human ECM. Unlike scaffolds and other collagen matrices used in TE, it has mechanical strength and is nondegradable. The EverMatrix™ is optimized as a natural habitat for human fibroblasts, stimulates migration colonization, and synthesizes ECM. Initial animal studies confirmed biointegration[88] and human implantation revealed good medium-term results.[89]

Bone marrow mesenchymal stem cells (MSCs), adipose-derived adult MSCs, umbilical cord MSCs, and ESCs and iPSCs have been used for corneal stromal regeneration. These cells were implanted on the ocular surface, implanted intrastromally alone or with a biodegradable, non-biodegradable, or decellularized corneal stromal scaffold, injected into the anterior chamber, or injected intravenously. Stem cells from MSC banks may be autologous or heterologous. Even MSC exosomes were used for their immunosuppressive and damage-repairing effects to reduce the stromal scarring size.[90]

Rama et al.[91] were the first to try expanding adult limbal stem cells *in vitro* to treat limbal stem cell deficiencies. Stem cells in culture are identified as small cells that express stem cell markers such as ABCG2, are negative for cell differentiation markers like cytokeratin 3, and have a high nuclear to cytoplasm ratio. High expression of DNp63a is a quality control measure that allows successful transplantation.[91] Strict patient inclusion criteria with a milder host microenvironment are crucial for clinical success.[92] Cell therapies other than *ex vivo* cultivated limbal epithelial cells have been described,[93,94] including cultivated oral mucosal epithelial cells, extraocular MSCs, and iPSC-derived limbal stem cells.[95]

Expanded adult or stem cell-derived CECs have been studied to treat corneal endothelial diseases.[47] CECs are quiescent cells that must be pushed to proliferate. At the same time, it is necessary to avoid endothelial-to-mesenchymal transition, which might lead to a myofibroblastic phenotype and cellular loss of function. The alternative of differentiating CECs from iPSCs requires the development of strict protocols to ensure that the final output resembles CECs.[47] Strategies to deliver those cells or acellular endothelial graft equivalents are being studied to alleviate the need for allograft surgeries.[47]

Meanwhile, to repair the tissue of the lacrimal glands, the feasibility of epithelial cell adhesion molecule-positive progenitor cell injection therapy has been demonstrated.[96] Lacrimal gland stem cells cultured from the lacrimal glands of healthy and

aqueous deficiency dry eye disease mice express progenitor cell markers (i.e., Krt14, Krt5, P63, nestin),[97] have self-renewal capacity, and differentiate into acinar or ductal-like cells *in vitro* and *in vivo*.[98] Conversely, a 3D TE technique with a direct reprogramming method to induce markers in the developmental process from human iPSCs has regenerated a secretory gland structure by reproducing embryogenesis *in vitro* and *in vivo*.[99] *In situ* regeneration of the partially damaged lacrimal gland is possible using stem cells in the glandular tissue. Organoids developed from iPSCs with TE methods can be transplanted for total glandular damage.[100] Indeed, the generation of organoids from iPSCs committed to neuro-ectodermal lineage displayed acinar, ductal, and myoepithelial structures specific for lacrimal glands and confirmed secretory function.[101]

For retinal stem cell therapy, retinal organoids seem to be a helpful resource.[77,102] RPCs are multipotent stem cells with mitotic capability, found in the neural retina of human fetuses between 16 and 20 weeks of gestation.[103] If manipulated *in vitro*, they can express photoreceptor markers, differentiate into neuronal cells of the retina,[104] and integrate into the outer nuclear layer of both intact and degenerating retinas in adult mice.[105] Timely selection of biochemically committed but not yet morphologically differentiated progenitors gives the best results.[106] RPCs at the peak of rod genesis can differentiate into rod photoreceptors when transplanted and form synaptic connections to integrate into the degenerating retina.[106,107] RPCs are transplanted subretinally or intravitreally. However, as in MSC procedures, subretinal implantation techniques are not risk-free.[108] Clinically, Stargardt's macular dystrophy, dry AMD, RP, and possibly retinal vascular diseases could benefit from ESCs.[109,110]

Replacing damaged RPE with healthy iPSCs can delay disease progression.[111,112] Transplantation of allogeneic or autologous RPE cells or sheets has been studied.[113] In a swine model, iPSC-derived RPE cells injected into the atrophic retina retained their typical morphology, RPE-related gene expression, and phagocytic ability.[114] Combined RPE and retinal sheet transplantation shows potential for complete replacement of the degenerated retina.[115]

Other stem cells have also been studied for RP with beneficial results, including the use of human iPSC-derived retinal cells in mice, bone marrow stem cells, and even conjunctival MSCs.[50,116,117,118] *In vivo* animal studies demonstrated that transplanting MSCs into the vitreous can improve photoreceptor survival in RP.[119]

Glaucoma and other optic neuropathies are the most common diseases expected to benefit from RGC replacement therapy.[110] However, donor neuron survival and retinal integration issues must be considered. Human iPSCs could be differentiated into RGCs, and aligned nanofiber matrices could be used for *in vitro* optic nerve-like modeling to guide the axonal outgrowth of these iPSC-derived RGCs. Forskolin, a cholinergic derivative, is also known to promote RGC differentiation.[120] Protocols for *ex vivo* human RGC transplantation for research on donor survival, dendritic stratification, topographic distribution, and donor-host interactions have been reported and hold promise for future applications.[121,122,123] When human iPSCs were differentiated into mature, functional RGCs *in vitro* and transplanted intravitreally in mice, their retinal localization, morphology, and functionality were similar to native RGCs.[124] A porcine decellularized optic nerve seeded with neurotrophin-3-overexpressing Schwann cells was shown to serve as a functional scaffold and promote directional growth and remyelination of regenerating axons, thus proving successful as an *in vivo* spinal cord defect model.[125]

On the other hand, Wharton's jelly-derived MSCs (WJ-MSCs) have been studied in terms of the effects of secretory exosomes, not neuronal transformation.[126] They are known to increase mitochondrial adenosine triphosphate synthesis and suppress neuroinflammation.[127,128] Umbilical cord WJ-MSC therapy has been suggested for the management of toxic optic neuropathies if performed soon after the incident and for RP, regardless of the causative mutations.[129,130]

3D Microtissues

3D culture systems ultimately aim to enhance cell-cell interactions and facilitate native-like microenvironments, thereby emulating tissue physiology. Cellular spheroids or 3D microarchitectures can either be formed naturally by aggregation of cells in hanging droplets or templated molds due to gravitational forces or by utilizing bioengineered platforms such as photolithography, droplet-microfluidics, or bioprinting.[131,132,133] Injectable ophthalmic microtissues have been generated from conjunctival stem cells to treat ocular surface diseases.[131] The 3D dynamic culture enabled constructs to maintain their stemness and facilitate efficient ocular differentiation. Hirayama et al.[134] successfully demonstrated the bioengineering of a functional mouse lacrimal gland from a microgerm composed of epithelial and mesenchymal cells. Following orthotopic implantation, the generated lacrimal germ could secrete tear proteins such as lactoferrin upon stimulation with pilocarpine. Similarly, spheroids generated in patterned molds and composed of lipoaspirate-derived pluripotent stem cells and MSCs were capable of preserving their differentiation capacity and restoring the cornea stroma in animal model.[132]

Regulation, Commercialization, and Ethics

The regulations on using and commercializing bioengineered products in humans are still being developed as new products emerge. However, using ESCs and animal experiments to create new therapeutic agents has been subject to severe ethical criticism for years. Using organ-on-a-chip technology for disease models might decrease the need for animal experiments by drugmakers. Ethical concerns in using human embryos and problems in matching patients based on compatible blood types can be overcome by using iPSCs. However, there are still safety concerns related to epigenetic memory, where derived cells retain gene expression from the original cells, and the ability of iPSCs to proliferate indefinitely, which can possibly lead to teratomas.[50]

Ethics

Authorship Contributions

Concept: C.A.U., S.G., Design: C.A.U., Data Collection or Processing: C.A.U., S.G., Literature Search: C.A.U., S.G., Writing: C.A.U., S.G.

Conflict of Interest: No conflict of interest was declared by the authors.

Financial Disclosure: The authors declared that this study received no financial support.

References

1. Bhumiratana S, Bernhard J, Cimetta E, Vunjak-Novakovic G. Principles of Bioreactor Design for Tissue Engineering. In: Lanza R, Langer R, Vacanti J, eds. Principles of tissue engineering (4th ed). San Diego CA; Elsevier; 2014:261-278.
2. Caplan AI. Embryonic development and the principles of tissue engineering. Novartis Found Symp. 2003;249:17-25.
3. Singh HP, Wang S, Stachelek K, Lee S, Reid MW, Thornton ME, Craft CM, Grubbs BH, Cobrinik D. Developmental stage-specific proliferation and retinoblastoma genesis in RB-deficient human but not mouse cone precursors. Proc Natl Acad Sci U S A. 2018;115:E9391-E9400.
4. Huh D, Torisawa YS, Hamilton GA, Kim HJ, Ingber DE. Microengineered physiological biomimicry: organs-on-chips. Lab Chip. 2012;12:2156-2164.
5. Hao N , Nie Y , Zhang JXJ . Microfluidics for silica biomaterials synthesis: opportunities and challenges. Biomater Sci. 2019;361:635-650.
6. Bellin M, Marchetto MC, Gage FH, Mummery CL. Induced pluripotent stem cells: the new patient? Nat Rev Mol Cell Biol. 2012;13:713-726.
7. Grskovic M, Javaherian A, Strulovici B, Daley GQ. Induced pluripotent stem cells--opportunities for disease modelling and drug discovery. Nat Rev Drug Discov. 2011;10:915-929.
8. Manafi N, Shokri F, Achberger K, Hirayama M, Mohammadi MH, Noorizadeh F, Hong J, Liebau S, Tsuji T, Quinn PMJ, Mashaghi A. Organoids and organ chips in ophthalmology. Ocul Surf. 2021;19:1-15.
9. Abdalkader R, Kamei KI. Multi-corneal barrier-on-a-chip to recapitulate eye blinking shear stress forces. Lab Chip. 2020;20:1410-1417.
10. Yu Z, Hao R, Chen X, Ma L, Zhang Y, Yang H. Protocol to develop a microfluidic human corneal barrier-on-a-chip to evaluate the corneal epithelial wound repair process. STAR Protoc. 2023;4:102122.
11. Bai J, Fu H, Bazinet L, Birsner AE, D'Amato RJ. A Method for Developing Novel 3D Cornea-on-a-Chip Using Primary Murine Corneal Epithelial and Endothelial Cells. Front Pharmacol. 2020;11:453.
12. Bikuna-Izagirre M, Aldazabal J, Extramiana L, Moreno-Montañés J, Carnero E, Paredes J. Technological advances in ocular trabecular meshwork in vitro models for glaucoma research. Biotechnol Bioeng. 2022;119:2698-2714.
13. Waxman S, Strzalkowska A, Wang C, Loewen R, Dang Y, Loewen NA. Tissue-engineered anterior segment eye cultures demonstrate hallmarks of conventional organ culture. Graefes Arch Clin Exp Ophthalmol. 2023;261:1359-1368.
14. Dautriche CN, Xie Y, Sharfstein ST. Walking through trabecular meshwork biology: Toward engineering design of outflow physiology. Biotechnol Adv. 2014;32:971-983.
15. Shimazawa M, Hara H. [Current Status of the Pharmacological Treatment of Glaucoma and Its Prospects]. Yakugaku Zasshi. 2021;141:61-66.
16. Zhang XH, Jin ZB. Patient iPSC-derived retinal organoids: Observable retinal diseases in-a-dish. Histol Histopathol. 2021;36:705-710.
17. Aoki H, Hara A, Nakagawa S, Motohashi T, Hirano M, Takahashi Y, Kunisada T. Embryonic stem cells that differentiate into RPE cell precursors in vitro develop into RPE cell monolayers in vivo. Exp Eye Res. 2006;82:265-274.
18. Song MJ, Quinn R, Nguyen E, Hampton C, Sharma R, Park TS, Koster C, Voss T, Tristan C, Weber C, Singh A, Dejene R, Bose D, Chen YC, Derr P, Derr K, Michael S, Barone F, Chen G, Boehm M, Maminishkis A, Singec I, Ferrer M, Bharti K. 3D vascularized eye tissue models age-related macular degeneration. Nat Methods. 2023;20:46-47.
19. Dalvi S, Chatterjee A, Singh R. AMD recapitulated in a 3D biomimetic: A breakthrough in retina tissue engineering. Cell Stem Cell. 2023;30:243-245.
20. Stowell C, Burgoyne CF, Tamm ER, Ethier CR; Lasker/IRRF Initiative on Astrocytes and Glaucomatous Neurodegeneration Participants. Biomechanical aspects of axonal damage in glaucoma: A brief review. Exp Eye Res. 2017;157:13-19.
21. Surma M, Anbarasu K, Dutta S, Olivera Perez LJ, Huang KC, Meyer JS, Das A. Enhanced mitochondrial biogenesis promotes neuroprotection in human pluripotent stem cell derived retinal ganglion cells. Commun Biol. 2023;6:218.
22. Ingber DE. Mechanobiology, Tissue Development and Organ Engineering. In: Lanza R, Langer R, Vacanti J, eds. Principles of tissue engineering (4th ed). San Diego CA; Elsevier; 2014:309-322.
23. Bennet D, Estlack Z, Reid T, Kim J. A microengineered human corneal epithelium-on-a-chip for eye drops mass transport evaluation. Lab Chip. 2018;18:1539-1551.
24. Beiβner N, Mattern K, Dietzel A, Reichl S. DynaMiTES - A dynamic cell culture platform for in vitro drug testing PART 2 - Ocular DynaMiTES for drug absorption studies of the anterior eye. Eur J Pharm Biopharm. 2018;126:166-176.
25. Ko J, Lee Y, Lee S, Lee SR, Jeon NL. Human Ocular Angiogenesis-Inspired Vascular Models on an Injection-Molded Microfluidic Chip. Adv Healthc Mater. 2019;8:e1900328.
26. Kern TJ. Topical cyclosporine therapy for keratoconjunctivitis sicca in dogs. Cornell Vet. 1989;79:207-209.
27. Power WJ, Mullaney P, Farrell M, Collum LM. Effect of topical cyclosporin A on conjunctival T cells in patients with secondary Sjögren's syndrome. Cornea. 1993;12:507-511.
28. Utine CA, Stern M, Akpek EK. Clinical review: topical ophthalmic use of cyclosporin A. Ocul Immunol Inflamm. 2010;18:352-361.
29. El-Feky YA, Fares AR, Zayed G, El-Telbany RFA, Ahmed KA, El-Telbany DFA. Repurposing of nifedipine loaded in situ ophthalmic gel as a novel approach for glaucoma treatment. Biomed Pharmacother. 2021;142:112008.
30. Yap ZL, Seet LF, Chu SW, Toh LZ, Ibrahim FI, Wong TT. Effect of valproic acid on functional bleb morphology in a rabbit model of minimally invasive surgery. Br J Ophthalmol. 2022;106:1028-1036.
31. Maneu V, Lax P, De Diego AMG, Cuenca N, García AG. Combined drug triads for synergic neuroprotection in retinal degeneration. Biomed Pharmacother. 2022;149:112911.
32. Ambati M, Apicella I, Wang SB, Narendran S, Leung H, Pereira F, Nagasaka Y, Huang P, Varshney A, Baker KL, Marion KM, Shadmehr M, Stains CI, Werner BC, Sadda SR, Taylor EW, Sutton SS, Magagnoli J, Gelfand BD. Identification of fluoxetine as a direct NLRP3 inhibitor to treat atrophic macular degeneration. Proc Natl Acad Sci U S A. 2021;118:e2102975118.
33. Manai F, Govoni S, Amadio M. The Challenge of Dimethyl Fumarate Repurposing in Eye Pathologies. Cells. 2022;11:4061.
34. Lu Y, Chan YK, Lau LH, Chao Y, Shih KC, Lai SM, Wong D, Shum HC. Adhesion of silicone oil and emulsification: an in vitro assessment using a microfluidic device and 'Eye-on-a-Chip'. Acta Ophthalmol. 2019;97:313-318.
35. Zhao Y, Hu G, Yan Y, Wang Z, Liu X, Shi H. Biomechanical analysis of ocular diseases and its in vitro study methods. Biomed Eng Online. 2022;21:49.
36. Su Y, Zhang B, Sun R, Liu W, Zhu Q, Zhang X, Wang R, Chen C. PLGA-based biodegradable microspheres in drug delivery: recent advances in research and application. Drug Deliv. 2021;28:1397-1418.
37. Leon RAL, Somasundar A, Badruddoza AZM, Khan SA. Microfluidic fabrication of multi-drug-loaded polymeric microparticles for topical glaucoma therapy. Part Syst Char. 2015;32:567-572.
38. Ali HS, York P, Ali AM, Blagden N. Hydrocortisone nanosuspensions for ophthalmic delivery: A comparative study between microfluidic nanoprecipitation and wet milling. J Control Release. 2011;149:175-181.
39. Kutlehria S, Sachdeva MS. Role of In Vitro Models for Development of Ophthalmic Delivery Systems. Crit Rev Ther Drug Carrier Syst. 2021;38:1-31.
40. Zhang H, Jackson JK, Chiao M. Microfabricated drug delivery devices: design, fabrication, and applications. Adv Funct Mater. 2017;27:1703606.
41. Kaczmarek JC, Tieppo A, White CJ, Byrne ME. Adjusting biomaterial composition to achieve controlled multiple-day release of dexamethasone from an extended-wear silicone hydrogel contact lens. J Biomater Sci Polym Ed. 2014;25:88-100.

42. Phan CM, Bajgrowicz M, Gao H, Subbaraman LN, Jones LW. Release of Fluconazole from Contact Lenses Using a Novel In Vitro Eye Model. Optom Vis Sci. 2016;93:387-394.
43. Phan CM, Walther H, Gao H, Rossy J, Subbaraman LN, Jones L. Development of an In Vitro Ocular Platform to Test Contact Lenses. J Vis Exp. 2016:e53907.
44. Pimenta AF, Valente A, Pereira JM, Pereira JC, Filipe HP, Mata JL, Colaço R, Saramago B, Serro AP. Simulation of the hydrodynamic conditions of the eye to better reproduce the drug release from hydrogel contact lenses: experiments and modeling. Drug Deliv Transl Res. 2016;6:755-762.
45. Silva D, de Sousa HC, Gil MH, Santos LF, Oom MS, Alvarez-Lorenzo C, Saramago B, Serro AP. Moxifloxacin-imprinted silicone-based hydrogels as contact lens materials for extended drug release. Eur J Pharm Sci. 2021;156:105591.
46. Mohan RR, Martin LM, Sinha NR. Novel insights into gene therapy in the cornea. Exp Eye Res. 2021;202:108361.
47. Català P, Thuret G, Skottman H, Mehta JS, Parekh M, Ní Dhubhghaill S, Collin RWJ, Nuijts RMMA, Ferrari S, LaPointe VLS, Dickman MM. Approaches for corneal endothelium regenerative medicine. Prog Retin Eye Res. 2022;87:100987.
48. McDougal Runner M, Gutekunst CA, Gross R. Promising new gene therapy for optic nerve regeneration and neuroprotection. Invest Ophthalmol Vis Sci. 2019;60:2251.
49. LUXTURNA_US_Prescribing_Information.pdf.https://www.fda.gov/media/109906/download.
50. Wu KY, Kulbay M, Toameh D, Xu AQ, Kalevar A, Tran SD. Retinitis Pigmentosa: Novel Therapeutic Targets and Drug Development. Pharmaceutics. 2023;15:685.
51. Maguire AM, Russell S, Wellman JA, Chung DC, Yu ZF, Tillman A, Wittes J, Pappas J, Elci O, Marshall KA, McCague S, Reichert H, Davis M, Simonelli F, Leroy BP, Wright JF, High KA, Bennett J. Efficacy, Safety, and Durability of Voretigene Neparvovec-rzyl in RPE65 Mutation-Associated Inherited Retinal Dystrophy: Results of Phase 1 and 3 Trials. Ophthalmology. 2019;126:1273-1285.
52. Maguire AM, Russell S, Chung DC, Yu ZF, Tillman A, Drack AV, Simonelli F, Leroy BP, Reape KZ, High KA, Bennett J. Durability of Voretigene Neparvovec for Biallelic RPE65-Mediated Inherited Retinal Disease: Phase 3 Results at 3 and 4 Years. Ophthalmology. 2021;128:1460-1468.
53. Hussain RM, Tran KD, Maguire AM, Berrocal AM. Subretinal Injection of Voretigene Neparvovec-rzyl in a Patient With RPE65-Associated Leber's Congenital Amaurosis. Ophthalmic Surg Lasers Imaging Retina. 2019;50:661-663.
54. Seitz IP, Michalakis S, Wilhelm B, Reichel FF, Ochakovski GA, Zrenner E, Ueffing M, Biel M, Wissinger B, Bartz-Schmidt KU, Peters T, Fischer MD; RD-CURE Consortium. Superior Retinal Gene Transfer and Biodistribution Profile of Subretinal Versus Intravitreal Delivery of AAV8 in Nonhuman Primates. Invest Ophthalmol Vis Sci. 2017;58:5792-5801.
55. Yi S, Ding F, Gong L, Gu X. Extracellular Matrix Scaffolds for Tissue Engineering and Regenerative Medicine. Curr Stem Cell Res Ther. 2017;12:233-246.
56. Thomas D, Gaspar D, Sorushanova A, Milcovich G, Spanoudes K, Mullen AM, O'Brien T, Pandit A, Zeugolis DI. Scaffold and scaffold-free self-assembled systems in regenerative medicine. Biotechnol Bioeng. 2016;113:1155-1163.
57. Chen Z, You J, Liu X, Cooper S, Hodge C, Sutton G, Crook JM, Wallace GG. Biomaterials for corneal bioengineering. Biomed Mater. 2018;13:032002.
58. Palchesko RN, Carrasquilla SD, Feinberg AW. Natural Biomaterials for Corneal Tissue Engineering, Repair, and Regeneration. Adv Healthc Mater. 2018;7:e1701434.
59. Mahdavi SS, Abdekhodaie MJ, Mashayekhan S, Baradaran-Rafii A, Djalilian AR. Bioengineering Approaches for Corneal Regenerative Medicine. Tissue Eng Regen Med. 2020;17:567-593.
60. Orash Mahmoud Salehi A, Heidari-Keshel S, Poursamar SA, Zarrabi A, Sefat F, Mamidi N, Behrouz MJ, Rafienia M. Bioprinted Membranes for Corneal Tissue Engineering: A Review. Pharmaceutics. 2022;14:2797.
61. Isaacson A, Swioklo S, Connon CJ. 3D bioprinting of a corneal stroma equivalent. Exp Eye Res. 2021;173:188-193.
62. Gouveia RM, Koudouna E, Jester J, Figueiredo F, Connon CJ. Template Curvature Influences Cell Alignment to Create Improved Human Corneal Tissue Equivalents. Adv Biosyst. 2017;1:e1700135.
63. Murphy SV, Atala A. 3D bioprinting of tissues and organs. Nat Biotechnol. 2014;32:773-785.
64. Ahearne M, Fernández-Pérez J, Masterton S, Madden PW, Bhattacharjee P. Designing scaffolds for corneal regeneration. Adv Funct Mater. 2020;30:1908996.
65. Yousaf S, Keshel SH, Farzi GA, Momeni-Moghadam M, Ahmadi ED, Asencio IO, Mozafari M, Sefat F. Scaffolds for corneal tissue engineering. In: Mozafari M, Sefat F, Atala A, eds. Handbook of Tissue Engineering Scaffolds (1st ed). Amsterdam; Elsevier; 2019:649-672.
66. Tayebi T, Baradaran-Rafii A, Hajifathali A, Rahimpour A, Zali H, Shaabani A, Niknejad H. Biofabrication of chitosan/chitosan nanoparticles/polycaprolactone transparent membrane for corneal endothelial tissue engineering. Sci Rep. 2021;11:7060.
67. Anitua E, Muruzabal F, de la Fuente M, Merayo J, Durán J, Orive G. Plasma Rich in Growth Factors for the Treatment of Ocular Surface Diseases. Curr Eye Res. 2016;41:875-882.
68. Chen L, Yan D, Wu N, Zhang W, Yan C, Yao Q, Zouboulis CC, Sun H, Fu Y. 3D-Printed Poly-Caprolactone Scaffolds Modified With Biomimetic Extracellular Matrices for Tarsal Plate Tissue Engineering. Front Bioeng Biotechnol. 2020;8:219.
69. Worthington KS, Wiley LA, Kaalberg EE, Collins MM, Mullins RF, Stone EM, Tucker BA. Two-photon polymerization for production of human iPSC-derived retinal cell grafts. Acta Biomater. 2017;55:385-395.
70. Wang P, Li X, Zhu W, Zhong Z, Moran A, Wang W, Zhang K, Shaochen Chen. 3D bioprinting of hydrogels for retina cell culturing. Bioprinting. 2018;11:e00029.
71. Kim J, Park JY, Kong JS, Lee H, Won JY, Cho DW. Development of 3D Printed Bruch's Membrane-Mimetic Substance for the Maturation of Retinal Pigment Epithelial Cells. Int J Mol Sci. 2021;22:1095.
72. Lorber B, Hsiao WK, Martin KR. Three-dimensional printing of the retina. Curr Opin Ophthalmol. 2016;27:262-267.
73. Lorber B, Hsiao WK, Hutchings IM, Martin KR. Adult rat retinal ganglion cells and glia can be printed by piezoelectric inkjet printing. Biofabrication. 2014;6:015001.
74. Song MJ, Quinn R, Nguyen E, Hampton C, Sharma R, Park TS, Koster C, Voss T, Tristan C, Weber C, Singh A, Dejene R, Bose D, Chen YC, Derr P, Derr K, Michael S, Barone F, Chen G, Boehm M, Maminishkis A, Singec I, Ferrer M, Bharti K. Bioprinted 3D outer retina barrier uncovers RPE-dependent choroidal phenotype in advanced macular degeneration. Nat Methods. 2023;20:149-161.
75. Jung SS, Son J, Yi SJ, Kim K, Park HS, Kang HW, Kim HK. Development of Müller cell-based 3D biomimetic model using bioprinting technology. Biomed Mater. 2022;18.
76. Sanie-Jahromi F, Azizi A, Shariat S, Johari M. Effect of Electrical Stimulation on Ocular Cells: A Means for Improving Ocular Tissue Engineering and Treatments of Eye Diseases. Biomed Res Int. 2021;2021:6548554.
77. Schwartz SD, Pan CK, Klimanskaya I, Lanza R. Retinal Degeneration. In: Lanza R, Langer R, Vacanti J, eds. Principles of tissue engineering (4th ed). San Diego CA; Elsevier; 2014:1427-1440.
78. Dzobo K, Thomford NE, Senthebane DA, Shipanga H, Rowe A, Dandara C, Pillay M, Motaung KSCM. Advances in Regenerative Medicine and Tissue Engineering: Innovation and Transformation of Medicine. Stem Cells Int. 2018;2018:2495848.
79. Jindal N, Banik A, Prabhakar S, Vaiphie K, Anand A. Alteration of Neurotrophic Factors After Transplantation of Bone Marrow Derived Lin-ve Stem Cell in NMDA-Induced Mouse Model of Retinal Degeneration. J Cell Biochem. 2017;118:1699-1711.
80. Parenteau NL, Nolte CM, Bilbo P, Rosenberg M, Wilkins LM, Johnson EW, Watson S, Mason VS, Bell E. Epidermis generated in vitro: practical considerations and applications. J Cell Biochem. 1991;45:245-251.

81. Zhao M, Chalmers L, Cao L, Vieira AC, Mannis M, Reid B. Electrical signaling in control of ocular cell behaviors. Prog Retin Eye Res. 2012;31:65-88.
82. Hu W, Wei X, Zhu L, Yin D, Wie A, Bi X, Liu T, Zhou G, Qiang Y, Sun X, Wen Z, Pan Y. Enhancing proliferation and migration of fibroblast cells by electric stimulation based on triboelectric nanogenerator. Nano Energy. 2019;57:600-607.
83. Chirila TV. An overview of the development of artificial corneas with porous skirts and the use of pHEMA for such application. Biomaterials. 2001;22:3311-3317.
84. Lambiase A, Rama P, Bonini S, Caprioglio G, Aloe L. Topical treatment with nerve growth factor for corneal neurotrophic ulcers. N Engl J Med. 1998;338:1174-1180.
85. Çelebi ARC. Yapay kornea uygulamaları ve kornea doku mühendisliği. In: Burcu A, Yıldız E, Erdem E, eds. Oküler Yüzey Cerrahileri (1st ed). Ankara; Anadolu Kitabevi; 2002:228-240.
86. Griffith M, Li F, Lohmann C, Sheardown HD, Shimmura S, Carlsson DJ. Tissue engineering of the cornea. In: Ma PX, Elisseeff J, eds. Scaffolding in Tissue Engineering. Florida; CRC Press Taylor & Francis Group; 2006:413-423.
87. Kaminski SL, Biowski R, Lukas JR, Koyuncu D, Grabner G. Corneal sensitivity 10 years after epikeratoplasty. J Refract Surg. 2002;18:731-736.
88. Litvin G, Klein I, Litvin Y, Klaiman G, Nyska A. CorNeat KPro: Ocular Implantation Study in Rabbits. Cornea. 2021;40:1165-1174.
89. Bahar I, Reitblat O, Livny E, Litvin G. The first-in-human implantation of the CorNeat keratoprosthesis. Eye (Lond). 2023;37:1331-1335.
90. Jorge L. Alió del Barrio. Cell Therapy of the Corneal Stroma Using Ex Vivo Cultured Extraocular Cells. In: Alio JL, Alio del Barrio JL, Arnalich-Montiel F, eds. Corneal regeneration Therapy and Surgery. (1st ed). Switzerland; Springer Nature; 2019:26;403-415.
91. Rama P, Matuska S, Paganoni G, Spinelli A, De Luca M, Pellegrini G. Limbal stem-cell therapy and long-term corneal regeneration. N Engl J Med. 2010;363:147-155.
92. Pellegrini G, Rama P, De Luca M. Vision from the right stem. Trends Mol Med. 2010;17:1-7.
93. Barut Selver Ö, Yağcı A, Eğrilmez S, Gürdal M, Palamar M, Çavuşoğlu T, Ateş U, Veral A, Güven Ç, Wolosin JM. Limbal Stem Cell Deficiency and Treatment with Stem Cell Transplantation. Turk J Ophthalmol. 2017;47:285-291.
94. Korkmaz I, Palamar M, Egrilmez S, Gurdal M, Yagci A, Barut Selver O. Evaluation of Limbal Stem Cell Transplant Success in Ocular Chemical Injury. Exp Clin Transplant. 2022;21:684-690.
95. Buenaga RF, Ahmad S. Cell therapy using cultivated oral mucosal epithelial transplant (COMET). In: Alio JL, Alio del Barrio JL, Arnalich-Montiel F. Corneal regeneration Therapy and Surgery. (1st ed). Switzerland; Springer Nature; 2019:16;225-230.
96. Gromova A, Voronov DA, Yoshida M, Thotakura S, Meech R, Dartt DA, Makarenkova HP. Lacrimal Gland Repair Using Progenitor Cells. Stem Cells Transl Med. 2017;6:88-98.
97. Xiao S, Zhang Y. Establishment of long-term serum-free culture for lacrimal gland stem cells aiming at lacrimal gland repair. Stem Cell Res Ther. 2020;11:20.
98. Chen H, Huang P, Zhang Y. Three-dimensional, serum-free culture system for lacrimal gland stem cells. J Vis Exp. 2022:(184).
99. Hirayama M. Advances in functional restoration of the lacrimal glands. Invest Ophthalmol Vis Sci. 2018;59:DES174-DES182.
100. Kasal K, Güven S, Utine CA. Current methodology and cell sources for lacrimal gland tissue engineering. Exp Eye Res. 2022;221:109138.
101. Asal M, Koçak G, Sarı V, Reçber T, Nemutlu E, Utine CA, Güven S. Development of lacrimal gland organoids from iPSC derived multizonal ocular cells. Front Cell Dev Biol. 2023;10:1058846.
102. Lund RD, Kwan AS, Keegan DJ, Sauvé Y, Coffey PJ, Lawrence JM. Cell transplantation as a treatment for retinal disease. Prog Retin Eye Res. 2001;20:415-449.
103. Wang NK, Tosi J, Kasanuki JM, Chou CL, Kong J, Parmalee N, Wert KJ, Allikmets R, Lai CC, Chien CL, Nagasaki T, Lin CS, Tsang SH. Transplantation of reprogrammed embryonic stem cells improves visual function in a mouse model for retinitis pigmentosa. Transplantation. 2010;89:911-919.
104. Klassen HJ, Ng TF, Kurimoto Y, Kirov I, Shatos M, Coffey P, Young MJ. Multipotent retinal progenitors express developmental markers, differentiate into retinal neurons, and preserve light-mediated behavior. Invest Ophthalmol Vis Sci. 2004;45:4167-4173.
105. Léveillard T, Mohand-Saïd S, Sahel JA. La transplantation de photorécepteurs immatures: un moyen pour réparer la rétine [Retinal repair by transplantation of photoreceptor precursors]. Med Sci (Paris). 2007;23:240-242.
106. MacLaren RE, Pearson RA, MacNeil A, Douglas RH, Salt TE, Akimoto M, Swaroop A, Sowden JC, Ali RR. Retinal repair by transplantation of photoreceptor precursors. Nature. 2006;444:203-207.
107. Gasparini SJ, Llonch S, Borsch O, Ader M. Transplantation of photoreceptors into the degenerative retina: Current state and future perspectives. Prog Retin Eye Res. 2019;69:1-37.
108. Oner A, Gonen ZB, Sinim N, Cetin M, Ozkul Y. Subretinal adipose tissue-derived mesenchymal stem cell implantation in advanced stage retinitis pigmentosa: a phase I clinical safety study. Stem Cell Res Ther. 2016;7:178.
109. Sanie-Jahromi F, Emadi Z, Khajehahmadi Z, Nowroozzadeh MH. The role of retinal pigment epithelium in the pathogenesis and treatment of age-related macular degeneration. J Infertil Reprod Biol. 2021;9:65-69.
110. Coco-Martin RM, Pastor-Idoate S, Pastor JC. Cell Replacement Therapy for Retinal and Optic Nerve Diseases: Cell Sources, Clinical Trials and Challenges. Pharmaceutics.. 2021;13:865.
111. Kashani AH, Uang J, Mert M, Rahhal F, Chan C, Avery RL, Dugel P, Chen S, Lebkowski J, Clegg DO, Hinton DR, Humayun MS. Surgical Method for Implantation of a Biosynthetic Retinal Pigment Epithelium Monolayer for Geographic Atrophy: Experience from a Phase 1/2a Study. Ophthalmol Retina. 2020;4:264-273.
112. Mandai M, Fujii M, Hashiguchi T, Sunagawa GA, Ito SI, Sun J, Kaneko J, Sho J, Yamada C, Takahashi M. iPSC-Derived Retina Transplants Improve Vision in rd1 End-Stage Retinal-Degeneration Mice. Stem Cell Reports. 2017;8:69-83.
113. Osakada F. [Development of Cellular and Tissue-based Products for Retinal Regenerative Medicine]. Yakugaku Zasshi. 2017;137:23-29.
114. Duarri A, Rodríguez-Bocanegra E, Martínez-Navarrete G, Biarnés M, García M, Ferraro LL, Kuebler B, Aran B, Izquierdo E, Aguilera-Xiol E, Casaroli-Marano RP, Trias E, Fernandez E, Raya Á, Veiga A, Monés J. Transplantation of Human Induced Pluripotent Stem Cell-Derived Retinal Pigment Epithelium in a Swine Model of Geographic Atrophy. Int J Mol Sci. 2021;22:10497.
115. Thomas BB, Lin B, Martinez-Camarillo JC, Zhu D, McLelland BT, Nistor G, Keirstead HS, Humayun MS, Seiler MJ. Co-grafts of Human Embryonic Stem Cell Derived Retina Organoids and Retinal Pigment Epithelium for Retinal Reconstruction in Immunodeficient Retinal Degenerate Royal College of Surgeons Rats. Front Neurosci. 2021;15:752958.
116. Surendran H, Nandakumar S, Reddy K VB, Stoddard J, Mohan K V, Upadhyay PK, McGill TJ, Pal R. Transplantation of retinal pigment epithelium and photoreceptors generated concomitantly via small molecule-mediated differentiation rescues visual function in rodent models of retinal degeneration. Stem Cell Res Ther. 2021;12:70.
117. Ferroni L, Gardin C, Tocco I, Epis R, Casadei A, Vindigni V, Mucci G, Zavan B. Potential for neural differentiation of mesenchymal stem cells. Adv Biochem Eng Biotechnol. 2013;129:89-115.
118. Soleimannejad M, Ebrahimi-Barough S, Nadri S, Riazi-Esfahani M, Soleimani M, Tavangar SM, Ai J. Retina tissue engineering by conjunctiva mesenchymal stem cells encapsulated in fibrin gel: Hypotheses on novel approach to retinal diseases treatment. Med Hypotheses. 2017;101:75-77.
119. Zhang J, Li P, Zhao G, He S, Xu D, Jiang W, Peng Q, Li Z, Xie Z, Zhang H, Xu Y, Qi L. Mesenchymal stem cell-derived extracellular vesicles protect retina in a mouse model of retinitis pigmentosa by anti-inflammation through miR-146a-Nr4a3 axis. Stem Cell Res Ther. 2022;13:394.
120. Sluch VM, Davis CH, Ranganathan V, Kerr JM, Krick K, Martin R, Berlinicke CA, Marsh-Armstrong N, Diamond JS, Mao HQ, Zack DJ.

Differentiation of human ESCs to retinal ganglion cells using a CRISPR engineered reporter cell line. Sci Rep. 2015;5:16595.
121. Zhang KY, Johnson TV. Analyses of transplanted human retinal ganglion cell morphology and localization in murine organotypic retinal explant culture. STAR Protoc. 2022;3:101328.
122. Zhang KY, Tuffy C, Mertz JL, Quillen S, Wechsler L, Quigley HA, Zack DJ, Johnson TV. Role of the Internal Limiting Membrane in Structural Engraftment and Topographic Spacing of Transplanted Human Stem Cell-Derived Retinal Ganglion Cells. Stem Cell Reports. 2021;16:149-167.
123. Zhang KY, Aguzzi EA, Johnson TV. Retinal ganglion cell transplantation: approaches for overcoming challenges to functional integration. Cells. 2021;10:1426.
124. Vrathasha V, Nikonov S, Bell BA, He J, Bungatavula Y, Uyhazi KE, Murthy Chavali VR. Transplanted human induced pluripotent stem cells- derived retinal ganglion cells embed within mouse retinas and are electrophysiologically functional. iScience. 2022;25:105308.
125. Bai YR, Lai BQ, Han WT, Sun JH, Li G, Ding Y, Zeng X, Ma YH, Zeng YS. Decellularized optic nerve functional scaffold transplant facilitates directional axon regeneration and remyelination in the injured white matter of the rat spinal cord. Neural Regen Res. 2021;16:2276-2283.
126. Rani S, Ryan AE, Griffin MD, Ritter T. Mesenchymal Stem Cell-derived Extracellular Vesicles: Toward Cell-free Therapeutic Applications. Mol Ther. 2015;23:812-823.
127. Paliwal S, Chaudhuri R, Agrawal A, Mohanty S. Human tissue-specific MSCs demonstrate differential mitochondria transfer abilities that may determine their regenerative abilities. Stem Cell Res Ther. 2018;9:298.
128. Millán-Rivero JE, Nadal-Nicolás FM, García-Bernal D, Sobrado-Calvo P, Blanquer M, Moraleda JM, Vidal-Sanz M, Agudo-Barriuso M. Human Wharton's jelly mesenchymal stem cells protect axotomized rat retinal ganglion cells via secretion of anti-inflammatory and neurotrophic factors. Sci Rep. 2018;8:16299.
129. Özmert E, Arslan U. Management of toxic optic neuropathy via a combination of Whartonıs jelly-derived mesenchymal stem cells with electromagnetic stimulation. Stem Cell Res Ther. 2021;12:518.
130. Özmert E, Arslan U. Management of retinitis pigmentosa by Whartonıs jelly-derived mesenchymal stem cells: prospective analysis of 1-year results. Stem Cell Res Ther. 2020;11:353.
131. Zhong Z, Deng X, Wang P, Yu C, Kiratitanaporn W, Wu X, Schimelman J, Tang M, Balayan A, Yao E, Tian J, Chen L, Zhang K, Chen S. Rapid bioprinting of conjunctival stem cell micro-constructs for subconjunctival ocular injection. Biomaterials. 2021;267:120462.
132. Guo Y, Xue Y, Wang P, Cui Z, Cao J, Liu S, Yu Q, Zeng Q, Zhu D, Xie M, Zhang J, Li Z, Liu H, Zhong J, Chen J. Muse cell spheroids have therapeutic effect on corneal scarring wound in mice and tree shrews. Sci Transl Med. 202012:eaaw1120.
133. Zhu L, Tang Q, Mao Z, Chen H, Wu L, Qin Y. Microfluidic-based platforms for cell-to-cell communication studies. Biofabrication. 2023;16.
134. Hirayama M, Ogawa M, Oshima M, Sekine Y, Ishida K, Yamashita K, Ikeda K, Shimmura S, Kawakita T, Tsubota K, Tsuji T. Functional lacrimal gland regeneration by transplantation of a bioengineered organ germ. Nat Commun. 2013;4:2497.

Case Report

In Vivo Confocal Microscopy and Anterior Segment Optical Coherence Tomography Findings of Patients with Iridocorneal Endothelial Syndrome

Gülay Güler Canözer, Emine Tınkır Kayıtmazbatır, Esra Öztürk, Ayşe Bozkurt Oflaz, Banu Bozkurt

Selçuk University Faculty of Medicine, Department of Ophthalmology, Konya, Türkiye

Abstract

This case report aims to present the findings of *in vivo* confocal microscopy (IVCM) and anterior segment optical coherence tomography (AS-OCT) in three patients with iridocorneal endothelial (ICE) syndrome. Three female patients 37, 50, and 57 years of age presented with complaints of unilateral visual impairment and elevated intraocular pressure (IOP). Biomicroscopy revealed unilateral pupil irregularities and anterior synechiae, and gonioscopy demonstrated synechiae in the iridocorneal angle. IOP was within normal limits with medical treatment in two patients, while one patient had an IOP of 44 mmHg despite maximal antiglaucomatous treatment. IVCM revealed large, polymorphic, and hyperreflective cells in the corneal endothelial layer of the affected eyes and normal corneal epithelium, stroma, and endothelium in the fellow eyes. AS-OCT findings were normal in healthy eyes, while the affected eye showed synechiae in the iridocorneal angle and a hyperreflective, thickened endothelial layer. The patient with refractory glaucoma underwent trabeculectomy surgery with 5-fluorouracil. In conclusion, IVCM and AS-OCT allow a detailed examination of endothelial cell abnormalities and iridocorneal membranes in ICE syndrome, which is characterized by unilateral pupil and iris irregularities and anterior synechiae mainly in women.

Keywords: Iridocorneal endothelial syndrome, *in vivo* confocal microscopy, anterior segment optical coherence tomography

Cite this article as: Güler Canözer G, Tınkır Kayıtmazbatır E, Öztürk E, Bozkurt Oflaz A, Bozkurt B. *In Vivo* Confocal Microscopy and Anterior Segment Optical Coherence Tomography Findings of Patients with Iridocorneal Endothelial Syndrome. Turk J Ophthalmol 2024;54:170-174

This study was presented as an oral presentation at the 45th TOA Winter Symposium (19-21 January 2024, Konya).

Address for Correspondence: Emine Tınkır Kayıtmazbatır, Selçuk University Faculty of Medicine, Department of Ophthalmology, Konya, Türkiye
E-mail: drtinkir@gmail.com **ORCID-ID:** orcid.org/0000-0002-8553-6992
Received: 24.01.2024 **Accepted:** 22.04.2024

DOI: 10.4274/tjo.galenos.2024.78861

Introduction

Iridocorneal endothelial (ICE) syndrome is a group of diseases in which corneal endothelial cells multiply and migrate to the iridocorneal angle and onto the iris.[1] There are three clinical variants: Chandler syndrome, progressive iris atrophy, and Cogan-Reese syndrome.[2] Yanoff[3] proposed the term ICE for these clinical entities, which have similar clinical findings and a common pathogenic mechanism characterized by abnormal endothelial proliferation.[4] In ICE syndrome, abnormally proliferating endothelial cells form a membrane on the iridocorneal angle and peripheral iris. This membrane can cause pupillary disorder, high intraocular pressure (IOP), corneal decompensation, and corneal edema due to peripheral anterior synechiae and peripheral iris traction. ICE syndrome occurs sporadically, is usually unilateral, and typically affects women 30-40 years of age.[5] Although its etiology is not fully known, it is thought to be of viral origin.[6] In the differential diagnosis, consideration should be given to conditions such as posterior polymorphous corneal dystrophy, Fuchs endothelial dystrophy, and Axenfeld-Rieger syndrome. In addition, findings such as aniridia, pupillary deformities, and corneal edema must also be evaluated alongside potential diagnoses including iris melanoma, inflammatory iris nodules, and glaucoma. This case report presents the clinical examination findings, *in vivo* confocal microscopy (IVCM, Heidelberg Retina Tomograph 3, Rostock Cornea Module, Germany) and anterior segment optical coherence tomography (AS-OCT, DRI Triton Topcon, Tokyo, Japan) findings, and treatment of 3 female patients with ICE syndrome.

Case Report

Case 1

A 50-year-old woman presented with decreased vision and elevated IOP in the left eye. The patient was using topical

brimonidine (Alphagan P 0.15%, AbbVie Pharmaceuticals, İstanbul, Türkiye), timolol/dorzolamide (Tomec 2% + 0.5% Abdi İbrahim Pharmaceuticals, İstanbul, Türkiye), and latanoprostene bunod (Vyzulta 0.024%, Bausch & Lomb Incorporated, Bridgewater, NJ, USA) drops in the left eye. On examination, her best-corrected visual acuity (BCVA) was 20/20 bilaterally and her IOP was 16 mmHg in the right eye and 44 mmHg in the left eye. Anterior segment findings in the right eye were normal, while the left eye showed inferonasal pupil displacement (Figure 1a, b) and peripheral anterior synechiae at 6-9 o'clock with a "beaten bronze" appearance in the endothelium. On gonioscopic examination of the left eye, extensive synechia at the iridocorneal angle was observed in the region corresponding to the iris irregularity (Figure 2a). On fundus examination, the cup/disc (C/D) ratio was 0.3 in the right eye and 0.7 in the left eye. Peripapillary nerve fiber layer thickness was 98 µm in the right eye and 63 µm in the left eye (Figure 3a, b). Visual field test revealed no visual field defect in the right eye and an altitudinal scotoma in the left eye (Figure 3c, d). The patient underwent trabeculectomy surgery with 5-fluorouracil (5-FU; Koçak Pharmaceuticals, Tekirdağ, Türkiye). IOP was 12 mmHg at postoperative 1 month.

Case 2

A 37-year-old woman presented with decreased vision and high IOP in the left eye. She was using topical brimonidine (Brimogut 0.15%, Bilim Pharmaceuticals, İstanbul, Türkiye) and brinzolamide/timolol (Azarga, Novartis International AG, Basel, Switzerland) in her left eye. Her BCVA was 20/20 in both eyes; IOP was 15 mmHg in the right eye and 12 mmHg in the left eye. On anterior segment examination, the right eye was normal, while the pupil of the left eye was rectangular in shape, elongated on a superotemporal-inferonasal axis (Figure 1c, d). There were peripheral anterior synechiae at 2 and 7 o'clock with a "beaten bronze" appearance in the endothelium. Gonioscopy also revealed extensive synechia at the iridocorneal angle in the region of the iris irregularity (Figure 2b). On fundus examination, the optic nerve and macula were normal in both eyes. The C/D ratio was 0.3 bilaterally. The patient was recommended follow-up with her current antiglaucoma therapy.

Case 3

A 57-year-old woman presented with decreased vision and high IOP. The patient was using brimonidine (Brimogut 0.15%, Bilim Pharmaceuticals, İstanbul, Türkiye) and brinzolamide/timolol (Azarga, Novartis International AG, Basel, Switzerland) antiglaucoma drops. On examination, BCVA was 20/40 in the right eye and 20/20 in the left eye. IOP was measured as 18 mmHg in the right eye and 13 mmHg in the left eye. On anterior segment examination, peripheral iridocorneal synechiae at 1-3 o'clock, iris atrophy, and corectopia were observed in the right eye (Figure 1e). Left anterior segment examination was normal

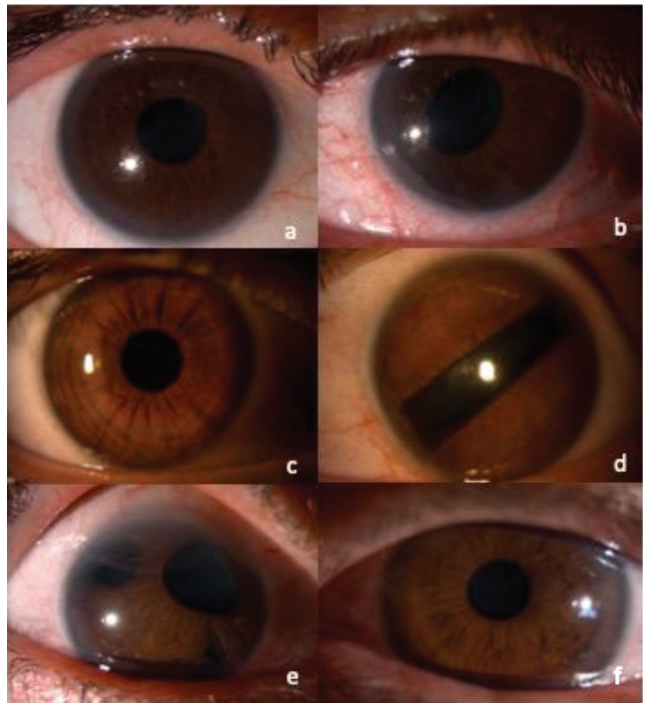

Figure 1. Anterior segment photographs of the patients: Patient 1: (a) healthy right eye, (b) affected eye showing inferonasal pupil displacement and anterior synechia in the same quadrant. Patient 2: (c) healthy right eye, (d) affected left eye showing an abnormal rectangular pupil extending along a superotemporal-inferonasal axis. Patient 3: (e) affected right eye showing peripheral iridocorneal synechia at 1-3 o'clock, iris atrophy, and corectopia, (f) healthy left eye

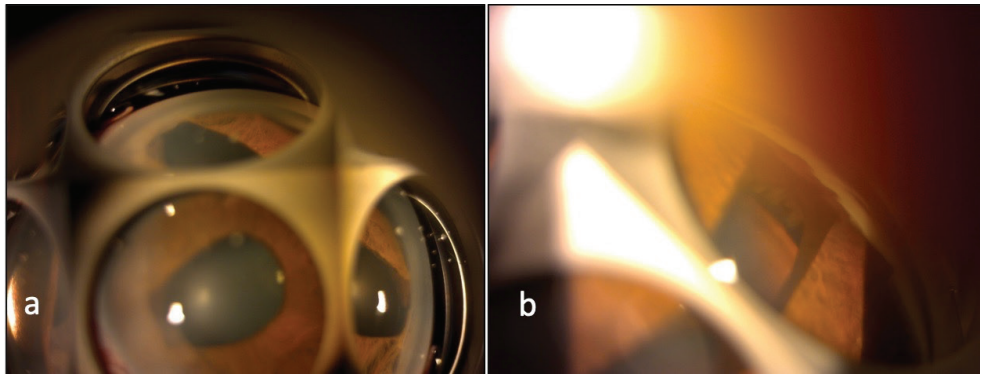

Figure 2. (a) Gonioscopy image of patient 1 shows extensive synechia at the iridocorneal angle in the lower nasal quadrant where the iris irregularity is located, and apparent ectropion uveae in the nasal quadrant, consistent with the anterior segment image. (b) Gonioscopy image of patient 2 shows extensive synechia at the iridocorneal angle in the region of the iris irregularity

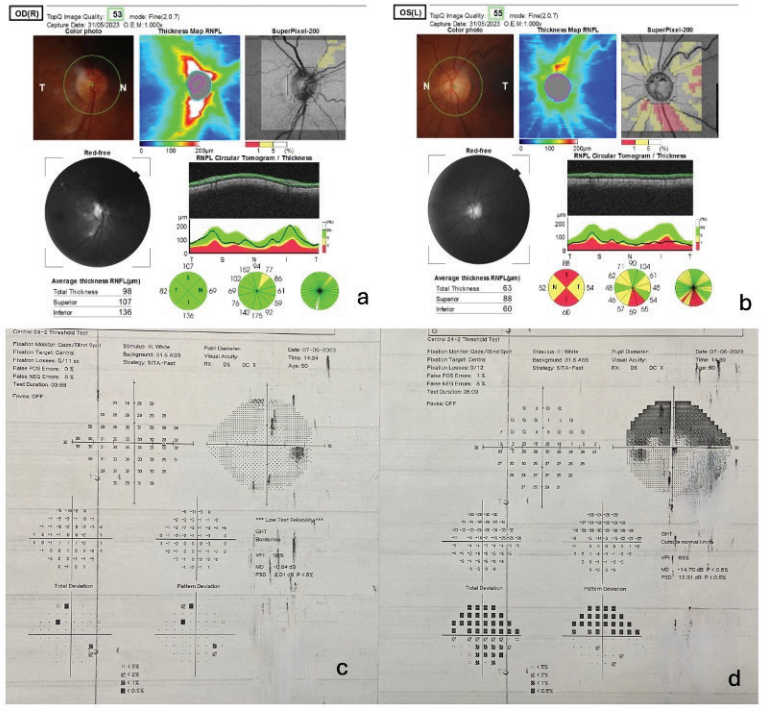

Figure 3. In patient 1, (a) peripapillary nerve fiber layer was 98 µm in the right eye, (b) 63 µm in the left eye, (c) visual field tests demonstrated no defect in the right eye, (d) altitudinal scotoma was detected in the left eye

(Figure 1f). On gonioscopy, there were extensive synechiae at the iridocorneal angle corresponding to the iris irregularity. Fundus examination revealed normal maculae bilaterally with a C/D ratio of 0.5 on the right and 0.3 on the left. The peripapillary nerve layer thickness was measured as 93 µm on the right and 105 µm on the left. The patient was recommended follow-up with her current medical treatment.

IVCM Findings

On IVCM, the corneal epithelium, stroma, and endothelial layers were normal in the patients' healthy eyes (Figure 4a, c, f). In the affected eyes, patient 1 exhibited cobblestone-like swollen endothelial cells, which were thought to correspond to the beaten bronze appearance observed on biomicroscopy, and occasional giant cells (Figure 4b). In patient 2, the endothelial cells were hyperreflective, highly polymorphic, and had lost their normal hexagonality, showing irregular borders and cobblestone pattern (Figure 4d), while hyperreflective uni- or binucleate giant endothelial cells were observed in patient 3 (Figure 4e).

AS-OCT Findings

AS-OCT parameters were within normal limits in the patients' healthy eyes. Corneal thicknesses were 559, 576, and 480 µm, respectively. In the affected eyes, there was extensive synechia at the iridocorneal angle, increased hyperreflectivity in the endothelial layer, and thickened hyperreflective tissue resembling an epiretinal membrane over the iridocorneal angle and iris. An increase in hyperreflectivity was observed in the endothelial layer of one patient, while another patient had several round hyperreflective formations on the membranous structure overlying the iris and one beneath the endothelial layer (Figure 5a-d). Corneal thicknesses were 552, 604, 561 µm, respectively.

Discussion

ICE syndrome is a rare condition characterized by proliferative and structural abnormalities in the corneal endothelium, iridocorneal angle obstruction, and iris defects such as atrophy and holes.[4] Patients usually present when they notice a change in the shape and position of the pupil or because of a decrease in visual acuity due to corneal edema and glaucoma. Two of our patients presented to our clinic with reduced vision and all were using antiglaucomatous treatment due to high IOP.

Although the etiology of ICE is still not fully understood, it is thought to be viral in origin. Using polymerase chain reaction (PCR) methods, Alvarado et al.[6] detected herpes simplex virus (HSV) DNA in over 60% of corneal and aqueous humor samples obtained from patients with ICE syndrome, but PCR results were negative in the patients' unaffected eyes. Histopathological studies have shown that corneal endothelial cells have epithelial-like morphological features, and these epithelial-like endothelial cells were called "ICE cells".[7] These abnormal endothelial cells obstruct the iridocorneal angle and advance through the anterior chamber to cover the iris, forming a basement membrane that leads to abnormal pupil shape and iris atrophic damage and adhesions to neighboring structures.[8] Being a rare disease with variable clinical presentations, ICE syndrome may be overlooked and misdiagnosed. Imaging the abnormal corneal endothelium

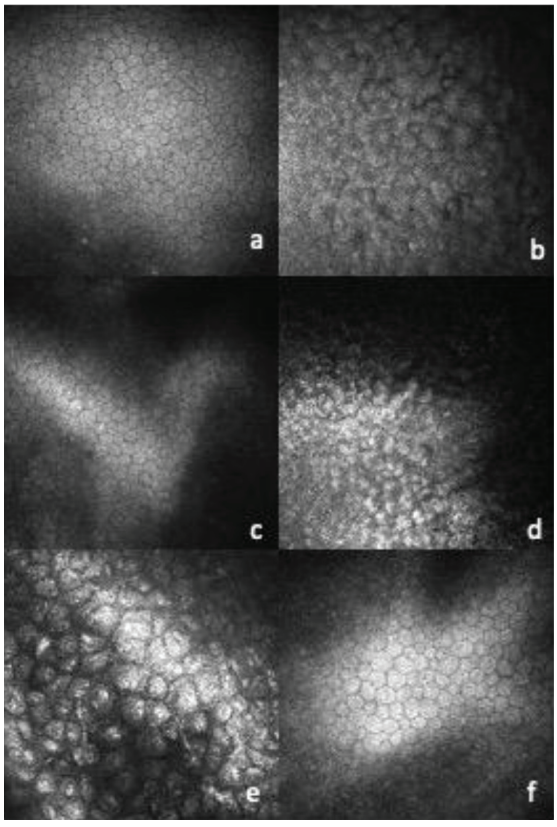

Figure 4. *In vivo* confocal microscopy images of the patients. Patient 1: (a) hexagonal endothelial layer in the healthy eye, (b) endothelial cells showing cobblestone-like swelling and occasional giant cells in the affected eye. Patient 2: (c) endothelial layer in the healthy eye, (d) hyperreflective, irregularly bordered endothelial cells showing cobblestone-like swelling in the affected eye. Patient 3: (e) hyperreflective uni- or binucleate giant endothelial cells in the affected right eye, (f) normal-looking endothelial cells in the healthy eye

during examination or evaluating the anterior chamber angle in glaucoma suspects is also important in terms of distinguishing it from other endotheliopathies. High-magnification slit-lamp examination may show a "beaten bronze" endothelium appearance. However, evaluating the endothelial layer and visualizing the anterior chamber and iris details might be difficult in patients with severe corneal edema.

IVCM is a non-interventional, high-resolution imaging technique that aids in the evaluation of corneal layers and cells, similar to histopathological sections. In a study of patients with ICE syndrome, two basic "epithelial-like endothelial cell" morphologies were described.[9] While the first type of abnormal endothelium cells were close in shape and size to the normal endothelial cell morphology, they lost normal hexagonality and had a distinct uniform "cobblestone-like" nucleus in their centers, with some having two nuclei or a single divided nucleus. The second type was more irregular in cellular size and shape, with hyperreflective variously shaped nuclei adjacent to the cell borders.[9]

In another IVCM and specular microscopy study conducted in patients with ICE syndrome, three types of cells were identified: smooth, epithelium-sized cells; cells resembling epithelial wing cells with a central hyperreflective nucleus; and highly irregular endothelial cells resembling superficial epithelial cells.[10] In another study conducted in Türkiye, ICE cells were identified on specular microscopy as white-bordered black cells, the reverse image of endothelial cells, and peripheral anterior synechiae and iris atrophy were shown in ultrasonic biomicroscopy in the same eye.[11]

In our cases, IVCM in eyes affected by ICE syndrome revealed highly polymorphic endothelial cells with cobblestone-like swelling, as well as hyperreflective uni- or binucleate giant cells in one patient.

A case report published by Hillard[12] evaluated angle and corneal changes in ICE syndrome with AS-OCT and demonstrated

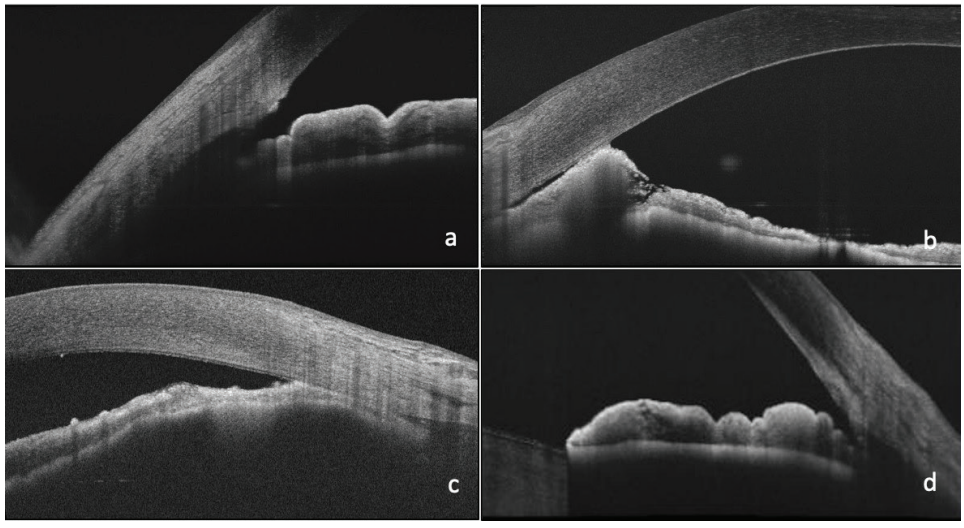

Figure 5. Anterior segment optical coherence tomography images. Patient 1: (a) healthy iridocorneal angle in left eye; (b) synechia at the iridocorneal angle, increased hyperreflectivity in the endothelial layer, thickening of hyperreflective tissue resembling an epiretinal membrane on the iridocorneal angle and iris in the affected right eye. Patient 3: (c) the affected right eye shows synechia at the iridocorneal angle, increased hyperreflectivity in the endothelial layer, irregular tissue thickening of the hyperreflective layer overlying the iris, several round hyperreflective formations on this membranous structure over the iris, and one under the endothelial layer; (d) normal iridocorneal angle appearance in the healthy left eye

in detail iridocorneal membrane formation, adhesions, and subepithelial bullae secondary to corneal edema. In our study, in addition to iridocorneal adhesions on swept-source OCT, we observed increased hyperreflectivity in the endothelial layer and a thickened hyperreflective tissue resembling an epiretinal membrane on the iridocorneal angle and iris.

In patients with high IOP, medical treatment and drugs that reduce aqueous production are preferred as the first-line treatment option. However, as the possible role of HSV in the pathogenesis has not been conclusively ruled out, prostaglandin analogues should be avoided in treatment. Surgical interventions such as goniotomy, trabeculectomy with antifibrotic agents such as mitomycin-C or 5-FU, glaucoma drainage implants, or cyclodestructive procedures should be considered in cases where medical treatment is insufficient.[1,2,13] However, recurrent obstructions resulting from proliferation of the endothelial membrane may cause surgical failure. Among our cases, one patient with high IOP despite medical treatment underwent trabeculectomy surgery combined with 5-FU.

In conclusion, ICE syndrome should be suspected in cases of unilateral IOP elevation accompanied by corectopia and corneal edema, especially in female patients. IVCM and AS-OCT are non-invasive, diagnostically useful imaging methods that can reveal the abnormal structure and anterior segment migration of endothelial cells with epithelial characteristics in ICE syndrome.

Ethics

Informed Consent: Obtained.

Authorship Contributions

Surgical and Medical Practices: G.G.C., E.Ö., B.B., Concept: G.G.C., E.T.K., E.Ö., A.B.O., B.B., Design: G.G.C., E.T.K., E.Ö., A.B.O., B.B., Data Collection or Processing: G.G.C., E.T.K., E.Ö., A.B.O., Analysis or Interpretation: G.G.C., E.T.K., E.Ö., A.B.O., B.B., Literature Search: G.G.C., E.T.K., E.Ö., B.B., Writing: G.G.C., E.T.K., A.B.O., B.B.

Conflict of Interest: No conflict of interest was declared by the authors.

Financial Disclosure: The authors declared that this study received no financial support.

References

1. Silva L, Najafi A, Suwan Y, Teekhasaenee C, Ritch R. The iridocorneal endothelial syndrome. Surv Ophthalmol. 2018;63:665-676.
2. Sacchetti M, Mantelli F, Marenco M, Macchi I, Ambrosio O, Rama P. Diagnosis and Management of Iridocorneal Endothelial Syndrome. Biomed Res Int. 2015;2015:763093.
3. Yanoff M. Iridocorneal endothelial syndrome: unification of a disease spectrum. Surv Ophthalmol. 1979;24:1-2.
4. Shields MB. Progressive essential iris atrophy, Chandler's syndrome, and the iris nevus (Cogan-Reese) syndrome: a spectrum of disease. Surv Ophthalmol. 1979;24:3-20.
5. Scheie HG, Yanoff M. Iris nevus (Cogan-Reese) syndrome. A cause of unilateral glaucoma. Arch Ophthalmol. 1975;93:963-970.
6. Alvarado JA, Underwood JL, Green WR, Wu S, Murphy CG, Hwang DG, Moore TE, O'Day D. Detection of herpes simplex viral DNA in the iridocorneal endothelial syndrome. Arch Ophthalmol. 1994;112:1601-1609.
7. Sherrard ES, Frangoulis MA, Muir MG, Buckley RJ. The posterior surface of the cornea in the irido-corneal endothelial syndrome: a specular microscopical study. Trans Ophthalmol Soc U K (1962). 1985;104(Pt 7):766-774.
8. Campbell DG, Shields MB, Smith TR. The corneal endothelium and the spectrum of essential iris atrophy. Am J Ophthalmol. 1978;86:317-324.
9. Le QH, Sun XH, Xu JJ. In-vivo confocal microscopy of iridocorneal endothelial syndrome. Int Ophthalmol. 2009;29:11-18.
10. Chiou AG, Kaufman SC, Beuerman RW, Ohta T, Yaylali V, Kaufman HE. Confocal microscopy in the iridocorneal endothelial syndrome. Br J Ophthalmol. 1999;83:697-702.
11. Altındal EU, Türkoğlu EB, Hasanreisoğlu M, Gülpınar G. Iridocorneal Endotheliıal Syndrome: A Case Report and Review of the Literature. Turkiye Klinikleri J Ophthalmol. 2016;25:66-70.
12. Hillard JG. Case Report: Iridocorneal Endothelial Syndrome Progression Documented by Anterior Segment Optical Coherence Tomography. Optom Vis Sci. 2019;96:309-313.
13. Laganowski HC, Kerr Muir MG, Hitchings RA. Glaucoma and the iridocorneal endothelial syndrome. Arch Ophthalmol. 1992;110:346-350.

Case Report

Endogenous Endophthalmitis Caused by *Aspergillus lentulus* in an Immunocompromised Patient with Lung Cancer

Mustafa Kayabaşı*, Ziya Ayhan**, Banu Lebe***, Ayşe Aydan Özkütük****, Meltem Söylev Bajin**, Arzu Nazlı*****, Eyüp Sabri Uçan******, Aziz Karaoğlu*******, Ali Osman Saatci**

*Muş State Hospital, Clinic of Ophthalmology, Muş, Türkiye
**Dokuz Eylül University Faculty of Medicine, Department of Ophthalmology, İzmir, Türkiye
***Dokuz Eylül University Faculty of Medicine, Department of Pathology, İzmir, Türkiye
****Dokuz Eylül University Faculty of Medicine, Department of Microbiology, İzmir, Türkiye
*****Dokuz Eylül University Faculty of Medicine, Department of Infectious Diseases, İzmir, Türkiye
******Dokuz Eylül University Faculty of Medicine, Department of Chest Diseases, İzmir, Türkiye
*******Dokuz Eylül University Faculty of Medicine, Department of Oncology, İzmir, Türkiye

Abstract

A 78-year-old man with a history of lung cancer, chemotherapy, radiotherapy, and coronavirus disease 2019 infection experienced visual deterioration of two-weeks' duration in his right eye. There was multifocal, yellowish-white retinitis foci, vascular engorgement, and scattered intraretinal hemorrhages extending from posterior pole to retinal periphery in the right eye, whereas the left eye was normal. Intravitreal vancomycin, ceftazidime, clindamycin, and dexamethasone were given for endogenous endophthalmitis initially. Vitreous culture confirmed the presence of *Aspergillus lentulus*, and he was treated with intravitreal amphotericin-B and voriconazole injections together with systemic amphotericin-B, voriconazole, posaconazole, and micafungin therapy. During follow-up, vitreoretinal surgery was performed because of rhegmatogenous retinal detachment, and he received one additional cycle of chemotherapy due to recurrence of the cancer. Although the retina was attached, enucleation was eventually required due to painful red eye. Atypical squamous cells beneath the neurosensory retina suggesting metastasis were noted on histopathological examination. Timely ocular examination is crucial for any immunocompromised patient having ocular symptoms. High level of suspicion for a fungal etiology is a must in these patients.

Keywords: *Aspergillus lentulus*, COVID-19 infection, endogenous endophthalmitis, immunosuppression, retinitis

Cite this article as: Kayabaşı M, Ayhan Z, Lebe B, Özkütük AA, Söylev Bajin M, Nazlı A, Uçan ES, Karaoğlu A, Saatci AO. Endogenous Endophthalmitis Caused by *Aspergillus lentulus* in an Immunocompromised Patient with Lung Cancer. Turk J Ophthalmol 2024;54:175-179

Address for Correspondence: Ali Osman Saatci, Dokuz Eylül University Faculty of Medicine, Department of Ophthalmology, İzmir, Türkiye
E-mail: osman.saatci@gmail.com **ORCID-ID:** orcid.org/0000-0001-6848-7239
Received: 29.03.2024 **Accepted:** 27.05.2024

DOI: 10.4274/tjo.galenos.2024.44045

Introduction

Endogenous endophthalmitis (EE) is typically associated with various risk factors such as systemic comorbidities, recent hospitalization, prolonged use of intravenous cannulas and catheters, intravenous drug use, and systemic infections.[1] Additionally, one or more factors contributing to an immunosuppressive state, such as early or advanced age, malignancy, diabetes mellitus, or the use of corticosteroids or non-corticosteroid immunosuppressive agents may also play a role.[2,3] Despite being less common than exogenous endophthalmitis, EE poses a greater danger to patients due to its life-threatening potential.[4,5] Coronavirus disease 2019 (COVID-19) has been shown to affect various organs and systems, including the eye.[6,7] Although both bacterial and fungal EE have been reported following COVID-19 infection, it has been shown that a fungal etiology is more likely than a bacterial etiology in these cases.[8,9]

Here, we present an extremely rare case in which a patient with lung cancer developed unilateral EE caused by *Aspergillus lentulus*.

Case Report

A 78-year-old man was referred to us with a gradual visual deterioration of two weeks' duration in his right eye. He previously received six cycles of chemotherapy based on paclitaxel and carboplatin, followed by four cycles of docetaxel, along with systemic radiation therapy for lung cancer diagnosed elsewhere 10 months earlier. He also had a history of systemic arterial hypertension, a recent hospitalization for COVID-19 infection just after the last chemotherapy session, and

uneventful bilateral cataract surgery with intraocular lens (IOL) implantation performed elsewhere 4 years ago.

On ophthalmological examination, his best-corrected Snellen visual acuity was counting fingers at 1 meter in the right eye and 8/10 in the left eye. Slit-lamp evaluation revealed 2+ anterior chamber cells, a posterior chamber IOL, and moderate vitritis in the right eye, while the left anterior segment was normal. Intraocular pressure was within normal limits bilaterally. Right fundus examination demonstrated a normal-looking optic disc and fovea but with grade 6 vitreous haze (according to the Miami scoring system[10]), white-yellowish presumed retinitis foci extending towards the superior retinal periphery, engorged vessels, and scattered intraretinal hemorrhages (Figure 1A and B). The left fundus was normal. A horizontal spectral-domain optical coherence tomographic section (Heidelberg Spectralis, Heidelberg Engineering, Heidelberg, Germany) passing through the retinitis area showed hyporeflective outer retinal layers related to the shadowing effect from the increased hyperreflectivity of the inner retinal layers, along with vitritis, vitreoretinal traction, and hyperreflective particles in the posterior vitreous (Figure 1C). We felt that the clinical presentation was compatible with right EE. A full systemic work-up was carried out, including complete blood count, routine biochemistry, sedimentation rate, C-reactive protein level, full infectious panel, and QuantiFERON-TB Gold test (Cellestis Inc., Carnegie, Victoria, Australia). A vitreous sample was obtained from the right eye by vitreous puncture using a 26-gauge needle for bacterial and fungal cultures and polymerase chain reaction (PCR) analysis for the viral etiology. Then, intravitreal injection of 1 mg/0.1 cc vancomycin (Vancotek, Koçak Farma, İstanbul, Türkiye), 2 mg/0.1 cc ceftazidime (Zidim, Tüm Ekip İlaç, İstanbul, Türkiye), 1 mg/0.1 cc clindamycin (Klinoksin, Deva İlaç, İstanbul, Türkiye), and 0.4 mg/0.1 cc dexamethasone (Dekort, Deva İlaç, İstanbul, Türkiye) was administered into the right eye under topical anesthesia. Topical 1% cyclopentolate (Siklоplejin, Abdi İbrahim, İstanbul, Türkiye) 3 times a day, 1% prednisolone (Maxidex, Alcon, Geneva, Switzerland) 8 times a day, and 0.5% moxifloxacin (Vigamox, Novartis, Basel, Switzerland) 6 times a day were commenced.

Serological tests for several infectious causes (including *Toxoplasma gondii*, cytomegalovirus, human immunodeficiency virus); QuantiFERON-TB Gold test; viral PCR analysis; and bacterial and fungal culture were negative. The vitreous haze briefly regressed, likely due to concurrent dexamethasone injection. The clinical findings then worsened despite three subsequent intravitreal injections of vancomycin, ceftazidime, and clindamycin administered over a 1-month period. Therefore, another vitreous sample was obtained, this time using a vitreous cutter set at 5000 cuts/min attached to a 2-mL syringe with manual suction under local anesthesia. Direct microscopic examination of the vitreous sample was unremarkable. Repeat viral PCR analysis and bacterial culture once again yielded

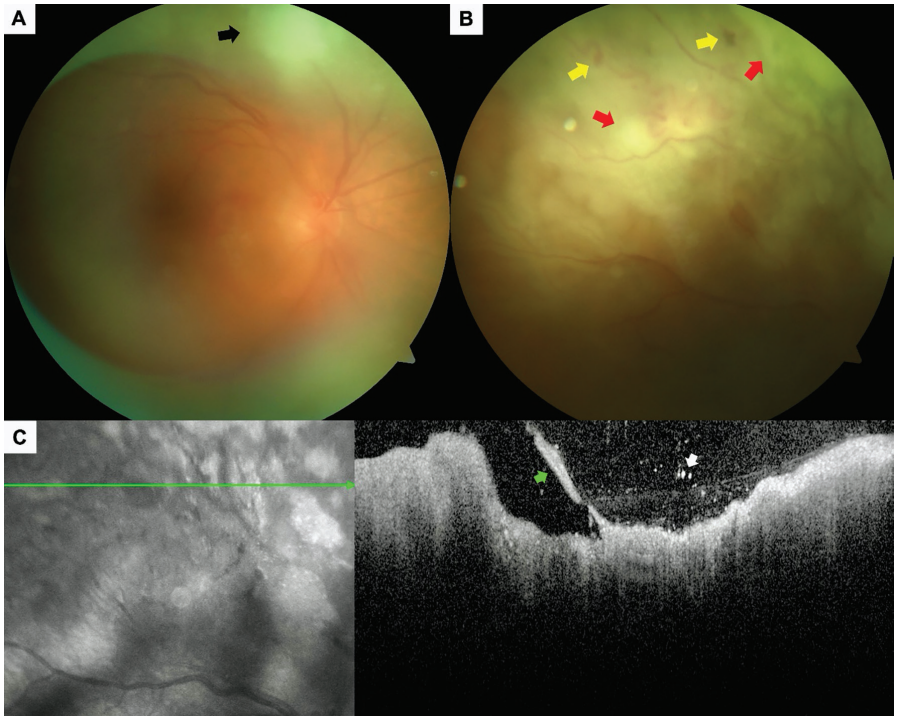

Figure 1. Right eye. Color fundus image of the posterior pole (A) showing the normal-looking optic disc and fovea, along with grade 6 vitreous haze and an area of retinitis (black arrow). Color fundus image of the superior retinal periphery (B) demonstrating the multifocal, yellowish-white presumed retinitis foci (red arrows), vascular engorgement, and scattered intraretinal hemorrhages (yellow arrows). Spectral-domain optical coherence tomographic section passing through the retinitis foci (C) depicting the hyporeflective outer retinal layers due to shadowing by the increased hyperreflectivity of the inner retinal layers, along with vitritis, vitreoretinal traction (green arrow), and hyperreflective particles in the posterior vitreous (white arrow)

negative results, but this time, fungal culture confirmed the presence of *A. lentulus* (Figure 2). Susceptibility testing for antifungal drugs could not be performed due to the unavailability of the testing kits at our hospital during that time. The patient received seven intravitreal injections of 5 mcg/0.1 cc amphotericin-B (AmBisome, Gilead Pharmaceuticals, Foster City, USA) and three intravitreal injections of 0.1 mg/0.1 cc voriconazole (Vfend, Pfizer, New York, USA) in the right eye and underwent parenteral administration of amphotericin-B (AmBisome, Gilead Pharmaceuticals), voriconazole (Vfend, Pfizer), posaconazole (Posectio, Polifarma, İstanbul, Türkiye), and micafungin (Mikafungus, Polifarma, İstanbul, Türkiye) followed by oral voriconazole (Vfend, Pfizer) therapy over a nearly 2-month period.

Three months after admission, the patient underwent right pars plana vitrectomy, laser photocoagulation, and silicone endotamponade surgery due to the development of rhegmatogenous retinal detachment. The oncology department administered one more cycle of chemotherapy based on paclitaxel due to the recurrence of the lung cancer detected by positron emission tomography. Unfortunately, the patient developed a painful red eye with corneal edema, 0.5 mm hypopyon, 3+ anterior chamber cells, and precipitates on the posterior IOL surface together with irideal lumps suggesting metastasis (Figure 3). Right enucleation was performed. Upon microscopic examination of the specimen, we observed atypical squamous cells forming solid islands beneath the sensory retinal epithelium, indicative of metastasis from the lung cancer (Figure 4).

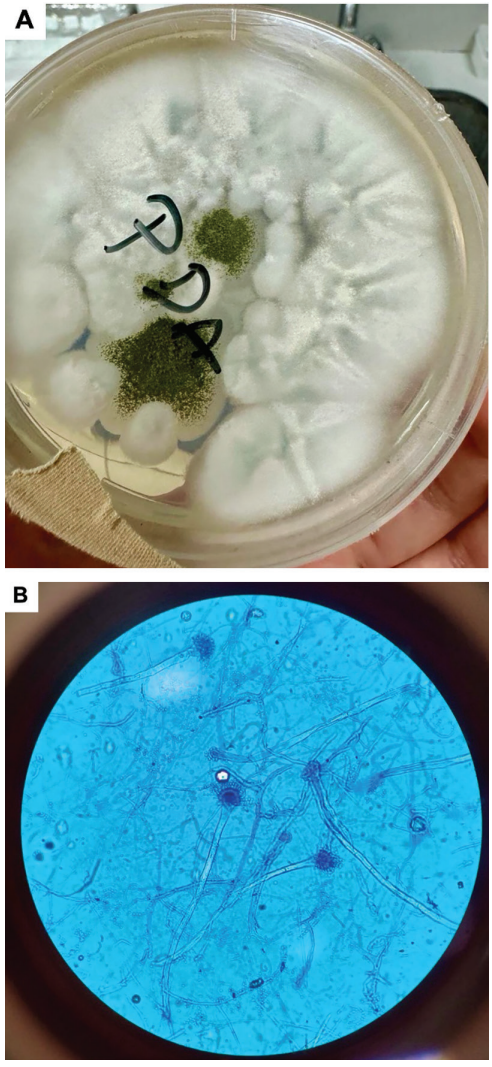

Figure 2. Morphologic appearance (A) of *Aspergillus lentulus* on potato dextrose agar showing colonies that are white and pale green-blue with slow sporulation. Microscopic image (B) showing the smaller, conidial heads with more diminutive vesicles compared to *Aspergillus fumigatus* (magnification 40x)

Discussion

EE constitutes almost 2-8% of all cases of endophthalmitis. Bacterial EE infections are mostly caused by gram-positive bacteria, notably *Staphylococcus* and *Streptococcus* spp., while gram-negative bacteria, especially *Klebsiella* spp., are more commonly encountered in Asian regions.[4,11] On the other hand, *Candida* spp. are the most common fungal cause of EE, followed by *Aspergillus* spp.[12]

A. lentulus, which has been phenotypically identified as *A. fumigatus*, is a genetically distinct and highly drug-resistant species of *Aspergillus*.[13,14] To the best of our knowledge, *A. lentulus* endophthalmitis was first described by Shivasabesan et al.[15] in a 72-year-old woman with a history of orthotopic heart transplantation due to idiopathic dilated cardiomyopathy. She developed invasive pulmonary aspergillosis caused by *A. lentulus* despite being under prophylactic itraconazole therapy that was commenced prior to transplantation. Subsequently, the authors switched itraconazole to voriconazole. Several days later, the patient experienced painless floaters in her right eye. Fine

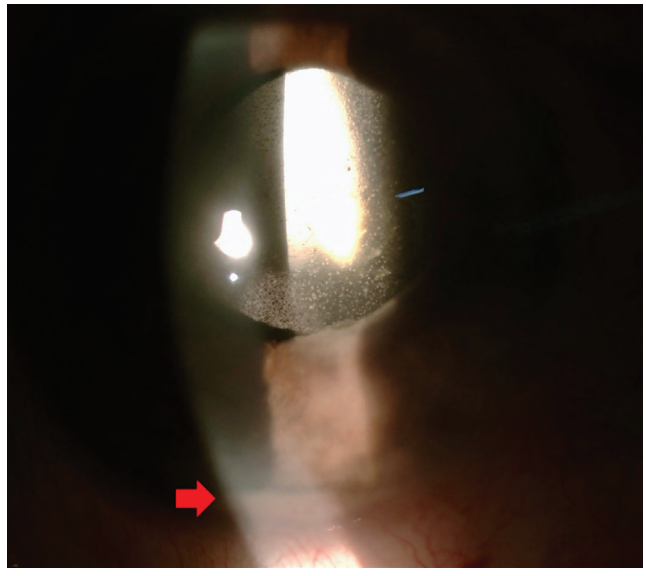

Figure 3. Right eye. Anterior segment photo revealing the mild corneal edema, 3+ anterior chamber cells, a 0.5 mm hypopyon (red arrow), and precipitates on the posterior intraocular lens surface

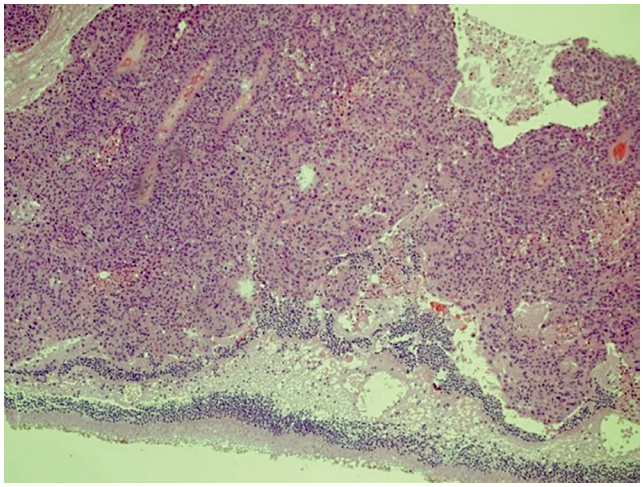

Figure 4. Microscopic image of the enucleation specimen depicting atypical squamous cells forming solid islands under the sensorineural retinal epithelium, indicating squamous cell carcinoma (original magnification 10x, stained with hematoxylin & eosin)

keratic precipitates and 2+ anterior chamber cells were observed upon ophthalmological examination, together with a large white mushroom-shaped subretinal mass projecting into the subhyaloid space with overlying mild to moderate vitreous haze in her right eye. 18s rRNA gene sequencing of the intravitreal aspirate confirmed the presence of *A. lentulus*, and twice weekly intravitreal voriconazole injections were commenced concurrent with the systemic voriconazole and anidulafungin therapy. Three weeks later, the patient underwent pars plana vitrectomy with removal of the fungal lesion, perilesional endolaser administration, intravitreal voriconazole injection, and fluid-air exchange due to lesion spread into the vitreous cavity. Intravitreal voriconazole injections were continued for 3 weeks post-vitrectomy.[15] Though systemic fungal infection was not present in our case, similar clinical progress was observed, where only an initial partial response could be obtained with intravitreal and systemic antifungal treatment. Moreover, rhegmatogenous retinal detachment developed, presumably secondary to intraocular inflammation and the burden of repeated intravitreal injections in the right eye, and vitreoretinal surgery was performed. Although the retina was attached, enucleation was eventually performed due to painful red eye.

Recently, Thompson et al.[16] evaluated the clinical course of EE in 37 eyes of 31 patients and reported vision loss, redness, and eye pain as the most common presenting symptoms. Only 7 eyes of 5 patients had fungal EE. They highlighted that all EE cases had at least one significant risk factor related to immunosuppression and concluded that prompt ocular examination was essential in immunocompromised patients experiencing any ocular symptoms to facilitate rapid diagnostic and therapeutic interventions.[16] Similarly, our patient was immunosuppressed because he had malignancy and a history of chemotherapy, and he had also experienced a recent COVID-19 infection prior to EE.

The primary treatment modality for fungal EE is intravenous and concomitant intravitreal administration of antifungal drugs. Polyenes (amphotericin B), azoles (voriconazole, isavuconazole, posaconazole), and echinocandins (micafungin, caspofungin) are among the preferred antifungal drugs. To date, voriconazole has been utilized as the first-line treatment of fungal EE via both the systemic and intravitreal routes as it attains higher concentrations in the intravitreal space. *A. lentulus* has been reported as a more drug-resistant subtype of *Aspergillus*, exhibiting reduced antifungal susceptibility for several antifungal agents.[15,17] We chose a combination of intravitreal amphotericin-B and voriconazole injections along with systemic amphotericin-B, voriconazole, posaconazole, and micafungin as the antifungal treatment in the present case, considering the possible drug resistance of *A. lentulus.*

In conclusion, a prompt ophthalmic examination to detect intraocular inflammation is crucial for any immunocompromised patient exhibiting presumptive ocular symptoms to facilitate early diagnosis and select the appropriate therapeutic regimen to prevent irreversible vision loss. As the differential diagnosis can be challenging, clinicians should have a high index of suspicion for potential fungal etiology and a proactive approach to ensure comprehensive care and optimized outcomes in this group of patients.

Ethics

Informed Consent: Obtained.

Authorship Contributions

Surgical and Medical Practices: Z.A., M.S.B., A.N., E.S.U., A.K., A.O.S., Concept: M.K., A.O.S., Design: M.K., B.L., A.A.Ö., A.O.S., Data Collection or Processing: M.K., B.L., A.A.Ö., Analysis or Interpretation: Z.A., M.S.B., A.O.S., Literature Search: M.K., A.N., E.S.U., A.K., A.O.S., Writing: M.K., A.O.S.

Conflict of Interest: No conflict of interest was declared by the authors.

Financial Disclosure: The authors declared that this study received no financial support.

References

1. Regan KA, Radhakrishnan NS, Hammer JD, Wilson BD, Gadkowski LB, Iyer SSR. Endogenous Endophthalmitis: yield of the diagnostic evaluation. BMC Ophthalmol. 2020;20:138.
2. Markan A, Dogra M, Katoch D, Tomar M, Mittal H, Singh R. Endogenous Endophthalmitis in COVID-19 Patients: A Case Series and Literature Review. Ocul Immunol Inflamm. 2023;31:1191-1197.
3. Takes O, Kocaoglu G, Saatci AO. Successful Treatment of a Case of Unilateral Endogenous Klebsiella pneumoniae Endophthalmitis. EEur Ophth. 2015;9:23-24.
4. Cunningham ET, Flynn HW, Relhan N, Zierhut M. Endogenous Endophthalmitis. Ocul Immunol Inflamm. 2018;26:491-495.
5. Ayhan Z, Karataş E, Yaman A, Saatci AO. *Endojen Endoftalminin Klinik Özellikleri* [Clinical Features of Endogenous Endophthalmitis]. Ret-Vit. 2019;28:51-56.
6. Cucinotta D, Vanelli M. WHO Declares COVID-19 a Pandemic. Acta Biomed. 2020;91:157-160.
7. Sen M, Honavar SG, Sharma N, Sachdev MS. COVID-19 and Eye: A Review of Ophthalmic Manifestations of COVID-19. Indian J Ophthalmol. 2021;69:488-509.

8. Agarwal M, Sachdeva M, Pal S, Shah H, Kumar R M, Banker A. Endogenous Endophthalmitis A Complication of COVID-19 Pandemic: A Case Series. Ocul Immunol Inflamm. 2021; 29:726-729.
9. Kaderli ST, Karalezli A, Çitil BE, Saatci AO. Endogenous Fungal Endophthalmitis in a Patient Admitted to Intensive Care and Treated with Systemic Steroid for COVID-19. Turk J Ophthalmol. 2022; 52:139-141.
10. Davis JL, Madow B, Cornett J, Stratton R, Hess D, Porciatti V, Feuer WJ. Scale for photographic grading of vitreous haze in uveitis. Am J Ophthalmol. 2010;150:637-641.e1.
11. Luong PM, Tsui E, Batra NN, Zegans ME. Endogenous endophthalmitis and other ocular manifestations of injection drug use. Curr Opin Ophthalmol. 2019;30:506-512.
12. Cunningham ET Jr, Rao NA, Gupta A, Zierhut M. Infections and Inflammation Occurring in the Subretinal Space. Ocul Immunol Inflamm. 2018;26:329-332.
13. Balajee SA, Kano R, Baddley JW, Moser SA, Marr KA, Alexander BD, Andes D, Kontoyiannis DP, Perrone G, Peterson S, Brandt ME, Pappas PG, Chiller T. Molecular identification of Aspergillus species collected for the Transplant-Associated Infection Surveillance Network. J Clin Microbiol. 2009;47:3138-3141.
14. Nematollahi S, Permpalung N, Zhang SX, Morales M, Marr KA. *Aspergillus lentulus:* An Under-recognized Cause of Antifungal Drug-Resistant Aspergillosis. Open Forum Infect Dis. 2021;8:ofab392.
15. Shivasabesan G, Logan B, Brennan X, Lau C, Vaze A, Bennett M, Gorrie N, Mirdad F, Deveza R, Koo CM, McCluskey P, Macdonald P, Marriott D, Muthiah K, Dharan NP. Disseminated Aspergillus lentulus Infection in a Heart Transplant Recipient: A Case Report. Clin Infect Dis. 2022;75:1235-1238.
16. Thompson KN, Alshaikhsalama AM, Wang AL. Evaluation of the Clinical Course of Endogenous Endophthalmitis. J Vitreoretin Dis. 2023;7:389-396.
17. Yagi K, Ushikubo M, Maeshima A, Konishi M, Fujimoto K, Tsukamoto M, Araki K, Kamei K, Oyamada Y, Oshima H. Invasive pulmonary aspergillosis due to Aspergillus lentulus in an adult patient: A case report and literature review. J Infect Chemother. 2019;25:547-551.

Orbital Cerebrospinal Fluid Leak After Dog Bite: A Case Report

Bilal Bahadır Akbulut, Elif Bolat

Ege University Faculty of Medicine, Department of Neurosurgery, İzmir, Türkiye

Abstract

A 4-year-old boy was referred to our tertiary hospital after a penetrating adnexal injury by a large-breed dog to the left orbital area. There was an increase in lacrimation, which was thought to be due to an inflammatory reaction. However, it was discovered that the lacrimation increased in the reverse-Trendelenburg position and with the Valsalva maneuver. Halo sign and beta transferrin test were positive, which led to the diagnosis of cerebrospinal fluid (CSF) fistula, and the patient was operated using a supraorbital craniotomy. A dural tear was visualized and sutured appropriately, then fibrin glue and an autologous galeal graft were applied to the tear. The CSF oculorrhea stopped postoperatively, and the patient was discharged after 10 days of follow-up. The patient had no recurrent CSF leakage at 4-year follow-up. Although CSF oculorrhea is rare and may be difficult to discern from lacrimation, the presence of pneumocephalus and halo sign should suggest fistula repair.

Keywords: CSF fistula, penetrating injury, dog bite, case report

Introduction

A variety of mechanisms may cause a cerebrospinal fluid (CSF) fistula in traumatic injury, and its incidence is 0.5 to 3% in cranial injuries.[1,2] It most commonly presents as rhinorrhea and otorrhea but rarely may present as oculorrhea, especially in patients with direct trauma to the eye.[3]

We present an uncommon case of oculorrhea in a young child admitted after an adnexal penetrating injury by a large-breed dog bite.

Case Report

A 4-year-old boy was referred to our tertiary care center after a penetrating dog bite to the left eyelid. There was marked periorbital and eyelid edema on the left side. A minor laceration was present at the time of referral, which was primarily closed by the consultant plastic and reconstructive surgeon (Figure 1).

Figure 1. The sutured entry wound can be seen adjacent to the patient's left eye, and there is edema over the eyelids

Cite this article as: Akbulut BB, Bolat E. Orbital Cerebrospinal Fluid Leak After Dog Bite: A Case Report. Turk J Ophthalmol 2024;54:180-182

Address for Correspondence: Bilal Bahadır Akbulut, Ege University Faculty of Medicine, Department of Neurosurgery, İzmir, Türkiye
E-mail: b.bahadirakbulut@gmail.com **ORCID-ID:** orcid.org/0000-0002-7983-5056
Received: 22.02.2024 **Accepted:** 22.04.2024

DOI: 10.4274/tjo.galenos.2024.45087

The patient was awake, slightly agitated, and had no neurological signs. An antibiotic regimen of cefotaxime 300 mg/kg/day (Tüm Ekip Pharmaceuticals, İstanbul, Türkiye), vancomycin 40 mg/kg/day (Koçak Pharmaceuticals, İstanbul, Türkiye), and metronidazole 30 mg/kg/day (Osel Pharmaceuticals, İstanbul, Türkiye) was initiated, and tetanus and rabies vaccinations were administered.

The ophthalmological examination showed that the globe was intact and the cornea clear. There was only conjunctival hyperemia and slight chemosis. While the visual examination was suboptimal due to poor patient cooperation, the patient was able to count fingers from at least 30 cm. Fundoscopic examination was unremarkable.

A computed tomography (CT) scan revealed a minor defect in the orbital roof and mild pneumocephalus without hematoma (Figure 2).

An increase in lacrimation was noted during the patient's first examination, but this was thought to be due to an inflammatory reaction after penetrating trauma. However, on follow-up, it was discovered that the lacrimation increased in the reverse-Trendelenburg position and sitting position. This suggested a CSF leak, and a subsequent test for the halo sign was positive. Three-dimensional reconstruction of the CT images yielded a more demonstrative image that increased our suspicion of a dural tear (Figure 3). A beta-2 transferrin test was performed on the clear secretions that were collected, and beta-2 transferrin was identified by immuno-fixation electrophoresis, thus confirming the presence of a CSF leak. No further imaging was performed since the only possible site of CSF leak was identified on the CT scan on admission. The patient was prepared for surgical repair of the dural tear.

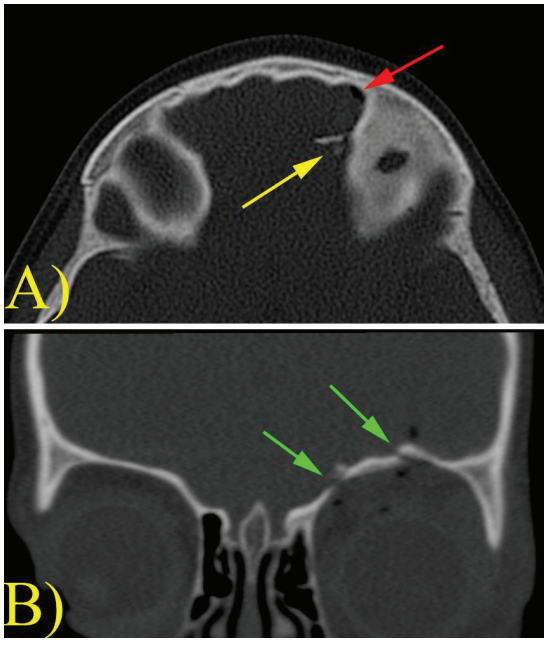

Figure 2. Cranial computed tomography scan. In the axial image (A), the pneumocephalus is marked with a red arrow, and the bone defect is marked with a yellow arrow. In the coronal view (B), the bone defect is marked with green arrows

A supraorbital craniotomy was performed via left eyebrow incision. After the dural tear was visualized, it was primarily sutured and supported with fibrin glue and an autologous galeal graft. A routine postoperative CT was obtained to rule out complications (Figure 4).

The patient was afebrile both on admission and follow-up. C-reactive protein levels reached a maximum of 12.58 mg/L, while white blood cell count reached a maximum of 6.38×10^3/μL.

Postoperatively, the patient's oculorrhea disappeared, and the patient was discharged after ten days of follow-up.

The patient had no recurrent CSF fistula or complications at 4-year follow-up. The healed surgical incision is shown in Figure 5.

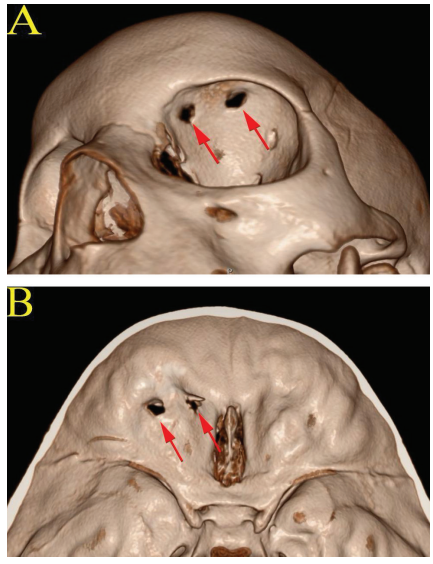

Figure 3. Three-dimensional reconstruction of the cranial computed tomography scan. The defect is visible from the exterior (A) and interior (B) aspects, marked by the red arrows

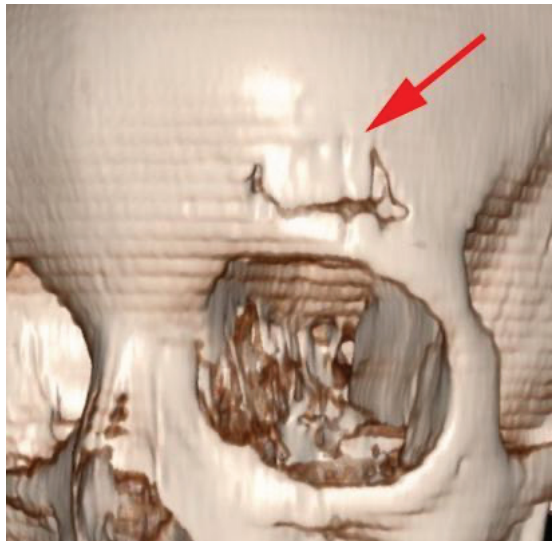

Figure 4. Three-dimensional construction of the postoperative cranial computed tomography scan. Note the small craniotomy (red arrow)

Figure 5. The patient's photograph at postoperative 4 years. The incision is indicated by a red arrow

Discussion

An orbital CSF leak in a pediatric patient following a periorbital dog bite is an uncommon phenomenon. CSF leaks are more commonly associated with cranial trauma or neurosurgical interventions.[1,4] While orbital roof defects occur in surgeries, direct penetrating trauma to the dura overlaying the anterior fossa was probably the underlying cause of this leak. Diagnosing CSF leaks associated with orbital injuries can be challenging, as CSF is not easily distinguishable from other fluids such as tears. In our case, the change in the fluid flow pattern after position change and the positive halo sign were key indicators of the CSF leak.[2]

In this case, supraorbital craniotomy combined with the use of fibrin glue and autologous galeal graft ensured a successful outcome. However, a more extensive approach, such as a bifrontal craniotomy, might be needed to expose more posteriorly positioned tears.[3,5] Managing CSF leaks in pediatric patients requires careful consideration due to their unique anatomical and physiological characteristics.[6,7]

This case underscores the importance of considering CSF leaks in patients with penetrating orbital trauma. It adds to the limited literature on orbital CSF leaks following animal bites and emphasizes the need for a high index of suspicion and appropriate management in similar cases.

Ethics

Informed Consent: Obtained.

Authorship Contributions

Surgical and Medical Practices: E.B., Concept: B.B.A., Design: B.B.A., Data Collection or Processing: B.B.A., Analysis or Interpretation: E.B., Literature Search: B.B.A., Writing: B.B.A., E.B.

Conflict of Interest: No conflict of interest was declared by the authors.

Financial Disclosure: The authors declared that this study received no financial support.

References

1. Pease M, Marquez Y, Tuchman A, Markarian A, Zada G. Diagnosis and surgical management of traumatic cerebrospinal fluid oculorrhea: case report and systematic review of the literature. J Neurol Surg Rep. 2013;74:57-66.
2. Oh JW, Kim SH, Whang K. Traumatic Cerebrospinal Fluid Leak: Diagnosis and Management. Korean J Neurotrauma. 2017;13:63-67.
3. Bunevicius A, Bareikis K, Kalasauskas L, Tamasauskas A. Penetrating Anterior Skull Base Fracture Inflicted by a Cow's Horn. J Neurosci Rural Pract. 2016;7(Suppl 1):S106-S108.
4. Schlosser RJ, Bolger WE. Nasal cerebrospinal fluid leaks: critical review and surgical considerations. Laryngoscope. 2004;114:255-265.
5. Couldwell WT, Weiss MH, Rabb C, Liu JK, Apfelbaum RI, Fukushima T. Variations on the standard transsphenoidal approach to the sellar region, with emphasis on the extended approaches and parasellar approaches: surgical experience in 105 cases. Neurosurgery. 2004;55:539-547; discussion 547-550.
6. Wang CS, Brown C, Mitchell RB, Shah G. Diagnosis and management of pediatric nasal CSF leaks and encephaloceles. Curr Treat Options Allergy. 2020;7:326-334.
7. Deng W, Liu J, Pang F, Zhang X. Diagnosis and management of pediatric cerebrospinal fluid leakage secondary to inner ear malformations: A report of 13 cases. Int J Pediatr Otorhinolaryngol. 2020;135:110049.